The Abdus Salam
International Centre for Theoretical Physics

United Nations
Educational, Scientific
and Cultural Organization

International Atomic
Energy Agency

SMR.1738 - 13

**WINTER COLLEGE**

**on**

**QUANTUM AND CLASSICAL ASPECTS**

**of**

**INFORMATION OPTICS**

***30 January - 10 February 2006***

**Lecture 2: Propagation dynamics of nondiffracting beams**

**Lecture 3: Scalar and vector Helmholtz-Gauss beams**

**Julio C. GUTIÉRREZ-VEGA**
Photonics and Mathematical Optics Group
Physics Department, Tecnológico de Monterrey
Garza-Sada 2501, Monterrey, N.L. México, 64849

The Abdus Salam
International Centre for Theoretical Physics

***WINTER COLLEGE ON***
***QUANTUM AND CLASSICAL ASPECTSOF INFORMATION OPTICS***

# *Lecture 2: Propagation dynamics of nondiffracting beams*
# *Lecture 3: Scalar and vector Helmholtz-Gauss beams*

***Julio C. Gutiérrez-Vega***

Photonics and
Mathematical Optics Group
Tecnológico de Monterrey, México

http://www.mty.itesm.mx/optica/pmog

http://homepages.mty.itesm.mx/jgutierr

# Outline

# Concept of a nondiffracting beam (NDB)

**Helmholtz equation:**

$$\left[\nabla^2 + k^2\right] U(\mathbf{r}) = 0, \quad \mathit{where} \quad \mathbf{r} = (x, y, z)$$

**Nondiffracting condition:**

$$I(x, y, z > 0) = I(x, y, z = 0)$$

$$U(\mathbf{r}) = U_t(x, y)\exp(ik_z z).$$

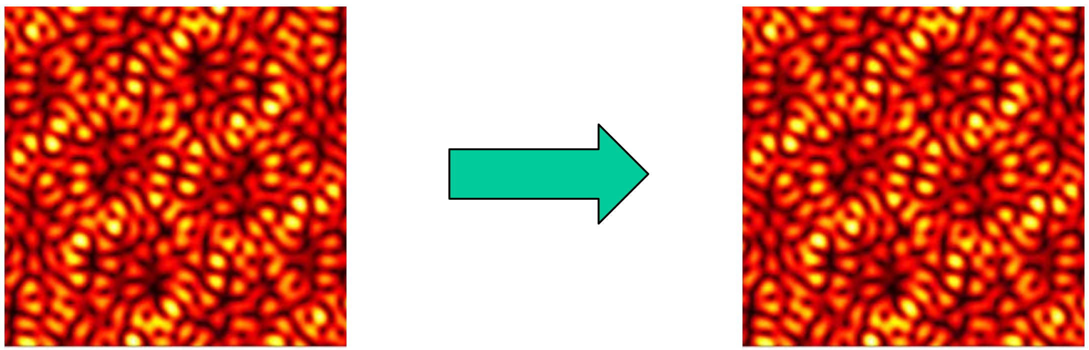

$z = 0$ $\qquad$ $z > 0$

# A little of history: Foundational papers 1987: Bessel beams

J. Durnin Vol. 4, No. 4/April 1987/J. Opt. Soc. Am. A 651

## Exact solutions for nondiffracting beams. I. The scalar theory

J. Durnin

*The Institute of Optics, University of Rochester, Rochester, New York 14627*

Received June 12, 1986; accepted November 24, 1986

We present exact, nonsingular solutions of the scalar-wave equation for beams that are nondiffracting. This means that the intensity pattern in a transverse plane is unaltered by propagating in free space. These beams can have extremely narrow intensity profiles with effective widths as small as several wavelengths and yet possess an infinite depth of field. We further show (by using numerical simulations based on scalar diffraction theory) that physically realizable finite-aperture approximations to the exact solutions can also possess an extremely large depth of field.

PHYSICAL REVIEW

LETTERS

VOLUME 58 13 APRIL 1987 NUMBER 15

## Diffraction-Free Beams

J. Durnin and J. J. Miceli, Jr.

*The Institute of Optics, University of Rochester, Rochester, New York 14627*

and

J. H. Eberly[a]

*Department of Physics and Astronomy, University of Rochester, Rochester, New York 14627*

(Received 20 October 1986)

It was recently predicted that nondiffracting beams, with beam spots as small as a few wavelengths, can exist and propagate in free space. We report the first experimental investigation of these beams.

PACS numbers: 03.50.−z, 03.65.−w, 41.10.Hv, 42.10.Hc

# *NDBs can be easily constructed using plane waves*

NDBs can be constructed by adding plane waves.

**REQUIRED CONDITION: All constituent plane waves must to have the same phase velocity $v_p$ along the propagation direction, i.e. all plane waves must to have the same longitudinal wavenumber $k_z$.**

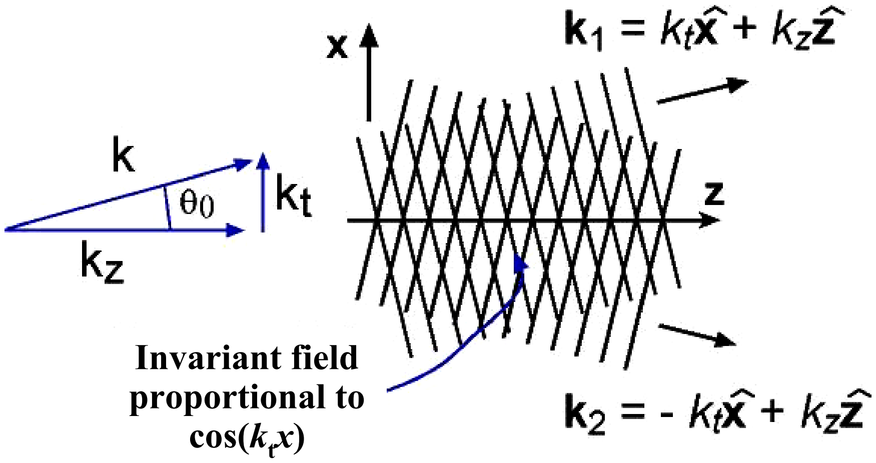


$$U(\mathbf{r}) = A\exp(i\mathbf{k}_1 \cdot \mathbf{r}) + A\exp(i\mathbf{k}_2 \cdot \mathbf{r})$$
$$= 2A\cos(k_t x)\exp(ik_z z)$$

$$v_p = \frac{c}{\cos\theta_0}$$

# *Plane wave expansion of the nondiffracting beams*

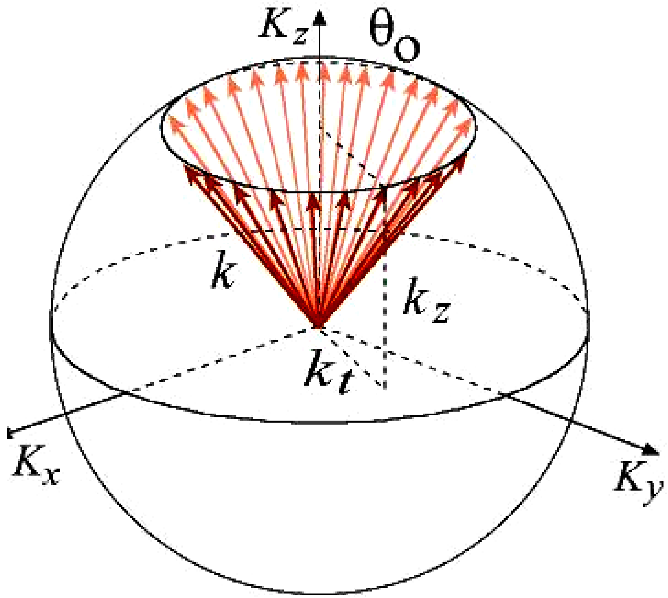


Three-dimensional expansion

$$U(\mathbf{r}) = \int_{\mathbf{K}} \widetilde{U}(\mathbf{K}) \exp\left[i\, \mathbf{K} \cdot \mathbf{r}\right] \, \mathrm{d}^3 K$$

$$\widetilde{U}(\mathbf{K}) = A(\varphi) \left[\frac{\delta(K-k)}{K}\right] \delta(K_z - k_z)$$

$$U(x, y, z \geq 0) = \exp(ik_z z) \int_{-\pi}^{\pi} A(\varphi) \exp\left[ik_t (x \cos\varphi + y \sin\varphi)\right] \, \mathrm{d}\varphi,$$

$$U(r, \theta, z \geq 0) = \exp(ik_z z) \int_{-\pi}^{\pi} A(\varphi) \exp\left[ik_t r \cos(\varphi - \theta)\right] \, \mathrm{d}\varphi,$$

## *An example of a nondiffracting field*

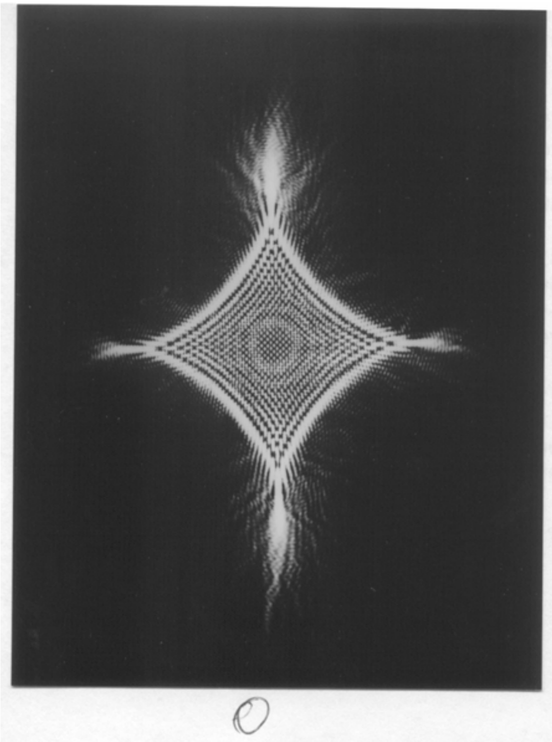

z = 0;

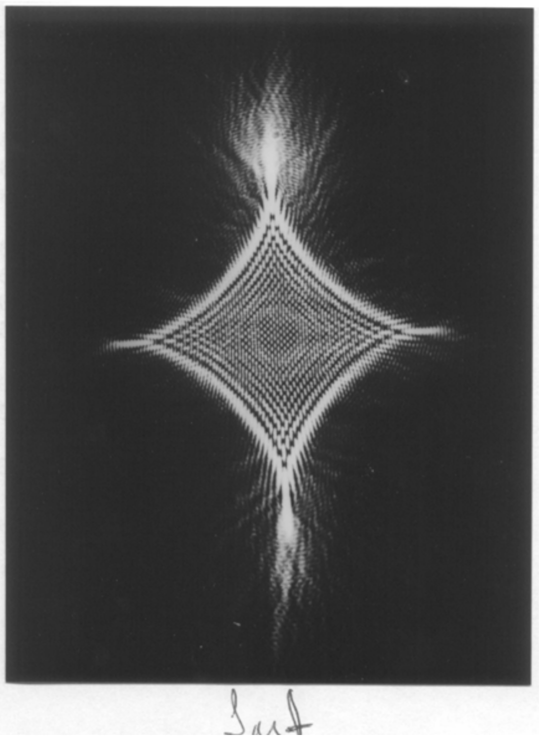

z = 1 m

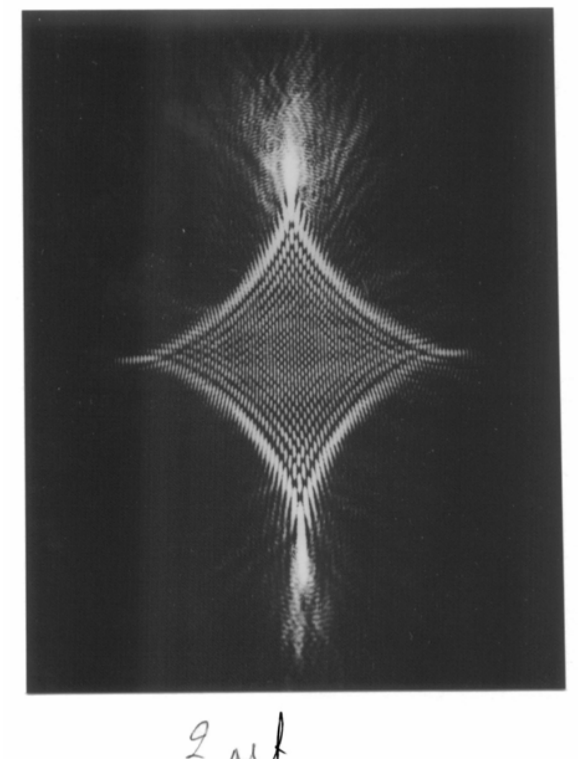

z = 2 m

Thanks to S. Chávez-Cerda and G. Ramirez

# *Apertured NDBs are restricted to a finite volume region*

Geometrical visualization of the nondiffracting region

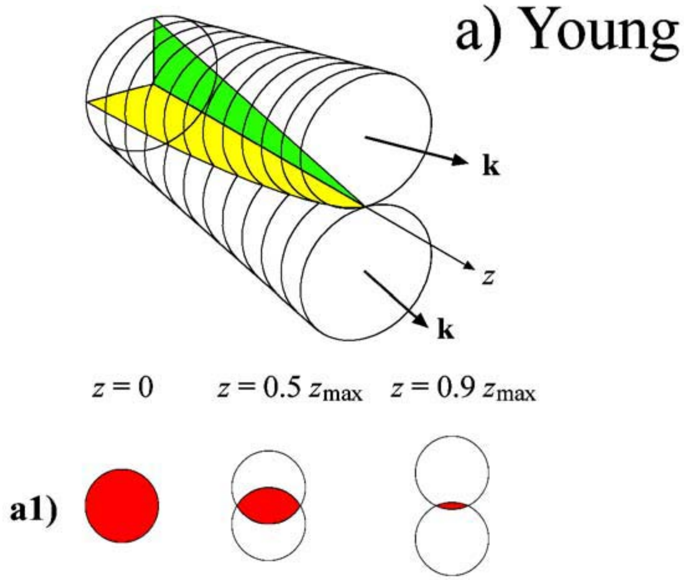


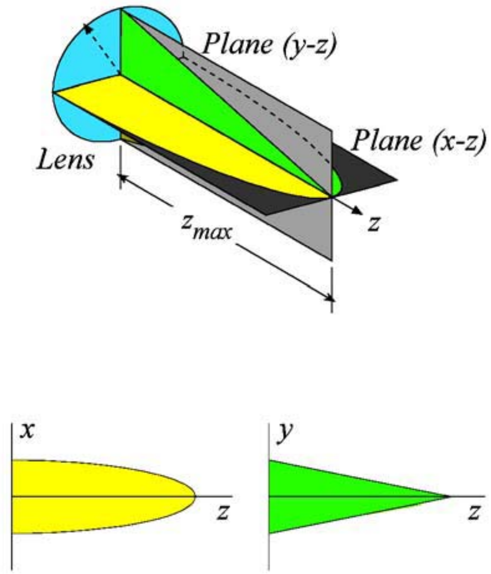


Interferring
2 plane waves:

Cosine fringes
$\cos(k_t x)\exp(ik_z z)$

Numerical propagation

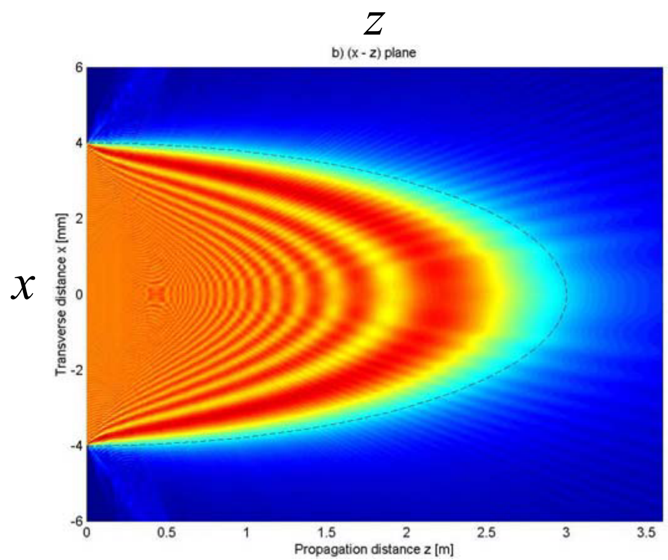


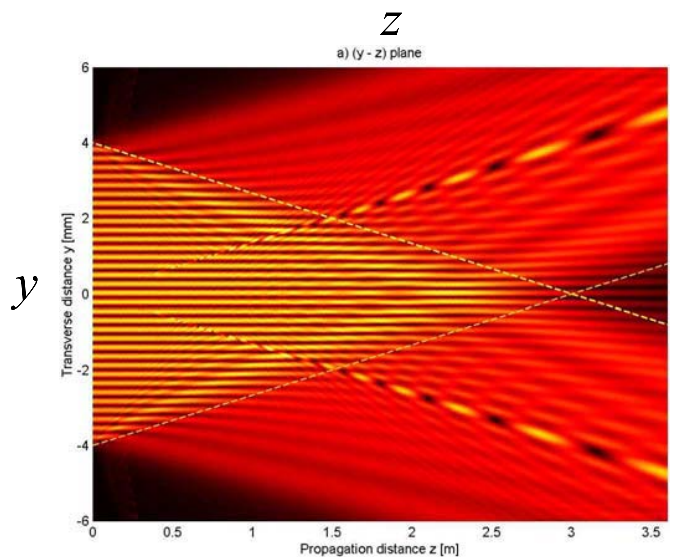

# Apertured NDBs are restricted to a finite volume region

Geometrical visualization of the nondiffracting region

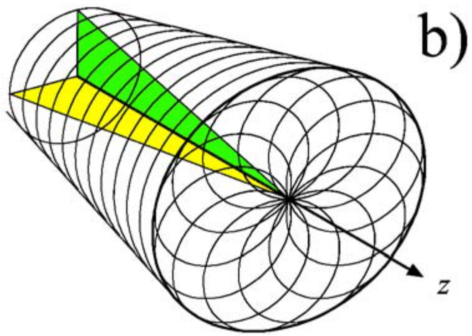


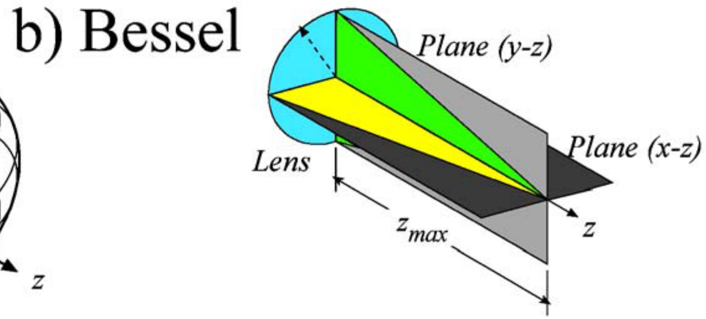


Bessel rings

$J_0(k_t r)\exp(ik_z z)$

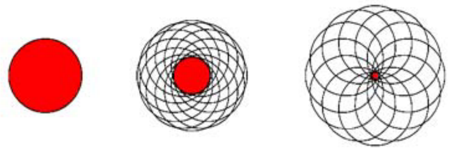

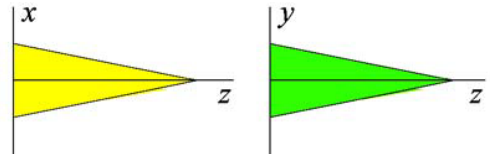


Numerical propagation

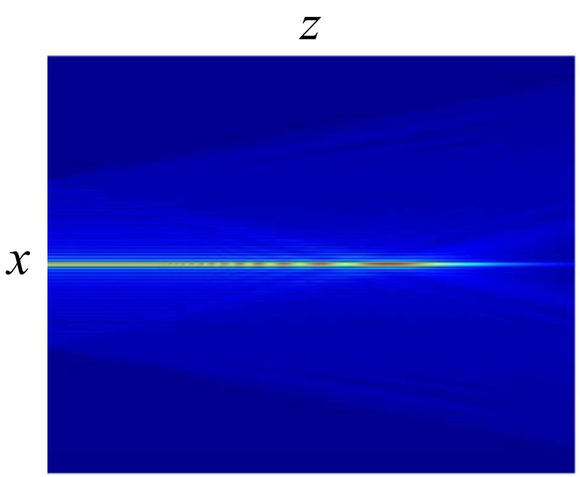


**Axial oscillations due to border waves**

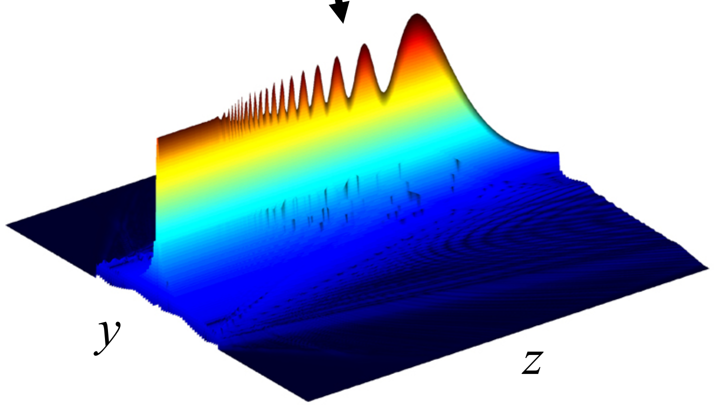


R. Borghi, M. Santarsiero, and F. Gori, "Axial intensity of apertured Bessel beams ," J. Opt. Soc. Am. A **14**, 23- (1997)

# Geometrical propagation of a focused NDBs

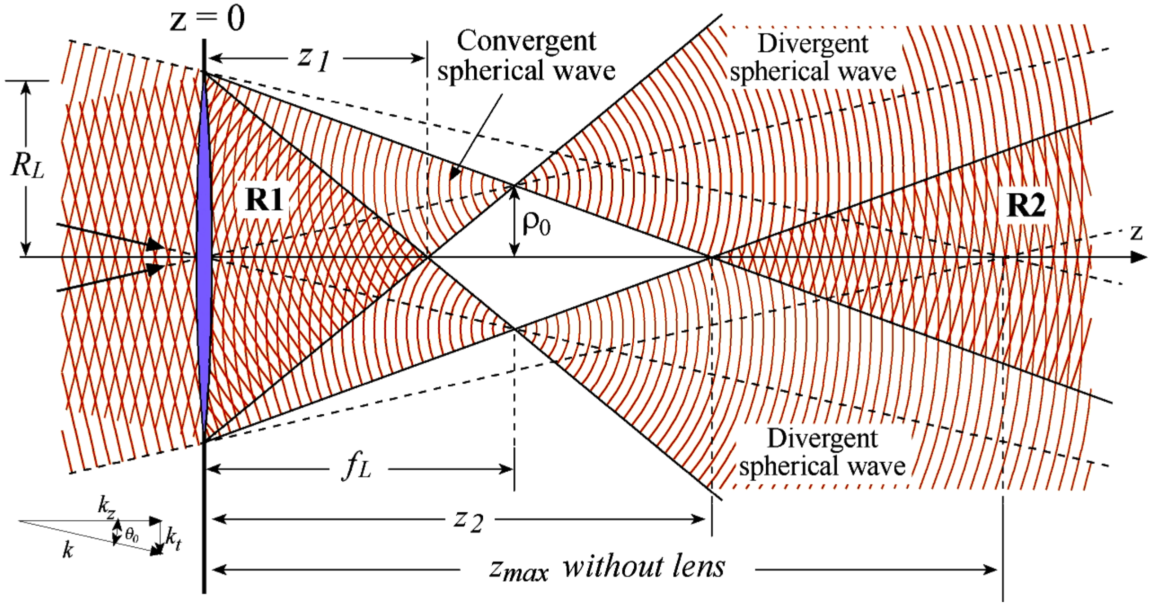


Numerical propagation

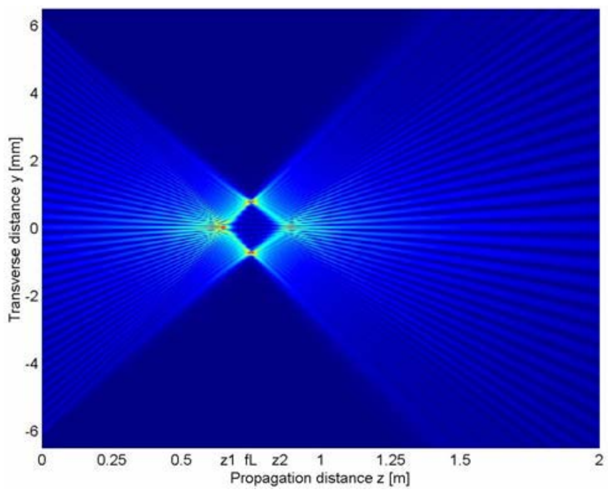


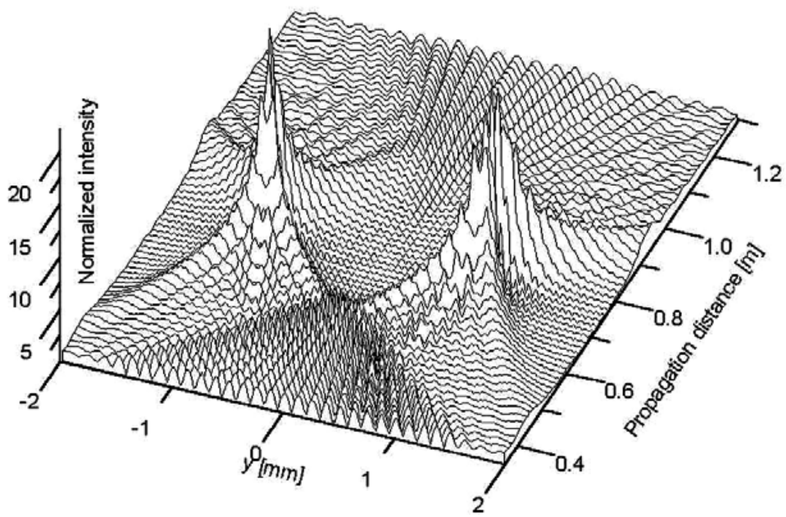


J. C. Gutiérrez-Vega, et al., *J. Opt. A*, **5**, 273 (2003)

# *Axial intensity of the focused NDB*

**The on-axis intensity of a focused NDB is a Lorentzian curve**

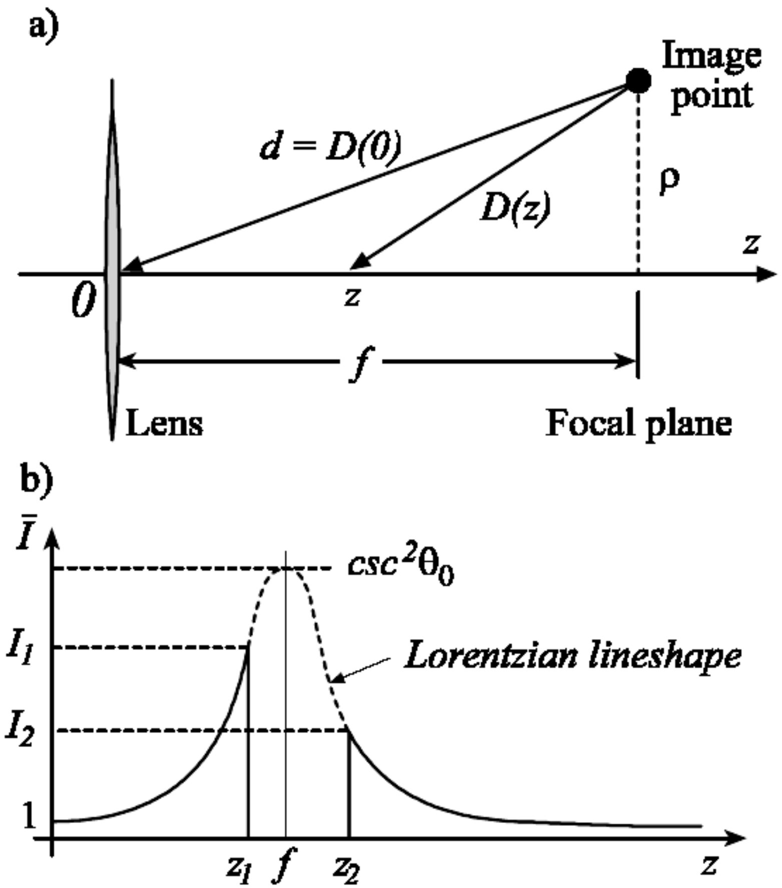


**Figure 3.** The geometric prediction of the axial intensity of a focused PIOF is given by a Lorentzian curve.

$$\frac{I(z)}{I_0} = \left[\frac{D(0)}{D(z)}\right]^2 = \frac{\rho_0^2 + f_L^2}{\rho_0^2 + (z - f_L)^2},$$

**Valid for any NDB!!**

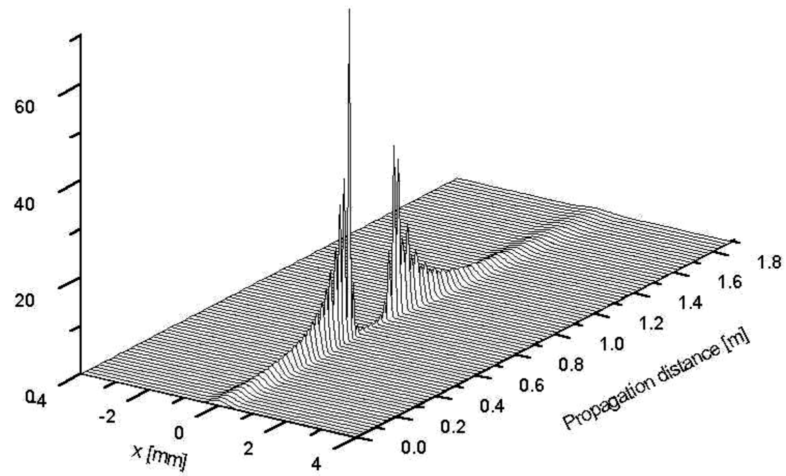


J. C. Gutiérrez-Vega, et al., *J. Opt. A*, **5**, 273 (2003)

# *There are four fundamental families of NDBs*

Helmholtz equation $\left[\nabla^2 + k^2\right] U(\mathbf{r}) = 0$ is separable in 11 orthogonal systems

Four of them are cylindrical i.e $\mathbf{r} = (\mathbf{r}_t, z)$

**Cartesian coordinates**
**Plane waves**

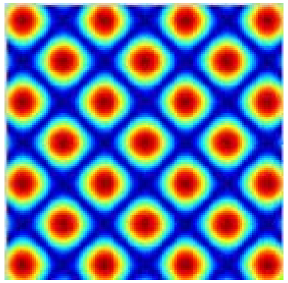

**Circular cylindrical coordinates**
**Bessel beams**

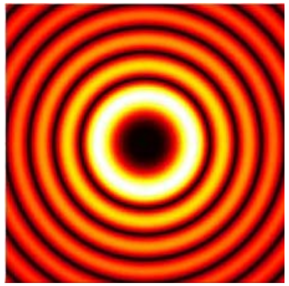

**Elliptic cylindrical coordinates**
**Mathieu beams**

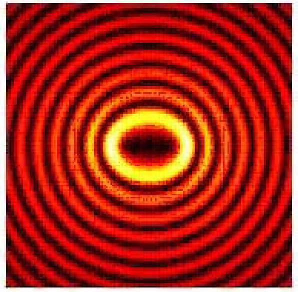

**Parabolic cylindrical coordinates**
**Parabolic beams**

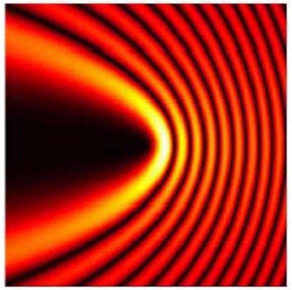

# Bessel beams

# *Bessel beams: Amplitude and phase distribution*

**Field distribution:**

$$
\begin{aligned}
U(\mathbf{r}) &= J_m(k_t r)\exp(im\theta)\exp(ik_z z) \\
&= \exp(ik_z z)\int_{-\pi}^{\pi} \underbrace{\left[\frac{(-i)^m}{2\pi}\exp(im\varphi)\right]}_{\textbf{Angular spectrum: } A(\varphi) \;\propto\; \exp(im\varphi)} \exp\left[ik_t r\cos(\varphi-\theta)\right]\,\mathrm{d}\varphi
\end{aligned}
$$

Intensity distribution has azimuthal symmetry

Phase distribution increases linearly along the angular coordinate from 0 to $2m\pi$.

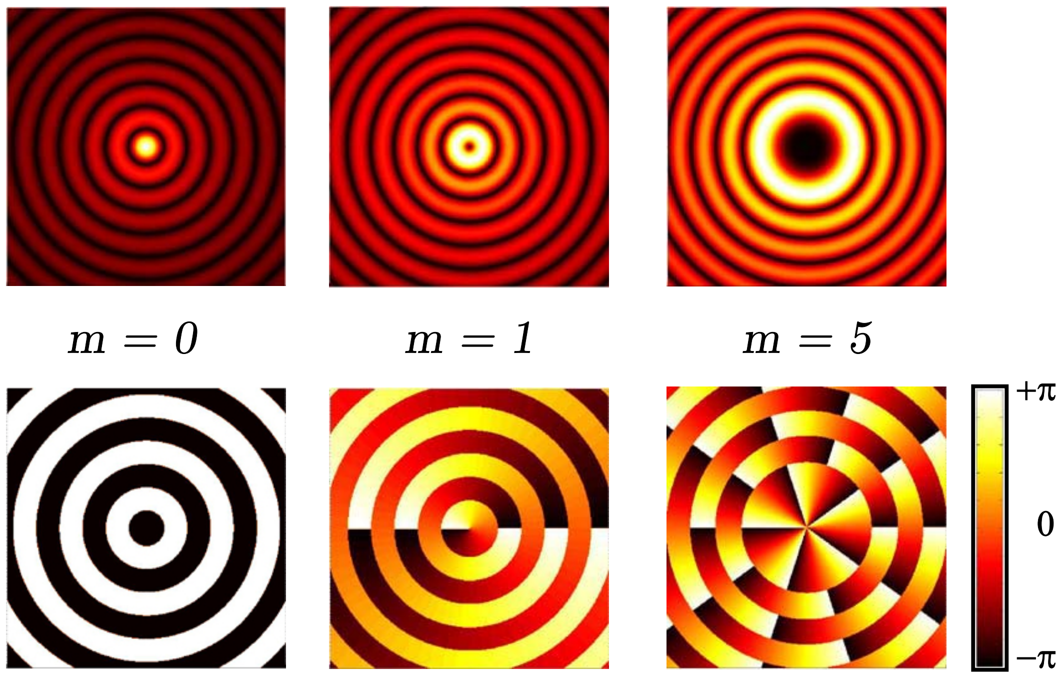

# *Adding plane waves to build up Bessel beams*

**Bessel beam $J_0$**

$A(\phi) = 1$

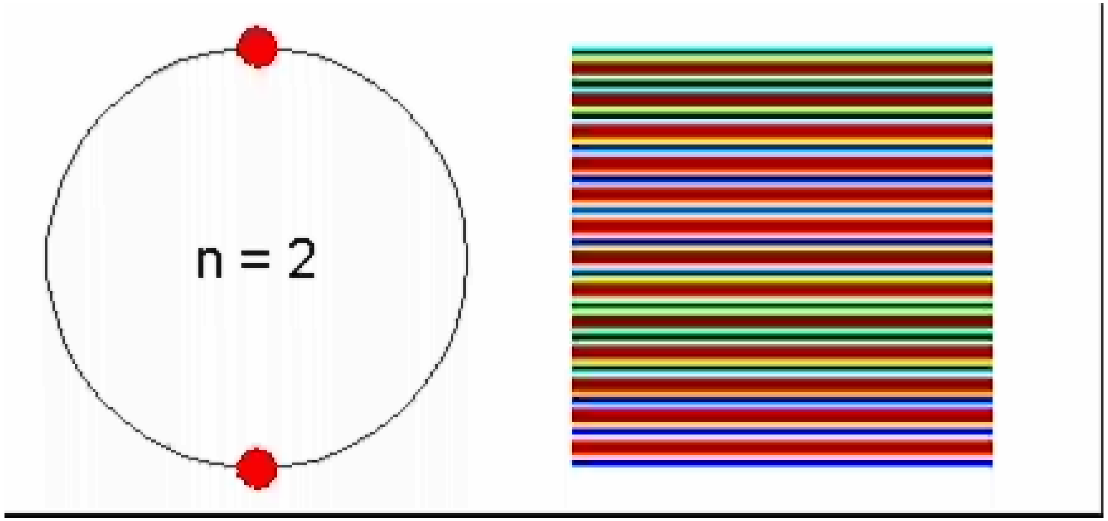


**Bessel beam $J_2$**

$A(\phi) = \exp(im\phi)$

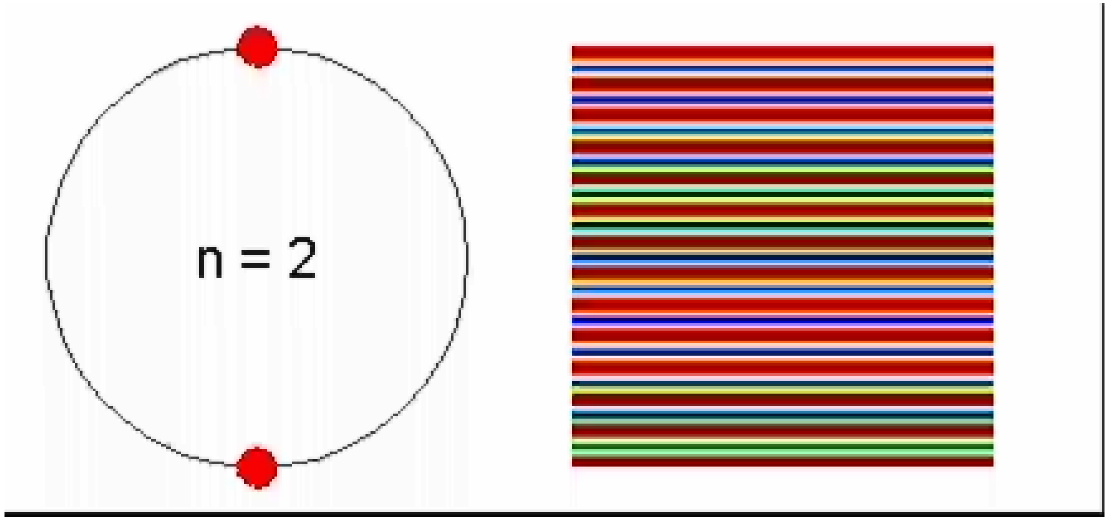

# *Bessel beams are vortex beams*

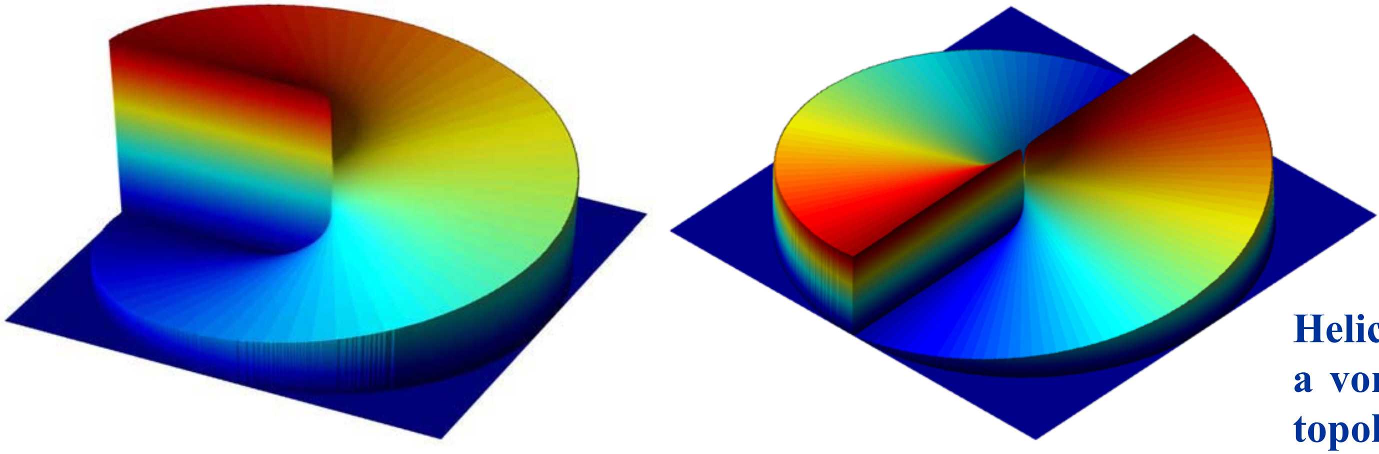

**Helical wavefronts of a vortex beam for the topological charge *m* = 1 and *m* = 2**

The point where the phase dislocation appears can be identified by the nonzero value of the integral

$$\oint \nabla\Phi \cdot \mathrm{d}\mathbf{l} \;=\; 2\pi m$$

where the integration is performed along the closed line surrounding the examined point.

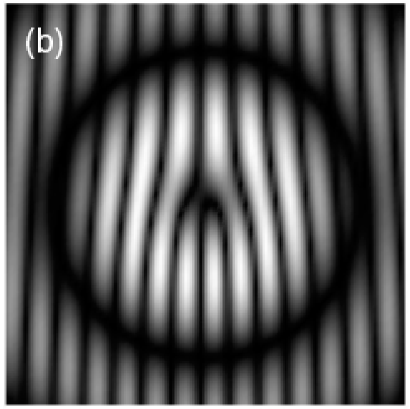


Interference of the optical vortex $m$ = 2 with the plane wave results in a fork-like interference patterns

[1] Z. Bouchal, "Nondiffracting optical beams," Czechoslovak J. Phys., **53**, 537-624 (2003)
[2] L. Allen, S. M. Barnett and M. Padgett, "Optical Angular Momentum" IOP Publishing (2003) and references therein

## *Simple experimental setup to produce NDBs: Durnin's setup*

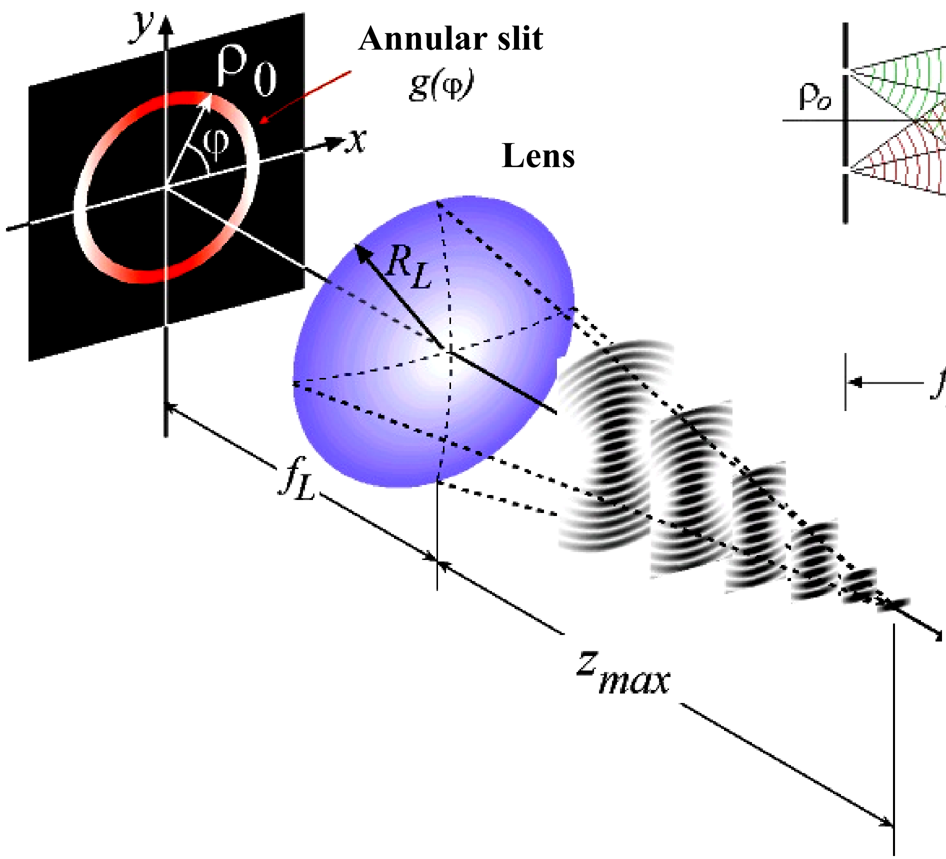


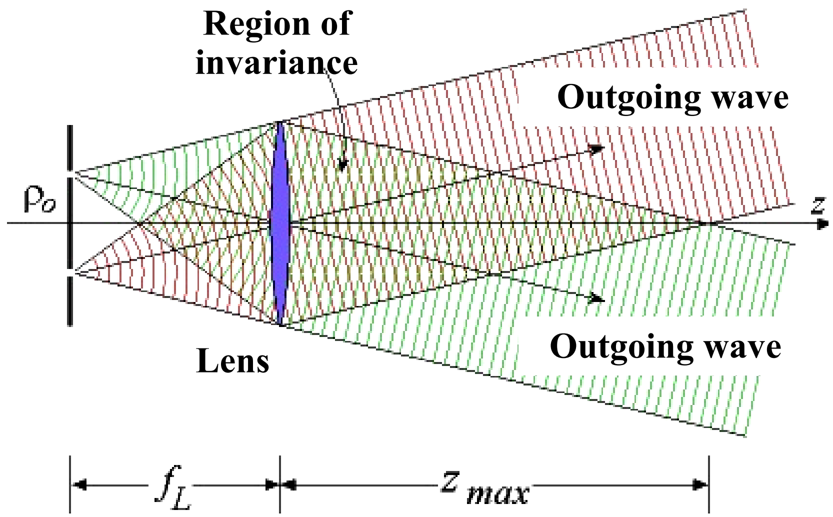


$$\theta_0 = \arctan\left(\frac{\rho_0}{f_L}\right)$$

$$z_{\max} = \frac{f_L}{\rho_0} R_L.$$

J. Durnin, "Exact solutions for nondiffracting beams," J. Opt. Soc. Am. A, 4, 651 (1987)

# BBs can also be produced with holograms or axicons

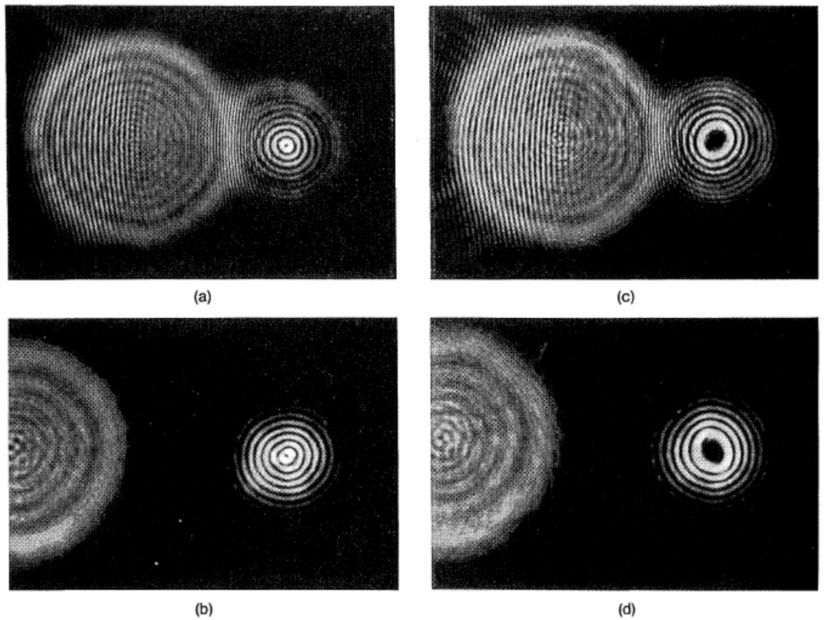


A. Vasara, J. Turunen, and A. Friberg, "Realization of general nondiffracting beams with computer-generated holograms," J. Opt. Soc. Am. A 6, 1748- (1989)

An axicon transforms a plane wave into a converging conical wave

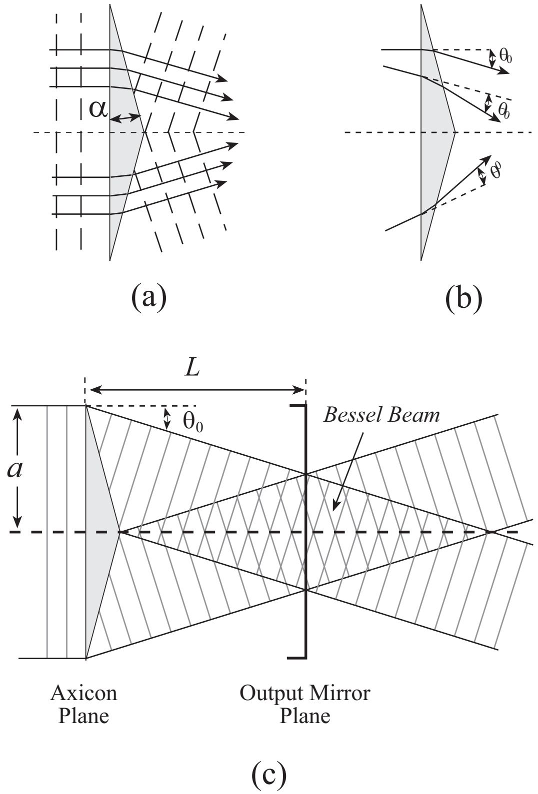


Converging conical waves build up the BB

Z. Jaroszewicz, A. Burvall, and A. T. Friberg, "Axicon - the Most Important Optical Element" Opt. Phot. News, **16**, 34-39 (2005)

## *BBs can be produced by superposing the even and odd components*

$$J_m(k_t r)\exp(im\varphi) = J_m(k_t r)\cos(m\varphi) + iJ_m(k_t r)\sin(m\varphi)$$

| | **Even: Bessel-Cosine** | **Odd: Bessel-Sine** | **Bessel** |
|---|---|---|---|
| | $J_m(k_t\rho)\cos(m\varphi)$ | $J_m(k_t\rho)\sin(m\varphi)$ | $J_m(k_t\rho)\exp(i\,m\varphi)$ |

Amplitude

Phase

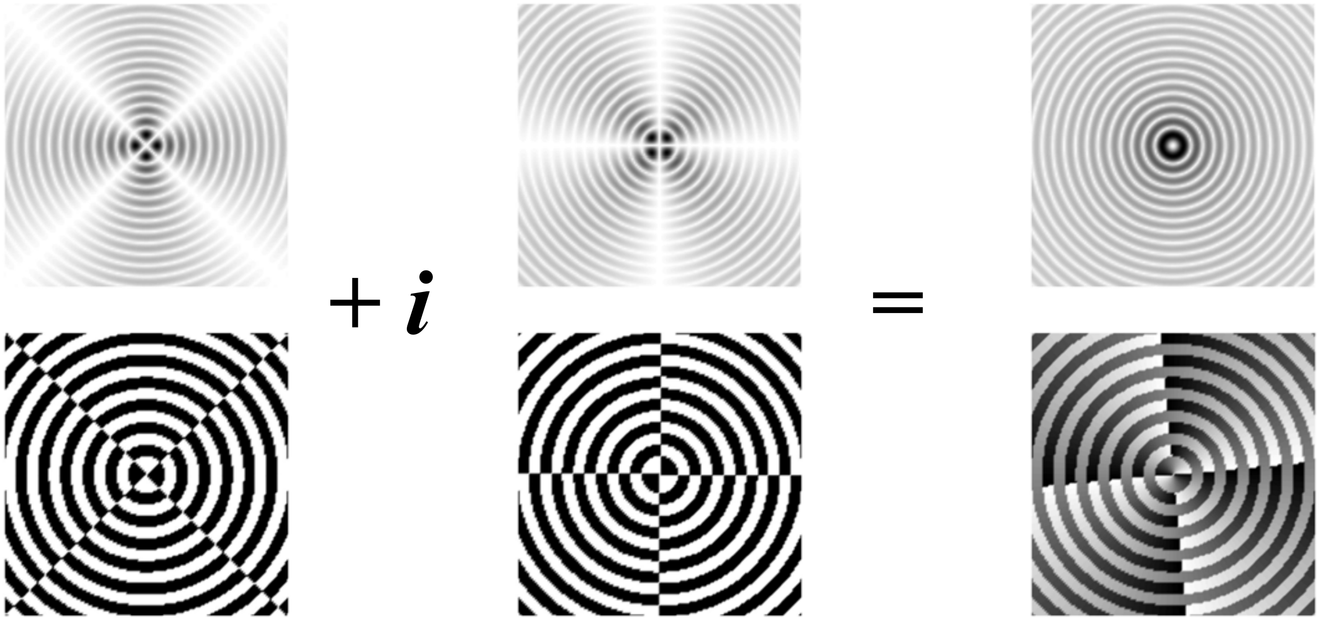


| | | | |
|---|---|---|---|
| **Angular spectrum** | $\cos(m\varphi)$ | $\sin(m\varphi)$ | $\exp(i\,m\varphi)$ |

# Constructing HOBBs with a Mach-Zehnder interferometer

$$J_m(k_t r)\exp(im\varphi) = J_m(k_t r)\cos(m\varphi) + iJ_m(k_t r)\sin(m\varphi)$$

$$g_1(\varphi) = \cos(m\varphi), \qquad g_2(\varphi) = \sin(m\varphi)$$

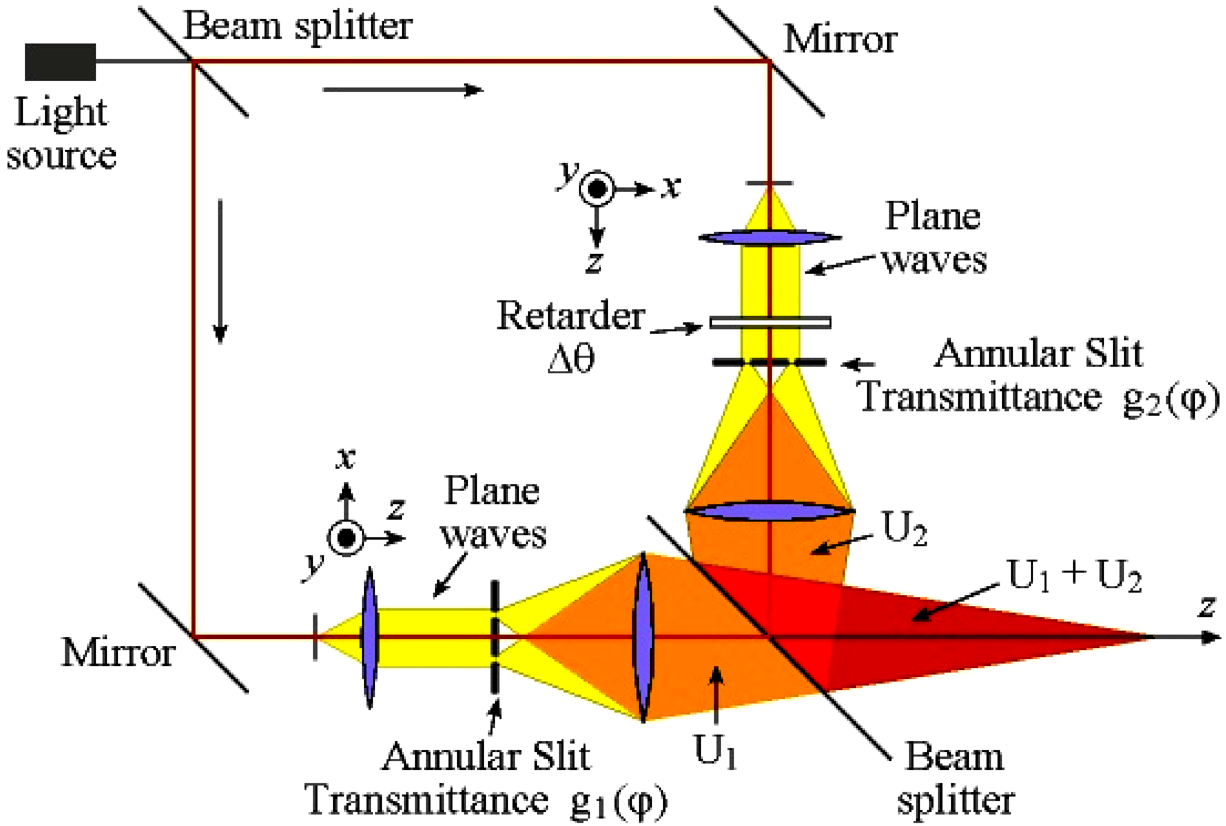


C. López-Mariscal, et al, "Production of high--order Bessel beams with a Mach--Zehnder interferometer," Appl. Opt. **43**, 5060-5063 (2004)

## *Some results*

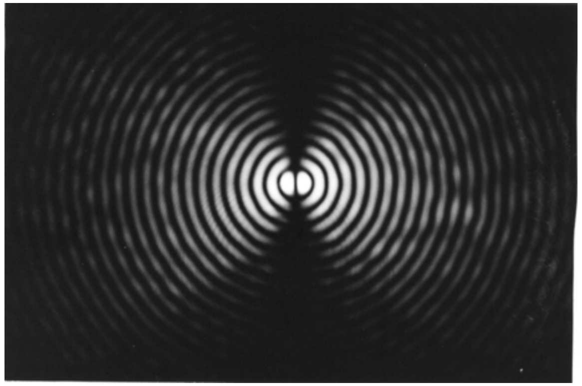

$+\,i$

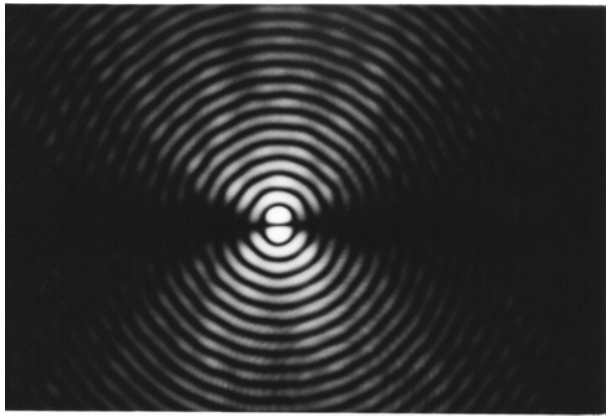

$J_1(k_t r)\cos(\varphi)$ $J_1(k_t r)\sin(\varphi)$

$$J_1(k_t r)\exp(i\varphi)$$

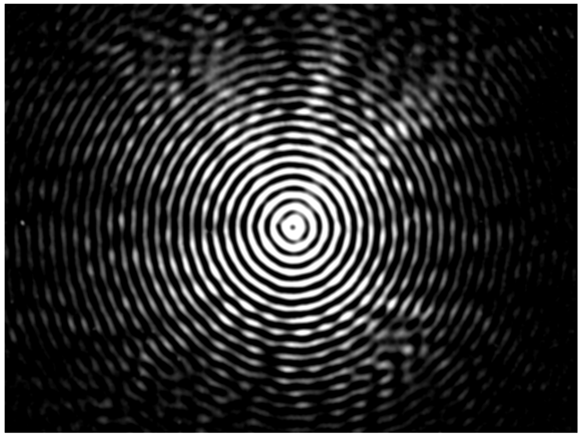

$0.8$ mm

C. López-Mariscal, et al, "Production of high--order Bessel beams with a Mach--Zehnder interferometer," Appl. Opt. **43**, 5060-5063 (2004)

## *Creating rotating waves with Bessel beams*

The interference of a HO-BB with spherical waves produces Spiraling waves (there is a scaling factor due the spherical wave)

Experiment

Order *m* = 4

L2 = 2 cm
L3 = 30 cm

Z-scan of 4th-HOBB interferred with a spherical wave

HOBBs carry Orbital Angular Momentum.

[1] C. López-Mariscal, et al, "Production of high--order Bessel beams with a Mach--Zehnder interferometer," Appl. Opt. **43**, 5063 (2004)
[2] K. Volke-Sepúlveda et al. *"Orbital angular momentum of a high order Bessel light beam,"* J. Opt. B, **4**, S82-S89 (2002).
[3] L. Allen, S. M. Barnett and M. Padgett, "Optical Angular Momentum" IOP Publishing (2003) and references therein

# *Active method to generate BBs: Bessel-Gauss Resonator*

An axicon transforms a plane wave into a converging conical wave

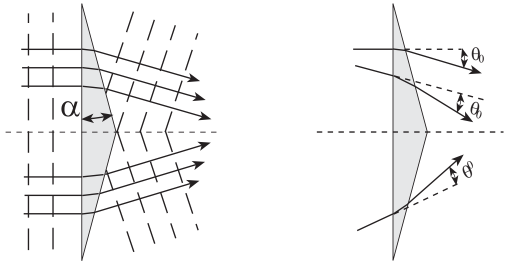


(a) (b)

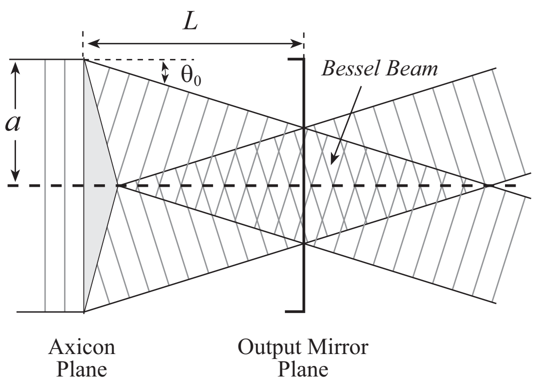


(c)

Converging conical waves build up the Bessel beam

Resonator with refractive and reflective axicon

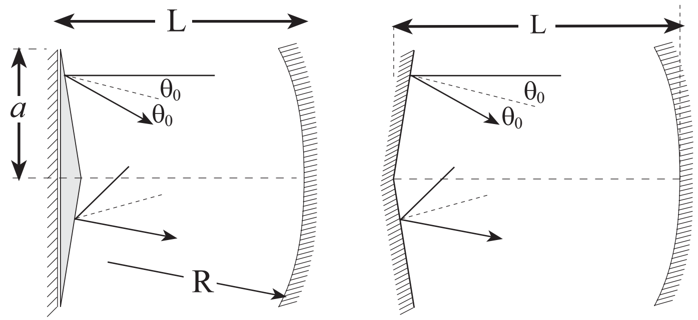


$$L = \frac{a}{2\tan\theta_0} \simeq \frac{a}{2\theta_0} = \frac{a}{2(n-1)\alpha}.$$

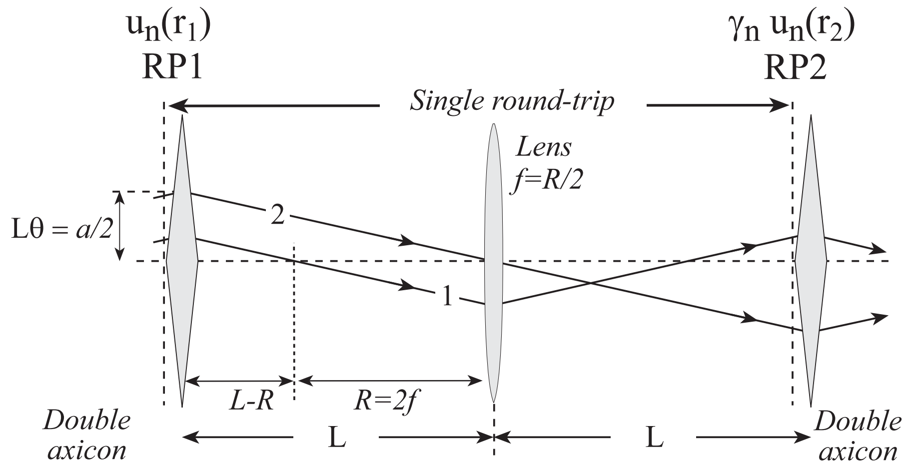

# *Wave optics analysis: Intracavity field distributions*

**Amplitude** **Phase**

**J0 BB**

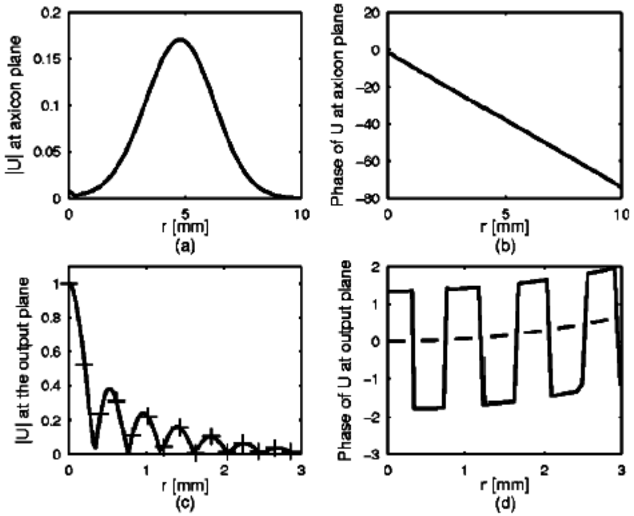


**AXICON PLANE**

**OUTPUT PLANE**

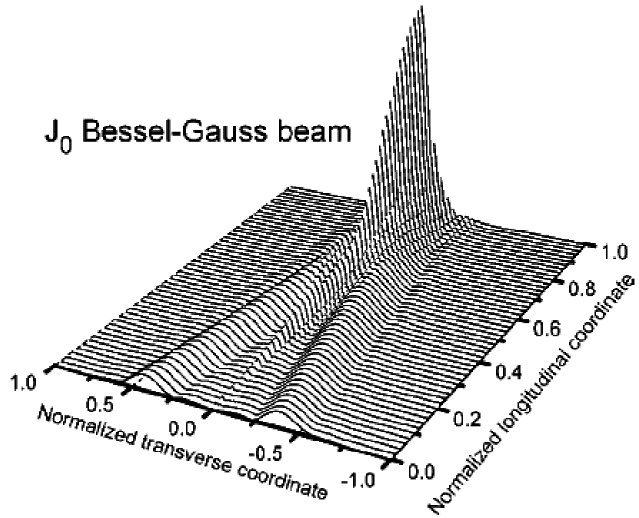


(a)

**J2 BB**

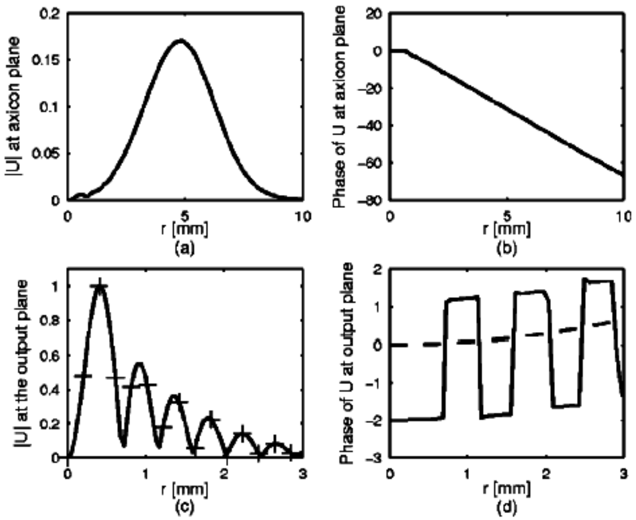


**AXICON PLANE**

**OUTPUT PLANE**

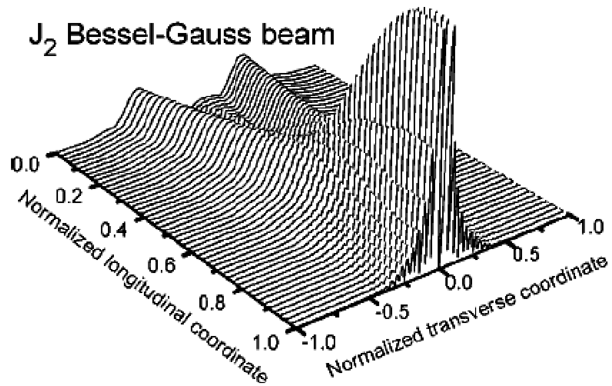


J. C. Gutiérrez-Vega, et al, JOSA A, **20**, 2113 (2003)

# Experiment: $CO_2$ Bessel-Gauss resonator

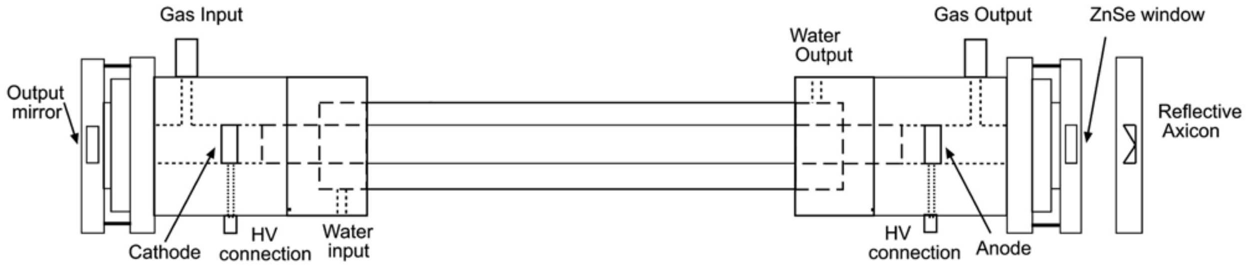


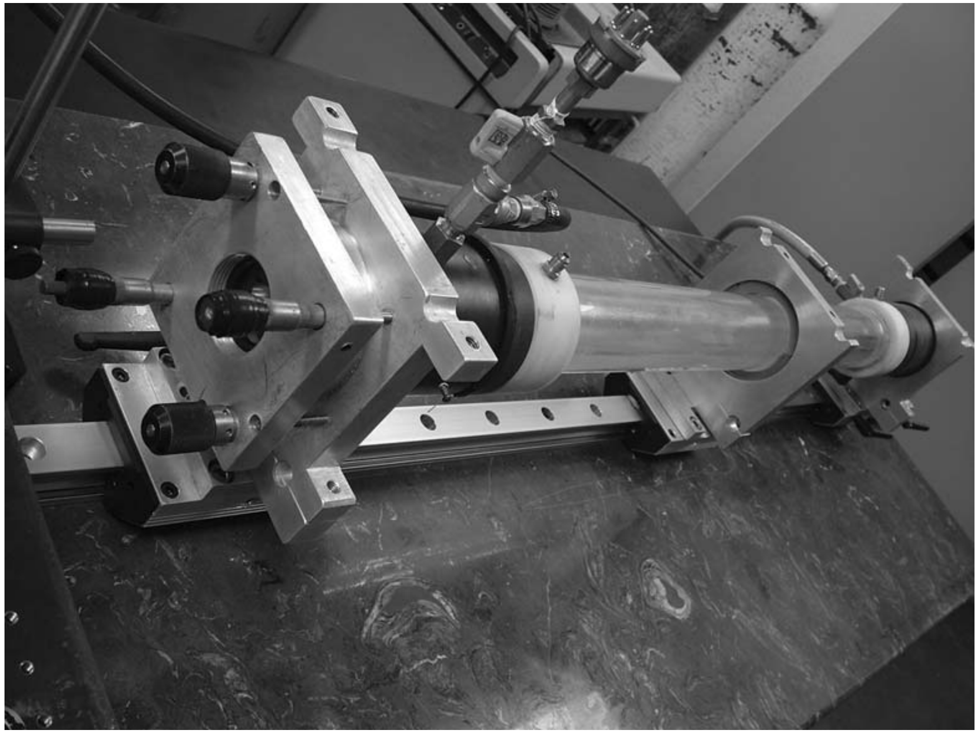

M. Alvarez, et al, "Construction and characterization of CO2 laser with an axicon based Bessel-Gauss resonator," SPIE Vol. 5708-19, 323-331 (2005)

# ***Focusing the Bessel-Gauss beam***

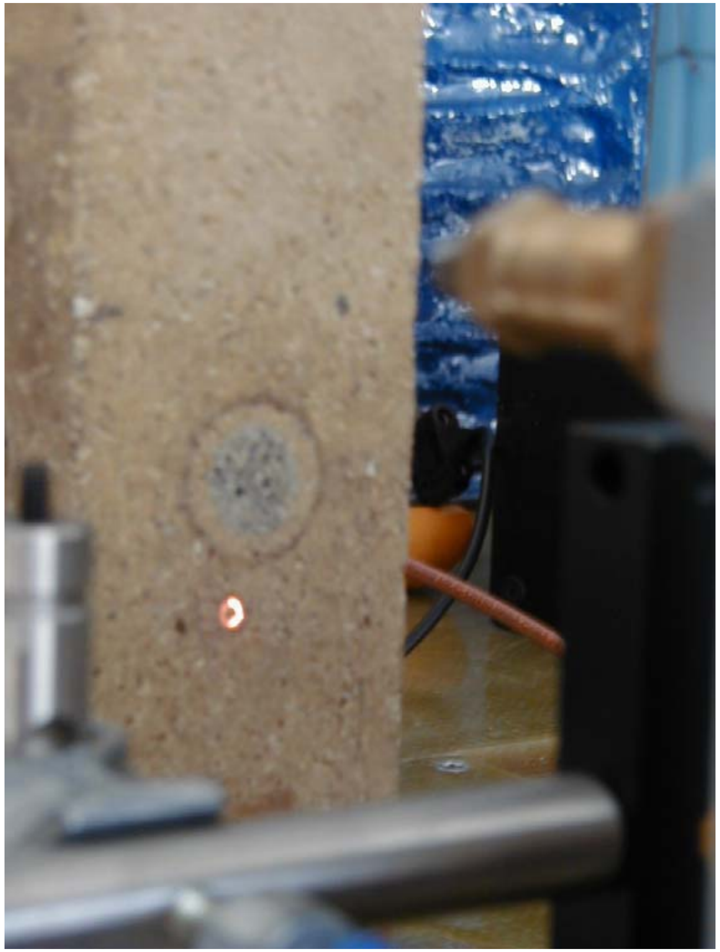

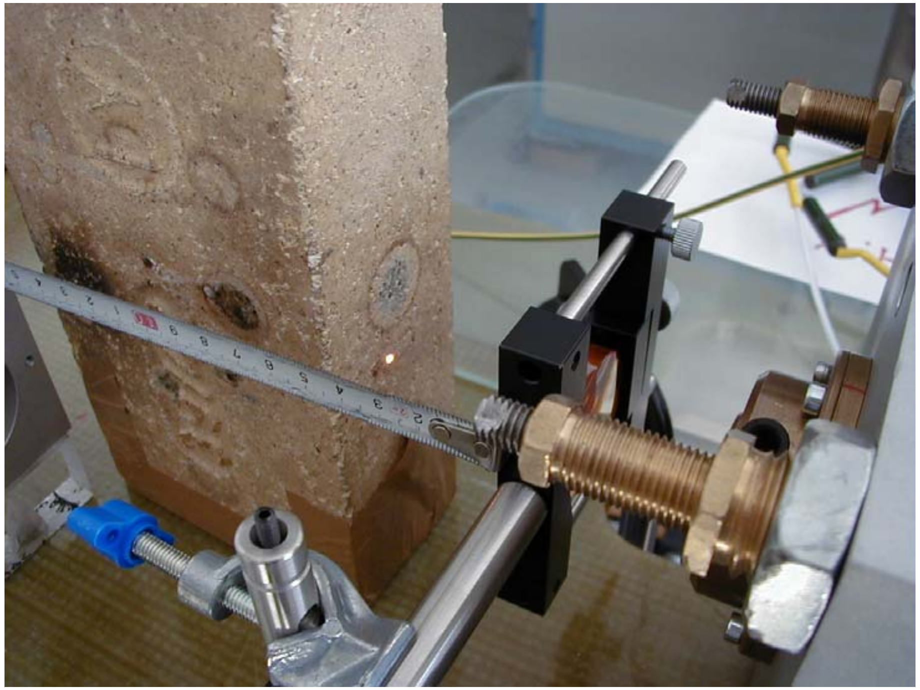

# Mathieu beams

# Mathieu beams: Elliptic coordinates

$$(x,y)\leftrightarrow(\xi,\eta)$$
$$x = f\cosh\xi\cos\eta$$
$$y = f\sinh\xi\sin\eta$$
$$z = z$$

For a given ellipse

$$f^2 = a^2 - b^2$$
$$e = \frac{f}{a} = \frac{1}{\cosh\xi_0}$$

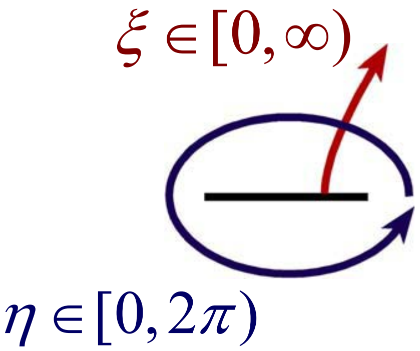


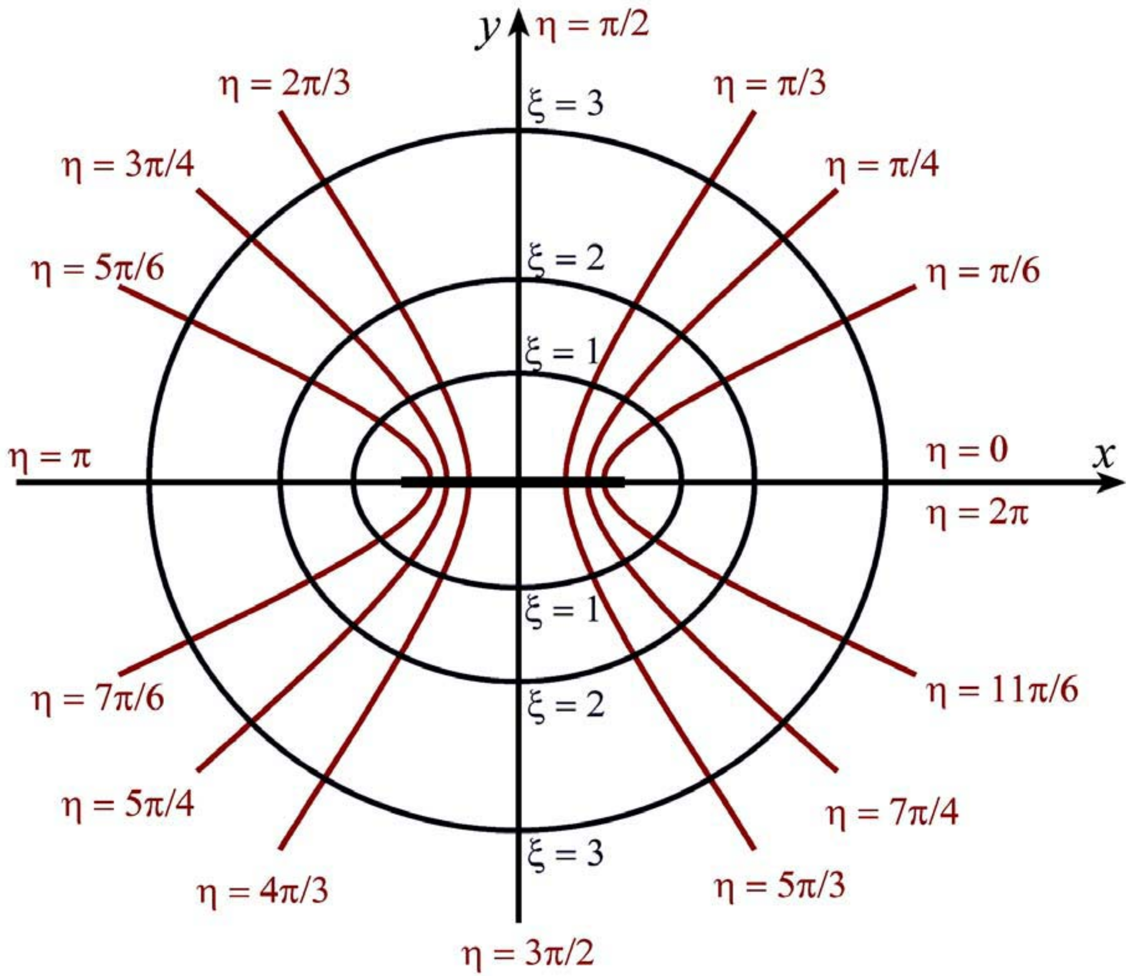

## Mathieu beams: Separation of the Helmholtz equation

Helmholtz equation in elliptic coordinates

$$\left[\frac{2}{f^2(\cosh 2\xi - \cos 2\eta)}\left(\frac{\partial^2}{\partial\xi^2} + \frac{\partial^2}{\partial\eta^2}\right) + \frac{\partial^2}{\partial z^2} - k^2\right]U(\mathbf{r}) = 0,$$

$$U(\mathbf{r}) = R(\xi)\Theta(\eta)Z(z),$$

$$R''(\xi) - (\alpha - 2q\cosh 2\xi)R(\xi) = 0,$$
$$\Theta''(\eta) + (\alpha - 2q\cos 2\eta)\Theta(\eta) = 0,$$
$$Z''(z) + k_z^2 Z(z) = 0,$$

$\alpha = eigenvalue$

$q = \dfrac{f^2}{4}k_t^2$

$k^2 = k_t^2 + k_z^2$

$$U(\mathbf{r}) = R(\xi;q)\Theta(\eta;q)\exp(\pm ik_z z).$$

## *Mathieu beams: Mathieu functions*

**Radial Mathieu equation**

$$\left[\frac{d^2}{d\xi^2} - (\alpha - 2q\cosh 2\xi)\right] R(\xi) = 0$$

| 1st. kind | 2nd kind | Mathieu-Hankel | |
|---|---|---|---|
| $Je_m(\xi;q)$ | $Ne_m(\xi;q)$ | $Me_m^{(1),(2)} = Je_m \pm iNe_m$ | **Even** |
| $Jo_m(\xi;q)$ | $No_m(\xi;q)$ | $Mo_m^{(1),(2)} = Jo_m \pm iNo_m$ | **Odd** |
| $J_m$ | $N_m$ | $H_m^{(1),(2)} = J_m \pm iN_m$ | **Bessel Analogy** |

**Angular Mathieu equation**

$$\left[\frac{\partial^2}{\partial\eta^2} + (\alpha - 2q\cos 2\eta)\right] \Theta(\eta) = 0$$

$ce_m(\eta;q)$

$se_m(\eta;q)$

J. C. Gutiérrez-Vega et al., "Mathieu functions, a visual approach," Am. J. Phys. 71, 233 (2003)

# *Visualization of Mathieu functions*

## Angular Mathieu functions

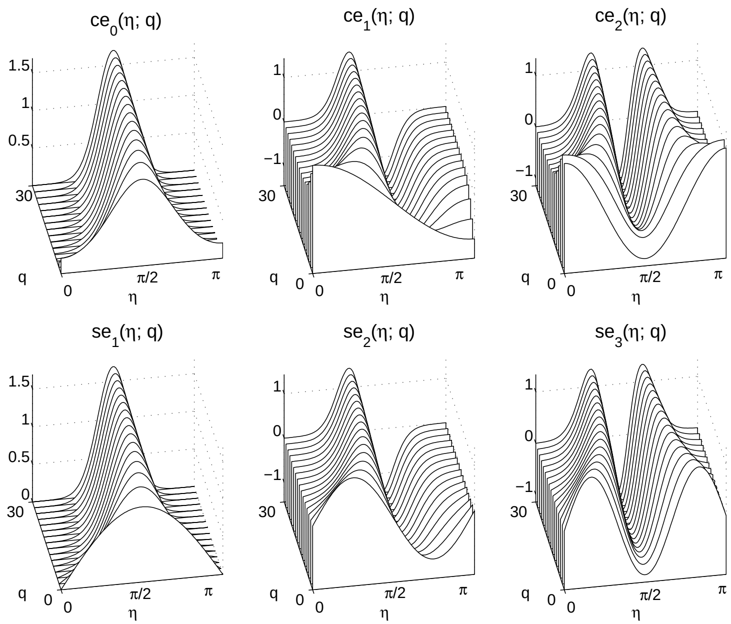


Fig. 2. Graphical visualization of angular Mathieu functions $\mathrm{ce}_m(\eta;q)$ and $\mathrm{se}_{m+1}(\eta;q)$ over the $(\eta,q)$ plane. The function $\mathrm{ce}_0(\eta;q)$ is never negative, although oscillatory.

## Radial Mathieu functions

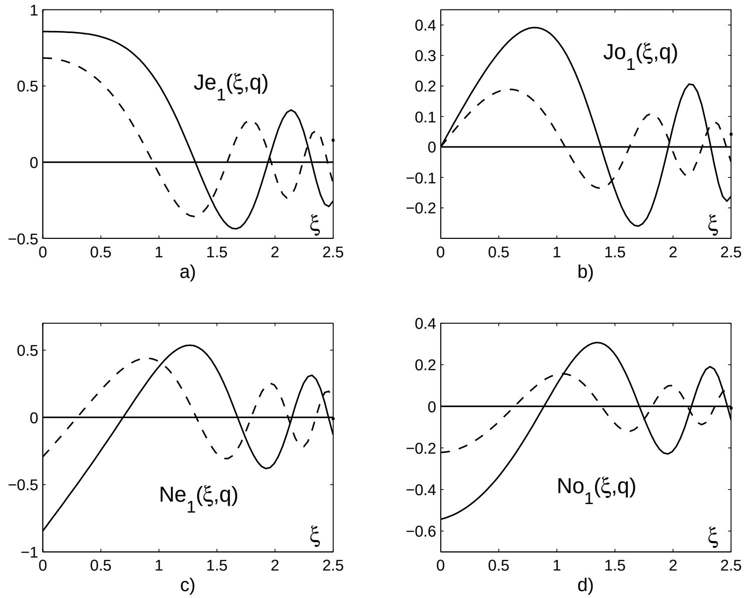


Fig. 4. Plots of radial Mathieu functions with $q=1$ (solid line), $q=2$ (dashed line), and $q=3$ (dotted line).

J. C. Gutiérrez-Vega et al., "Mathieu functions, a visual approach," Am. J. Phys. 71, 233 (2003)

# Mathieu beams: Transverse intensity distribution

$$ {}_{e}U_{m}(\mathbf{r}) = Je_{m}(\xi,q)\, ce_{m}(\eta,q)\, \exp\left(ik_{z}z\right), \quad m = \{0,1,2,3\ldots\}, $$
$$ {}_{o}U_{m}(\mathbf{r}) = Jo_{m}(\xi,q)\, se_{m}(\eta,q)\, \exp\left(ik_{z}z\right), \quad m = \{1,2,3\ldots\}. $$

## Fundamental Mathieu beam

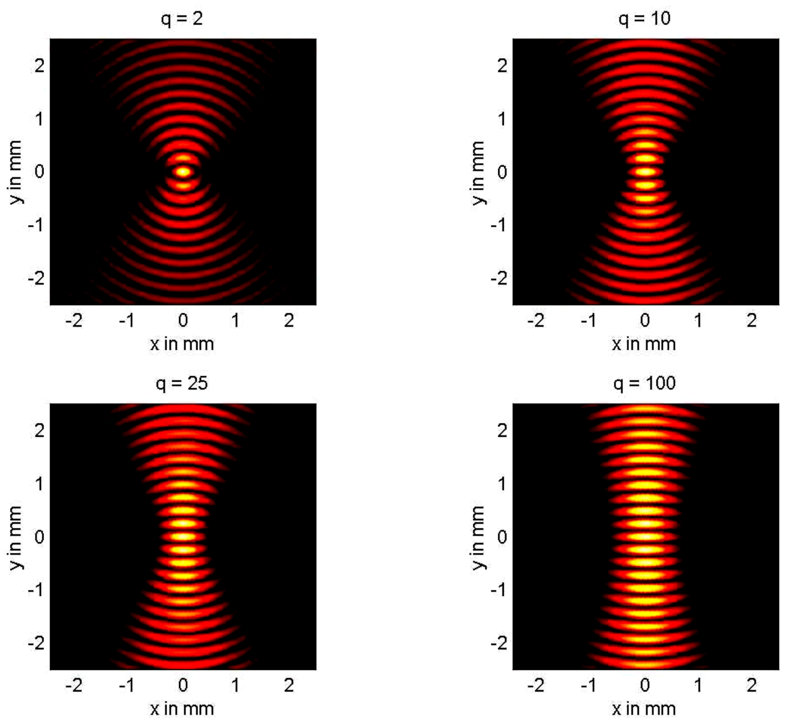


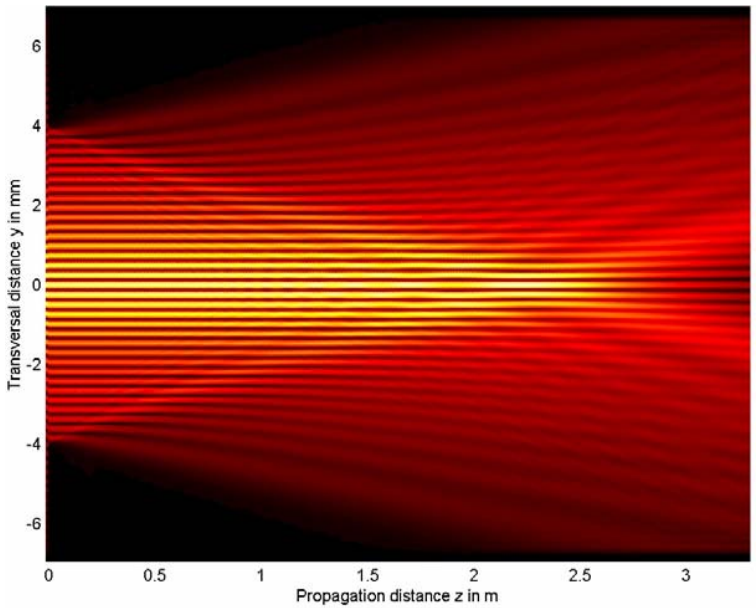


J. C. Gutiérrez-Vega, et al., *Opt. Lett.*, **25**, 1493-1495 (2000)

# Mathieu beams: Angular spectrum

$$\mathrm{Je}_m(\xi,q)\,\mathrm{ce}_m(\eta,q) \propto \int_{-\pi}^{\pi} \mathrm{ce}_m(\phi)\exp\left[ik_t r\cos(\phi-\theta)\right]\,\mathrm{d}\phi$$

$$\mathrm{Jo}_m(\xi,q)\,\mathrm{se}_m(\eta,q) \propto \int_{-\pi}^{\pi} \mathrm{se}_m(\phi)\exp\left[ik_t r\cos(\phi-\theta)\right]\,\mathrm{d}\phi$$

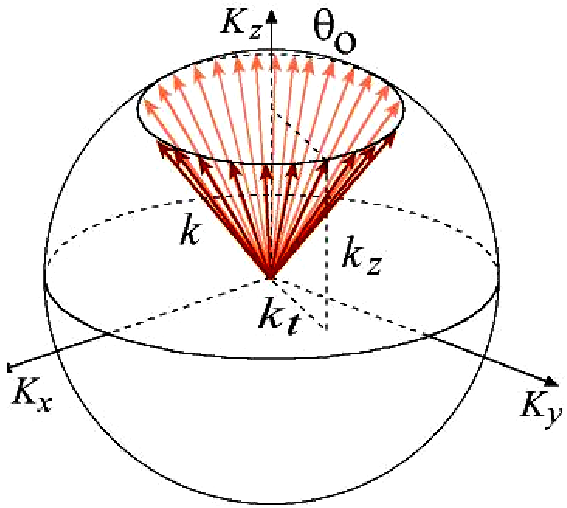


$ce_3(\eta,35)$ $\quad Je_3(\xi,35)\,ce_3(\eta,35)$

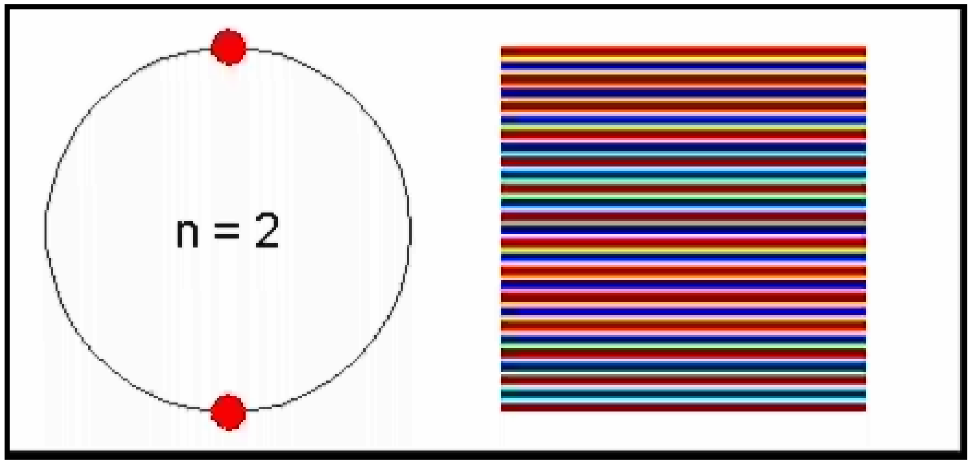


J. C. Gutiérrez-Vega, et al., *Opt. Lett.*, **25**, 1493-1495 (2000)

# *Experimental observation:  Fundamental Mathieu beam*

**Using the classical Durnin's setup**

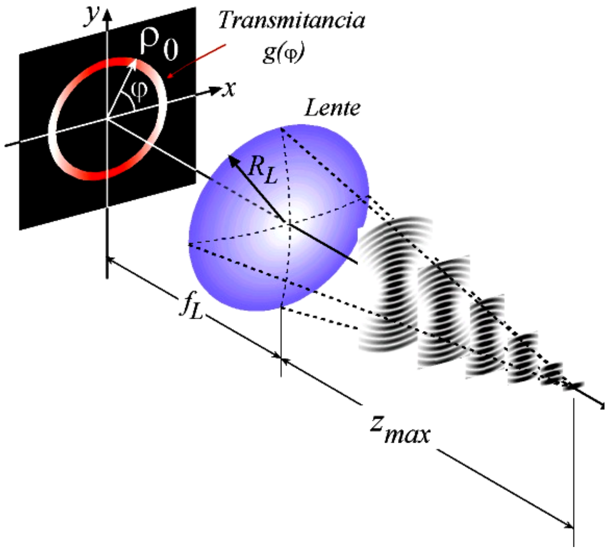


J. C. Gutiérrez-Vega *et al.*,
Opt. Comm., **195**,  35-40, 2001

**Theory**

**Experiment**

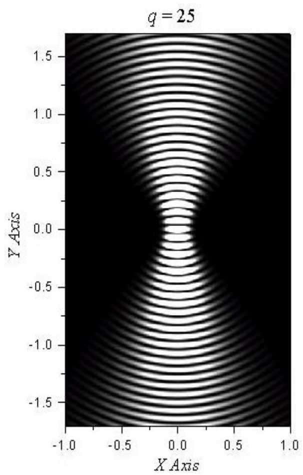


**q = 25**

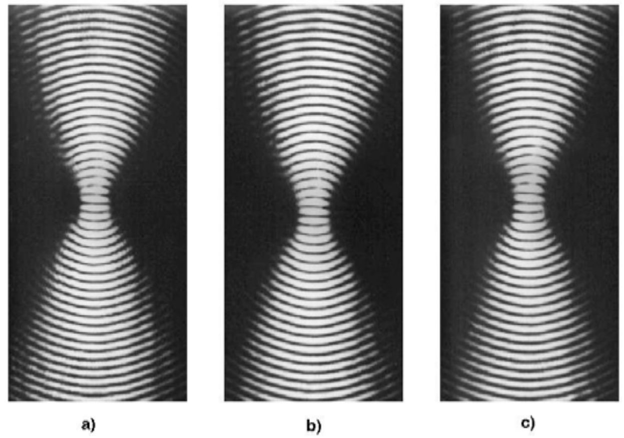


**a) 0 m** **b) 5 m** **c) 10 m**

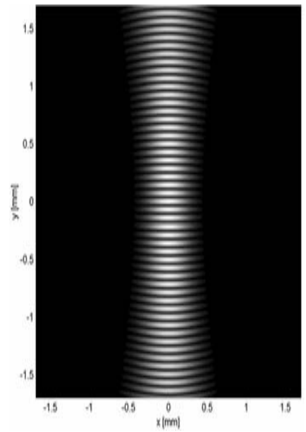

**q = 525**

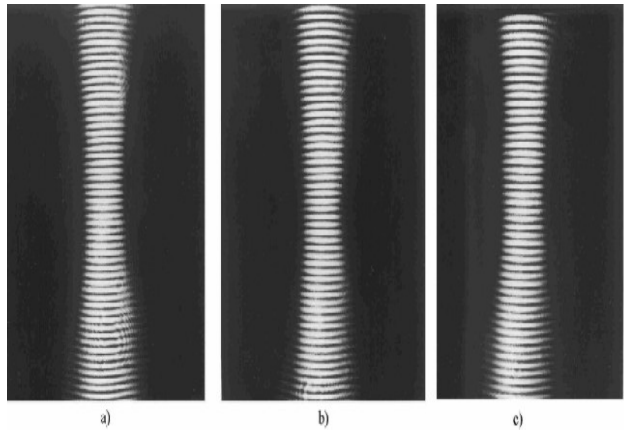

# ***Even*** ***Mathieu beam order 1:*** *$Je_1(\xi)\ ce_1(\eta)$*

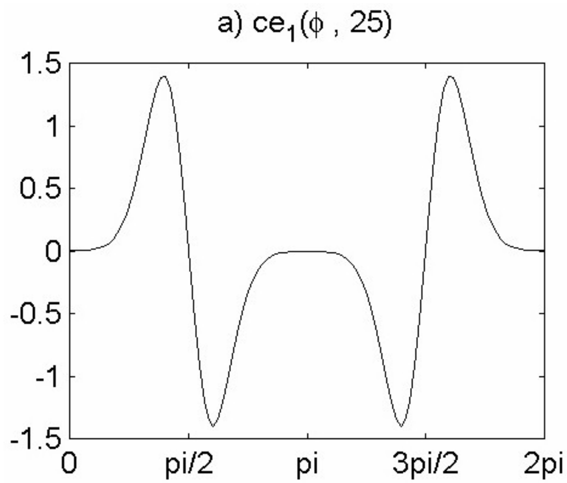


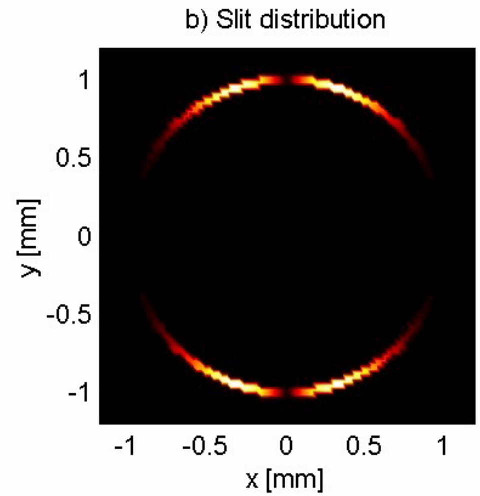


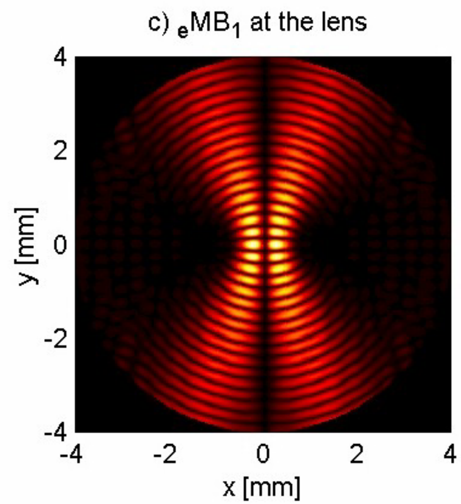


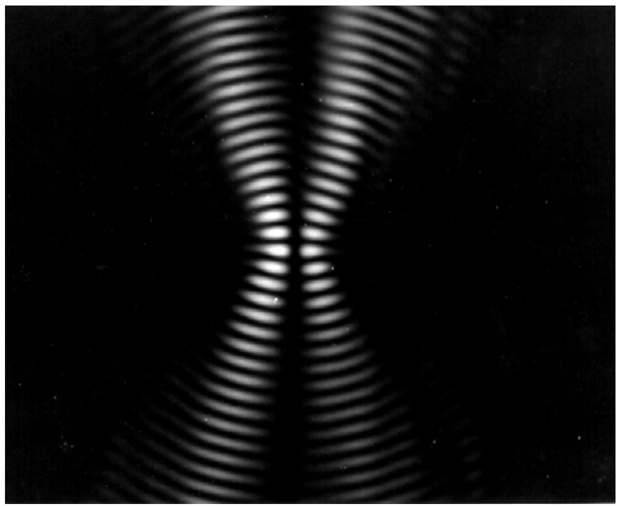

**Theory** **Experiment**

# **Even Mathieu beam order 2:** $Je_2(\xi)\ ce_2(\eta)$

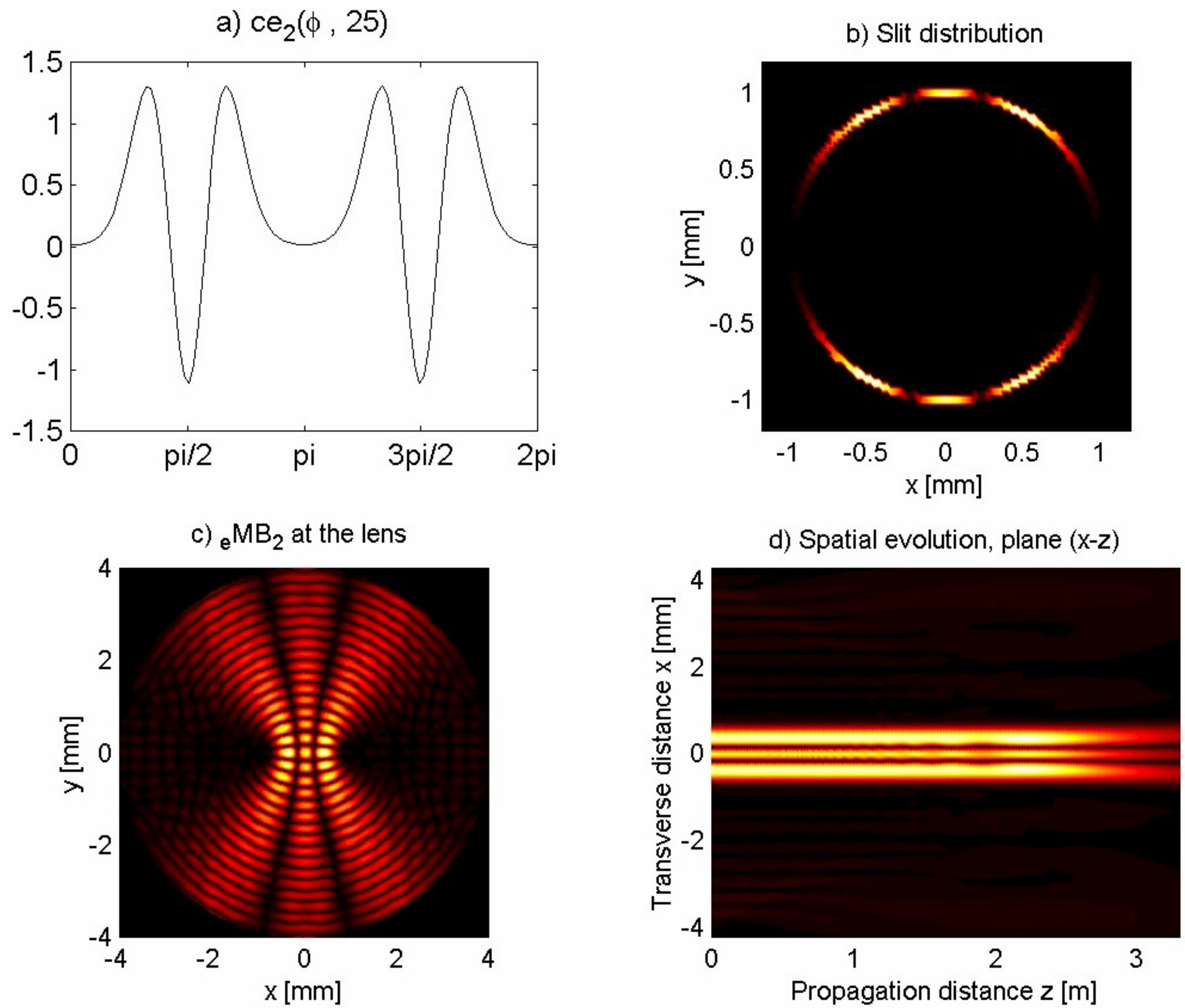

# ***Helical*** $MB_m(\xi,\eta)$ = $Je_m(\xi)\ ce_m(\eta) + \iota\ Jo_m(\xi)\ se_m(\eta)$

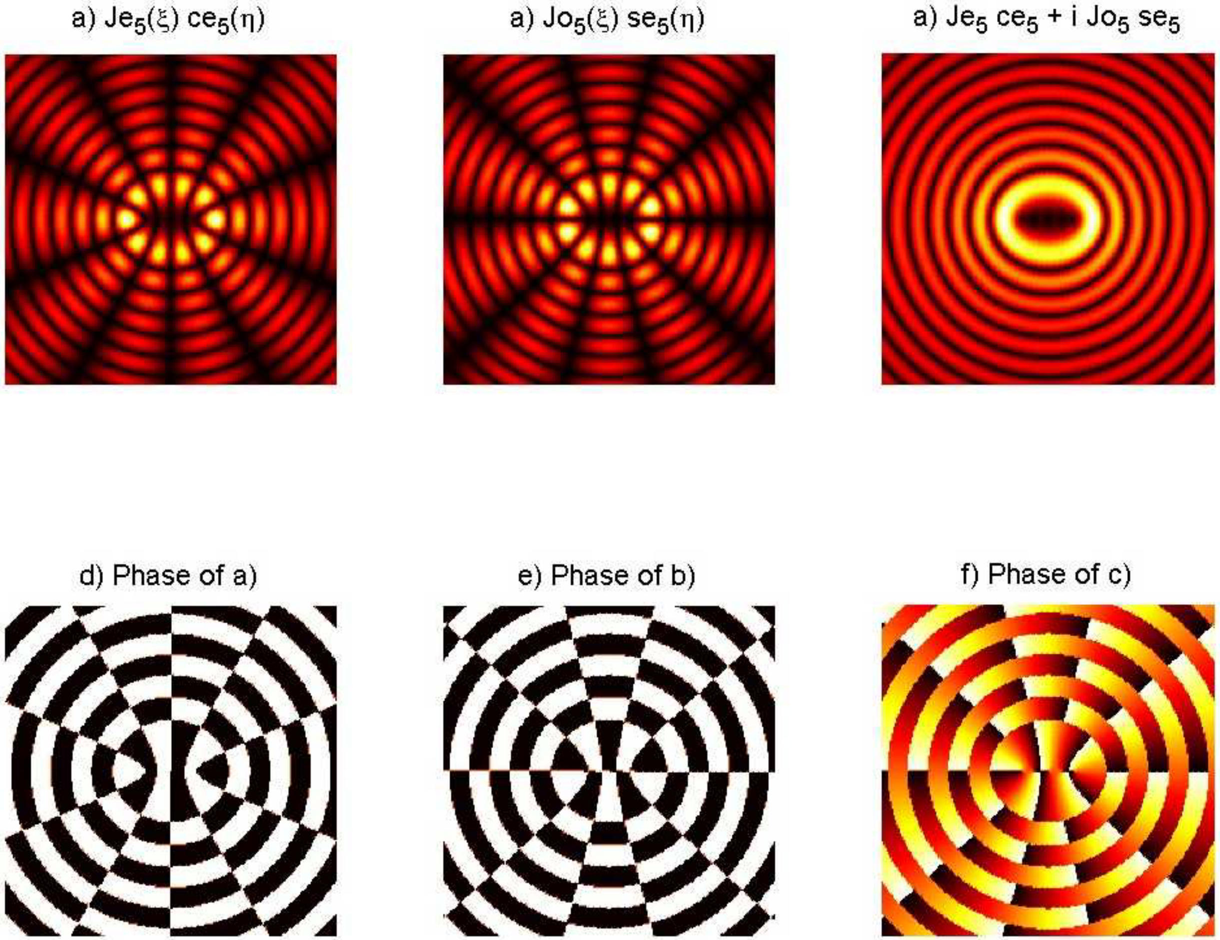

# **Evolution** $MB_m(\xi,\eta)$ = $Je_m(\xi)\, ce_m(\eta) + \iota\, Jo_m(\xi)\, se_m(\eta)$

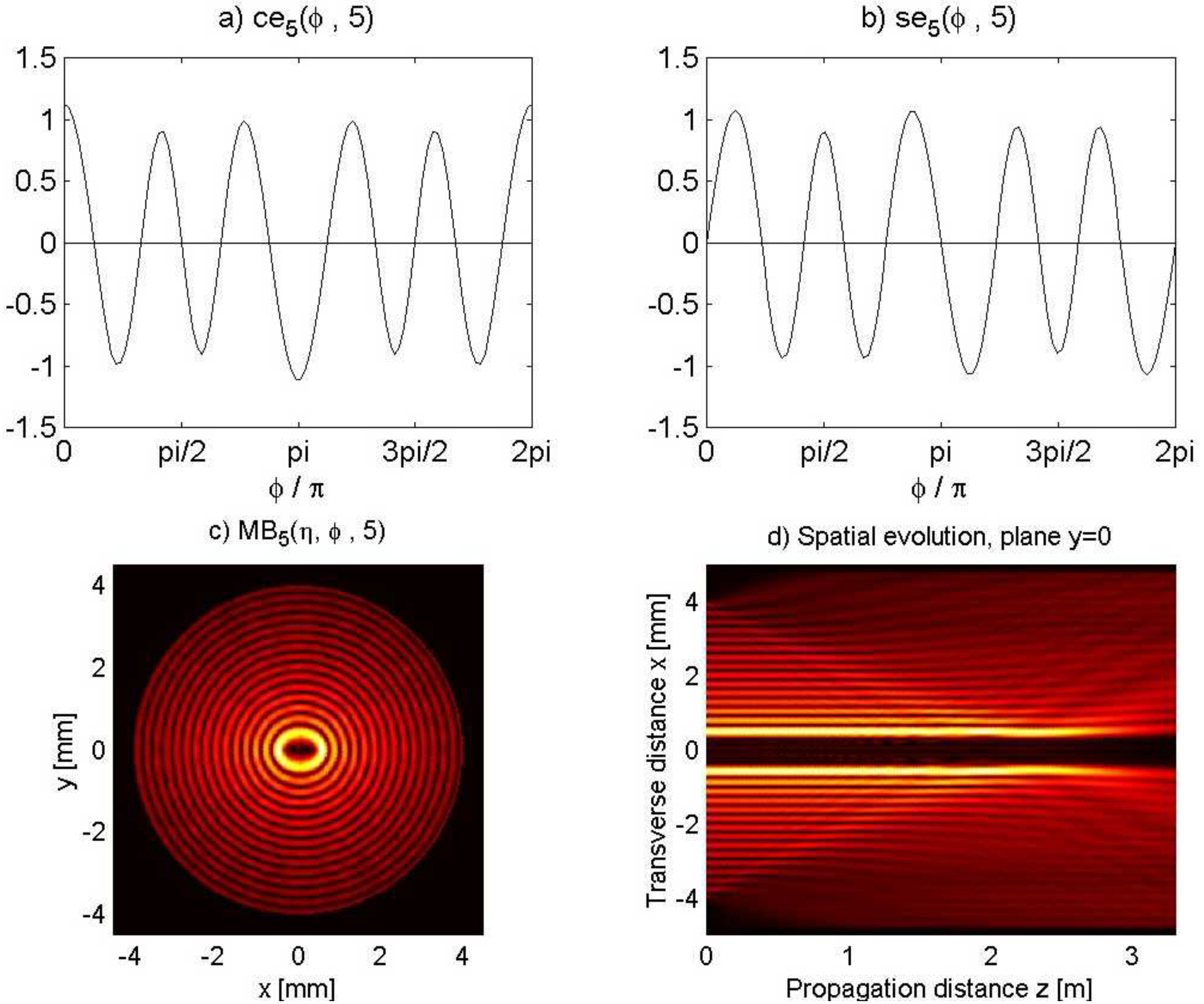

# Effect of changing the ellipticity parameter

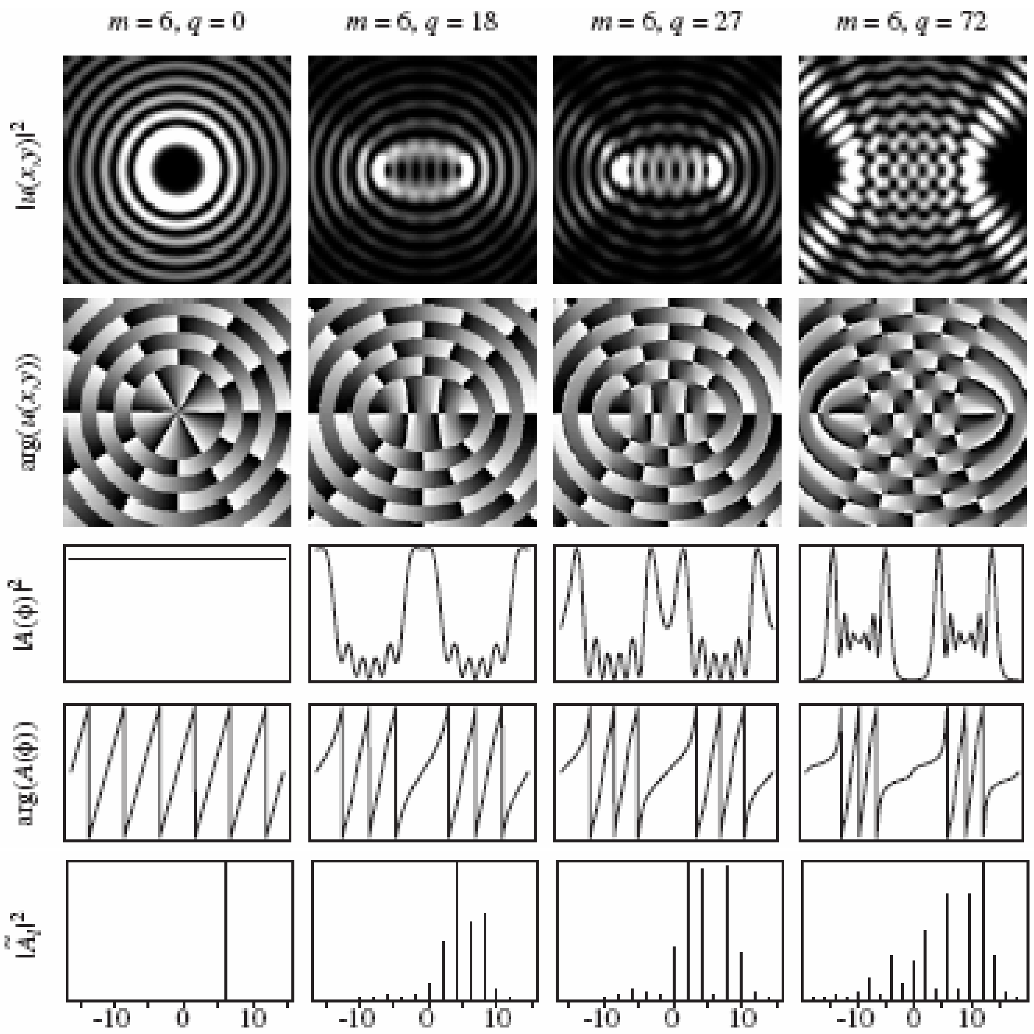


Intensity pattern

Phase pattern

Abs of the angular spectrum

Phase of the angular spectrum

Bessel beam spectra of the corresponding MB

S. Chávez-Cerda, et al, "Holographic generation and orbital angular momentum of high-order momentum", J. Opt. B: Quantum Semiclass. Opt. 4, S52–S57, Apr. 2002

# *Effect of changing the ellipticity parameter*

Helical Mathieu beam: $m = 7$

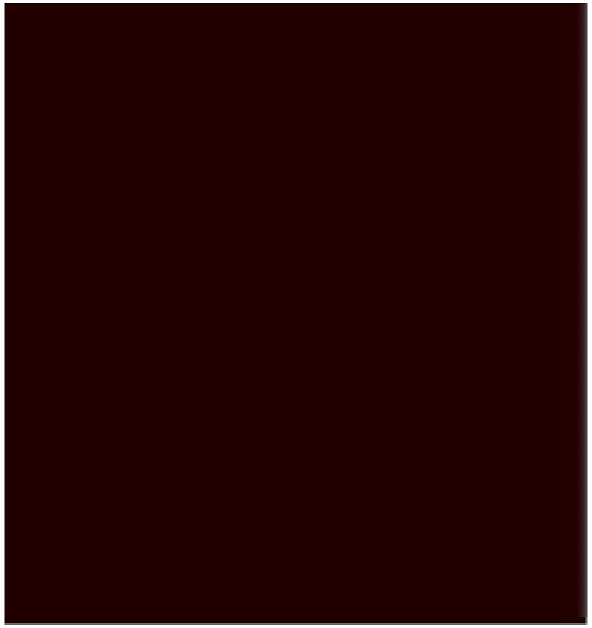

Intensity

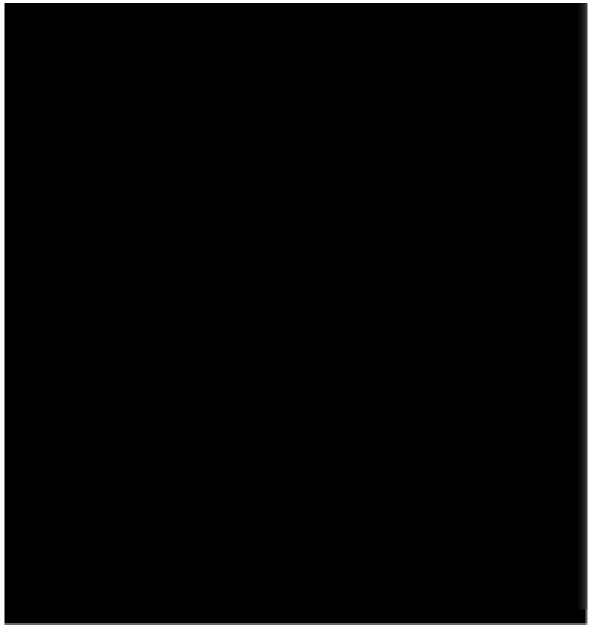

Phase

# Vortices in Mathieu beams are along the interfocal line

Phase structure of an fifth-order MB 5 propagating invariant vortices are aligned along the interfocal line.

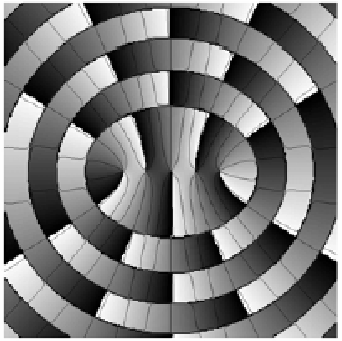

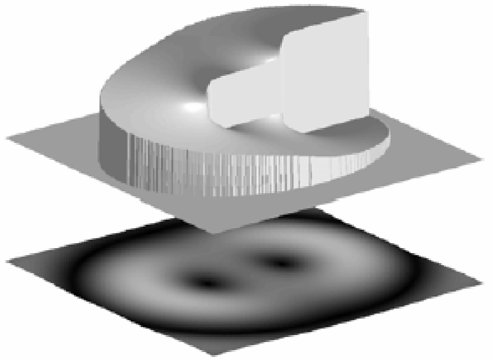

Central phase structure of an 2nd-order MB

Fork-like patterns resulting from the interferogram with a plane wave

***m* =3; *q* = 0**

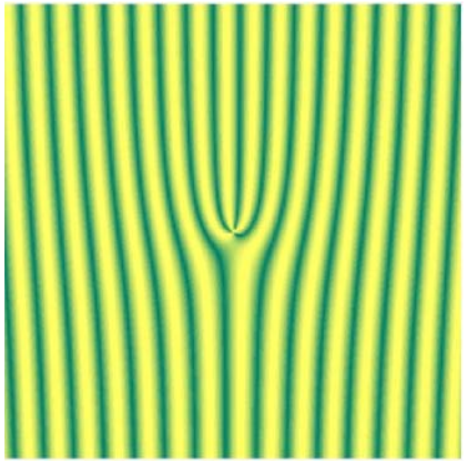

***m* =3; *q* = 3.5**

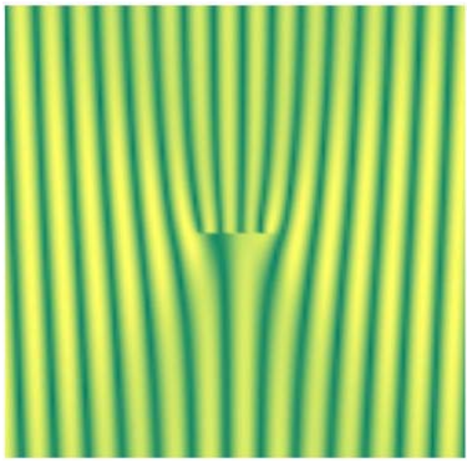

***m* =3; *q* = 10**

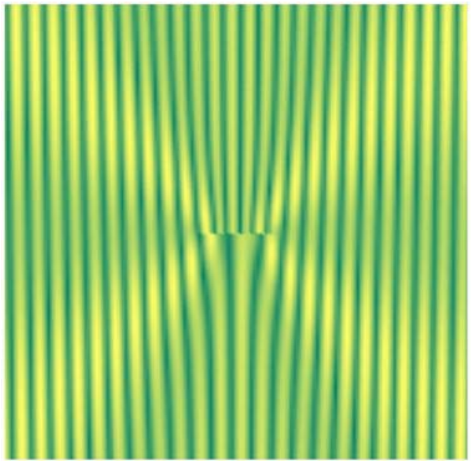

J. C. Gutiérrez-Vega et al., Opt. Lett., 26 (22), 1803-1805, 2001

# Holographic generation of Helical Mathieu beams

Holographic setup

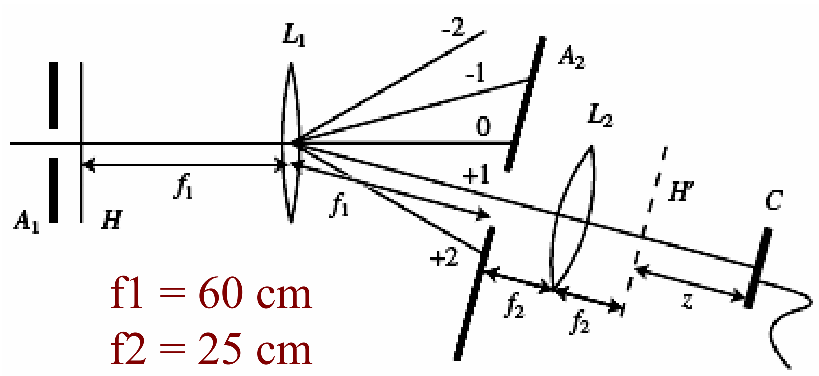


f1 = 60 cm
f2 = 25 cm

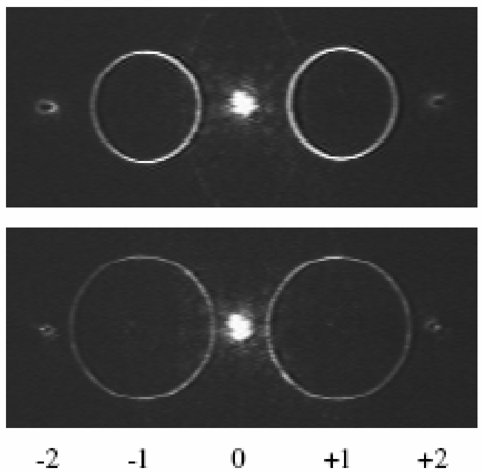


Intensity at focal plane of L1
Diffraction order are identified at bottom

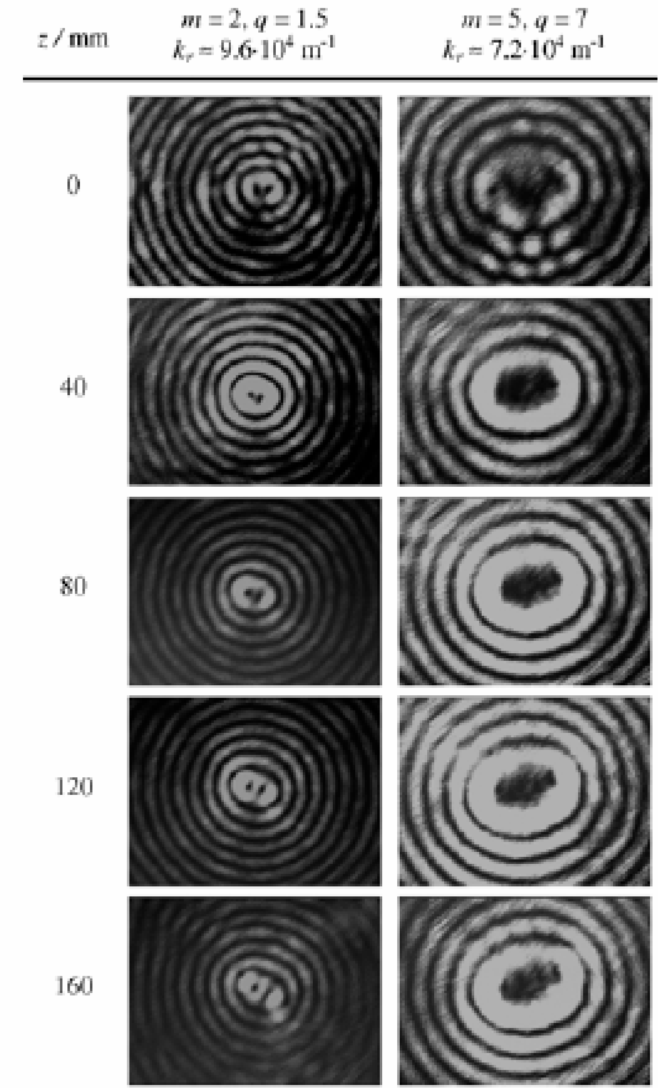


0.4 mm

Chavez-Cerda *et al*, J. Opt. B: **4,** 52, 2002

# Mathieu art: Gallery of nondiffracting patterns

$q = 5$ $q = 25$ $q = 75$ $q = 125$

$m = 0$

$m = 1$

$m = 2$

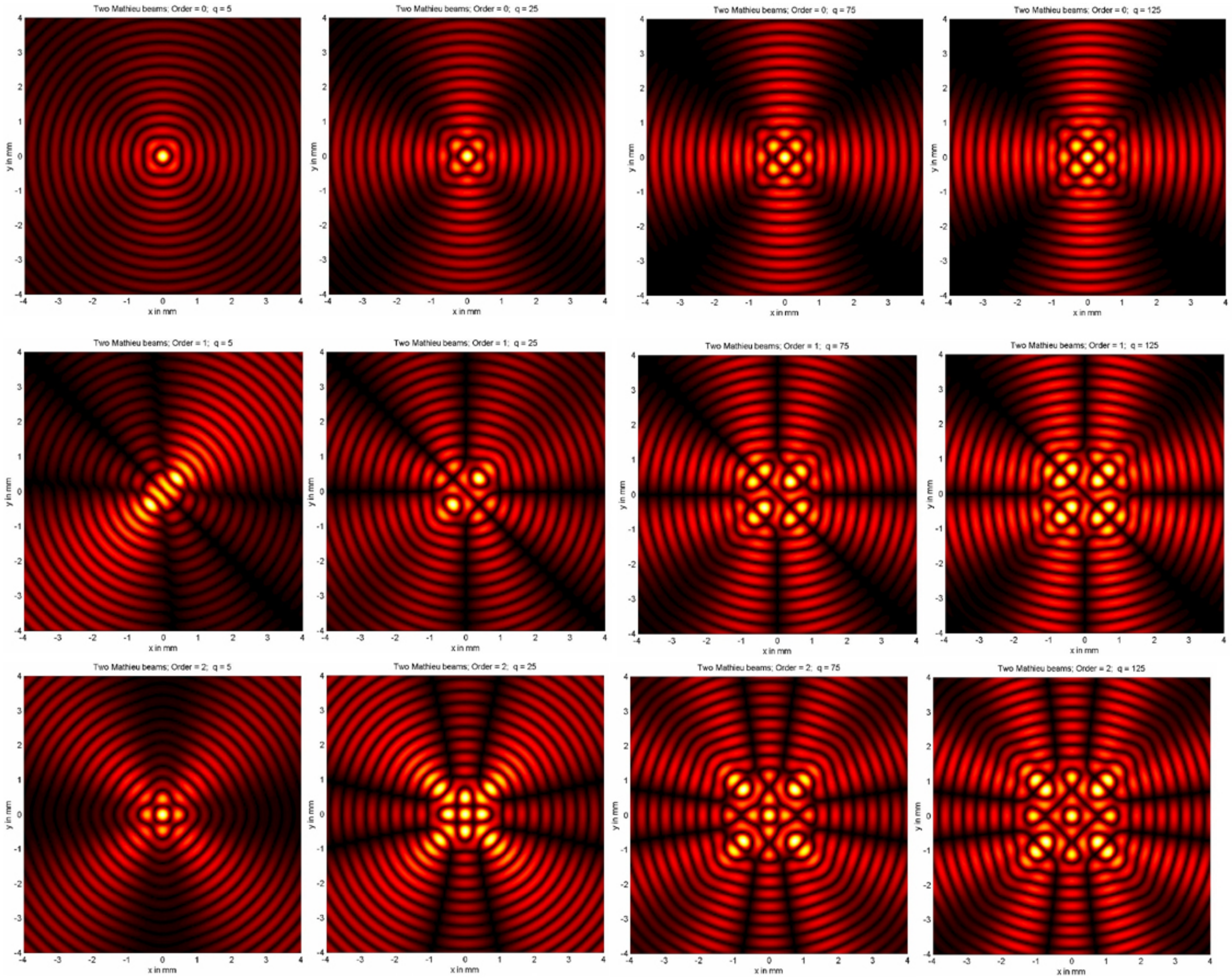

# Self-imaging patterns with Mathieu beams (Talbot effect)

In general, two collinear IOFs with different longitudinal propagation constant interfere to produce self-images separated by a distance:

$$L_B = \frac{2\pi}{\left|k_{z,2} - k_{z,1}\right|}$$

Interferring two fundamental Mathieu beams

Evolution along the plane ($y$-$z$)

$$k_{t1} = 2k_{t2}$$

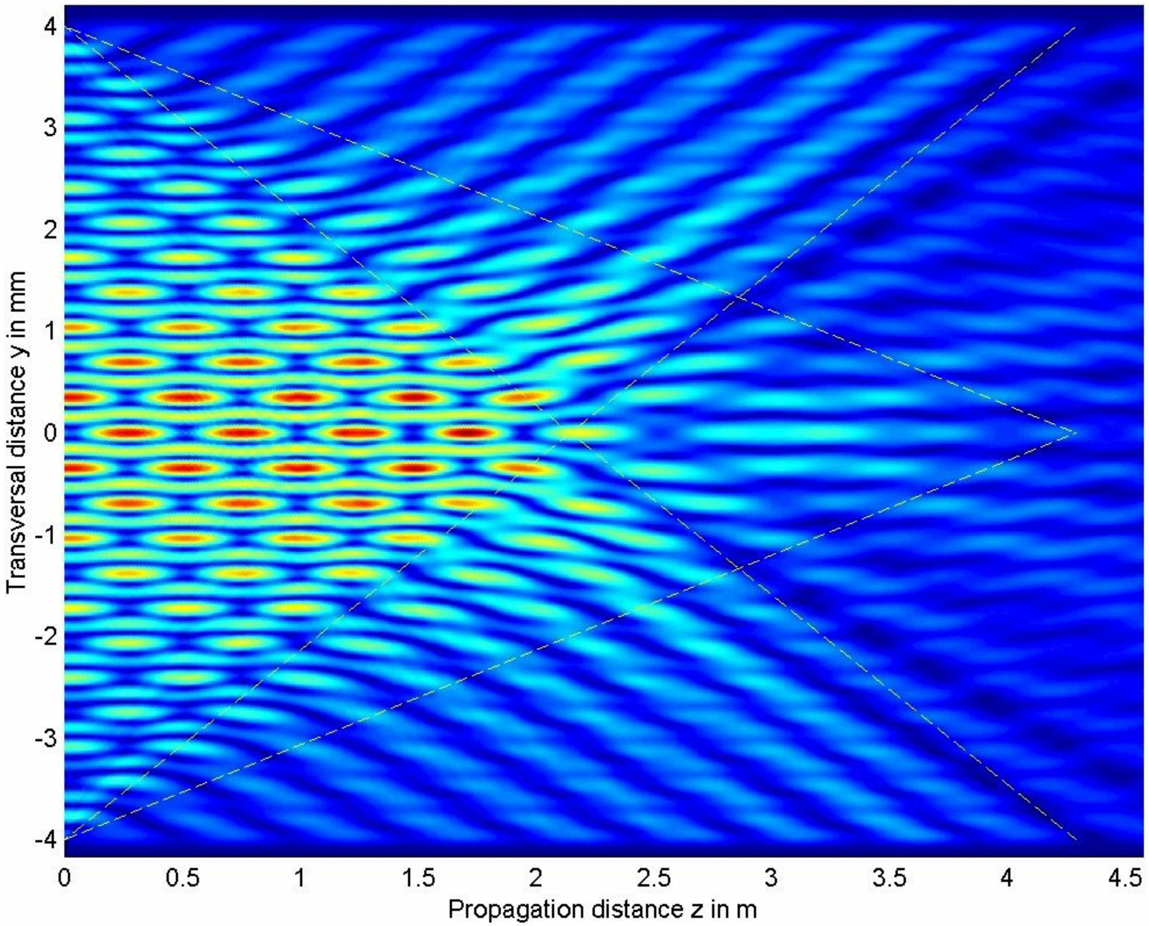

# Evolution of a focused Mathieu beam: (y,z) plane

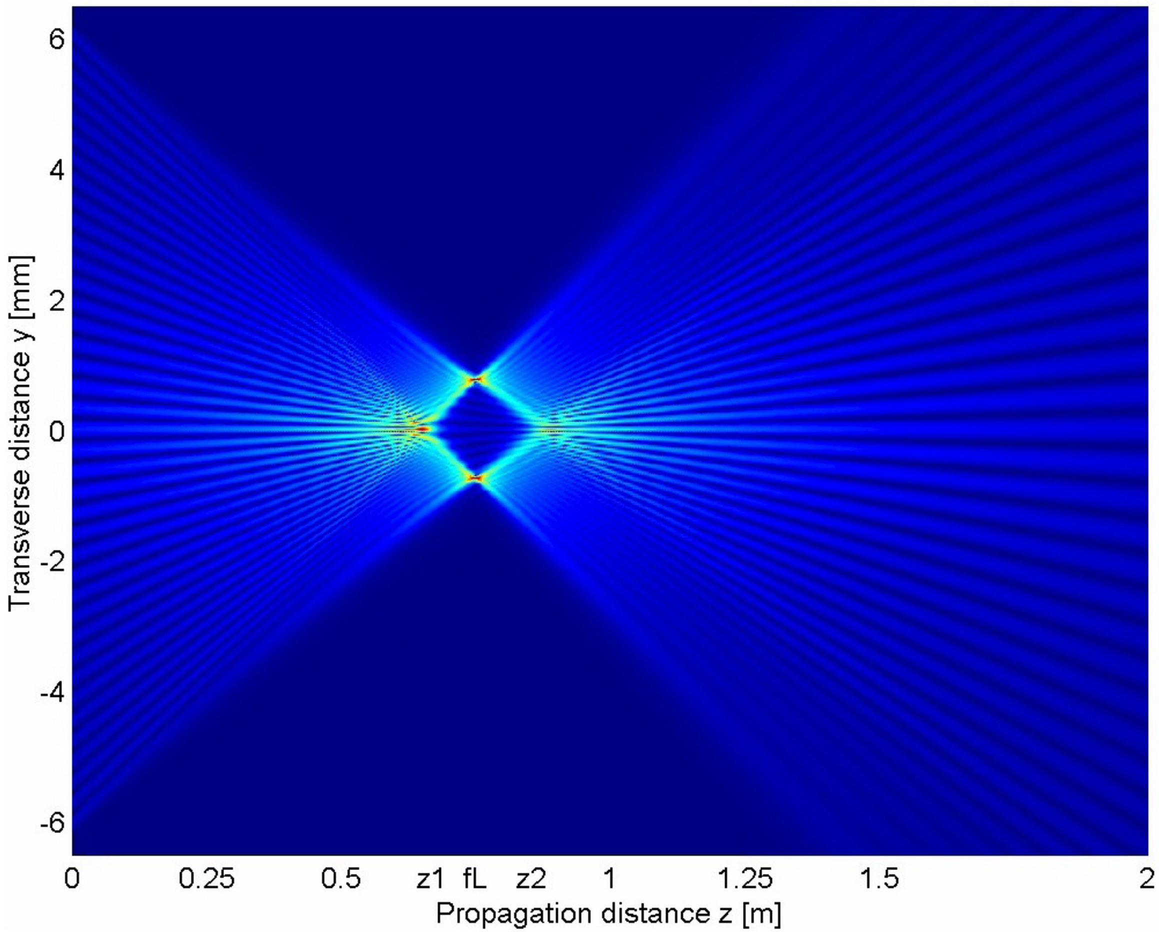

# *Evolution of elliptical rotating waves produced by superposing Mathieu beams and spherical waves*

$$U(\mathbf{r}) = [Je_m(\xi;q)ce_m(\varphi,q) + iJo_m(\xi;q)se_m(\varphi,q)]\exp(ik_z z) + \frac{C}{\sqrt{\rho^2+z^2}}\exp\left(ik\sqrt{\rho^2+z^2}\right)$$

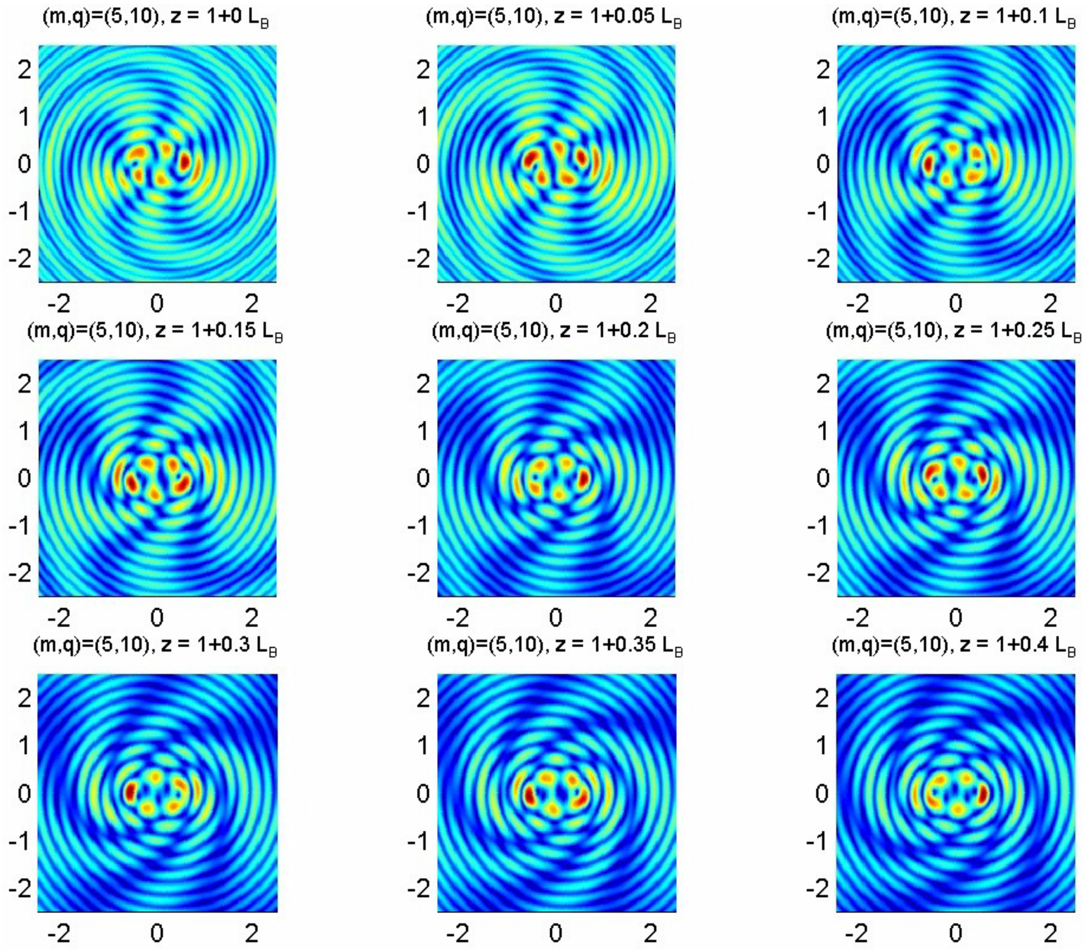

# Mathieu beams in an axicon resonator

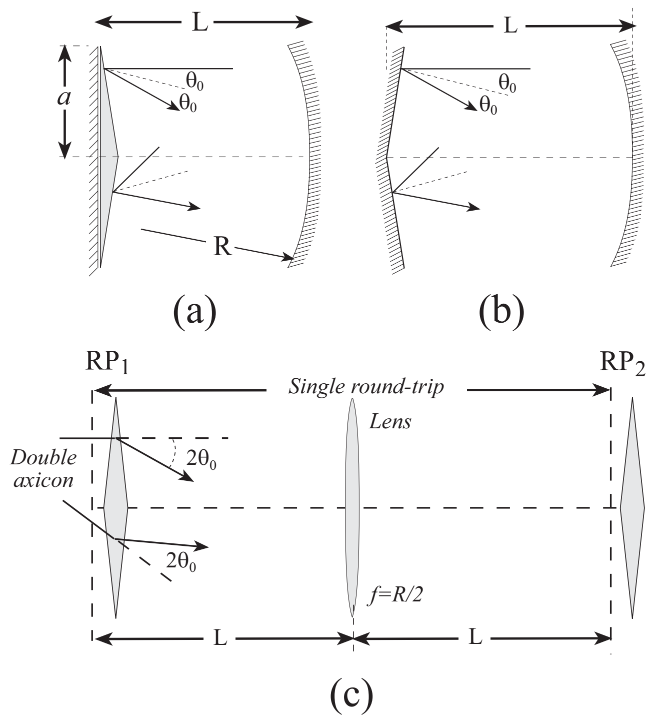


## Disaligned cavity

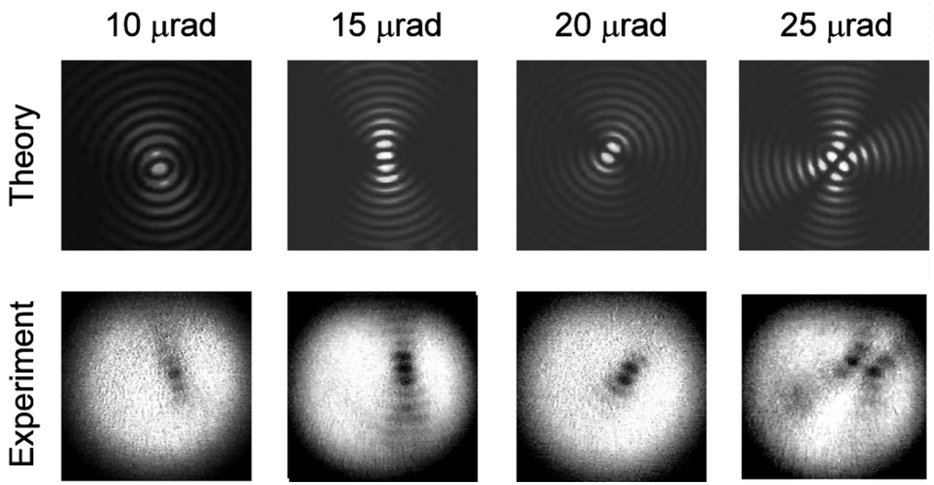


## and at the focal plane

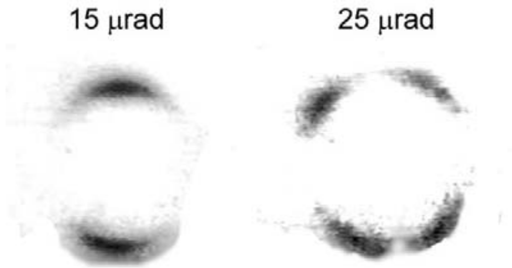


M. Alvarez, et al, "Construction and characterization of $CO_2$ laser with an axicon based Bessel-Gauss resonator," SPIE Vol. 5708-19, 323-331 (2005)

# *Bessel beams as Hankel waves*

$$U(\mathbf{r},t) = \underbrace{J_m(k_t r) \pm i N_m(k_t r)}_{H_m^{(1),(2)}(k_t r)} \exp(im\theta)\exp(ik_z z - i\omega t)$$

Hankel function

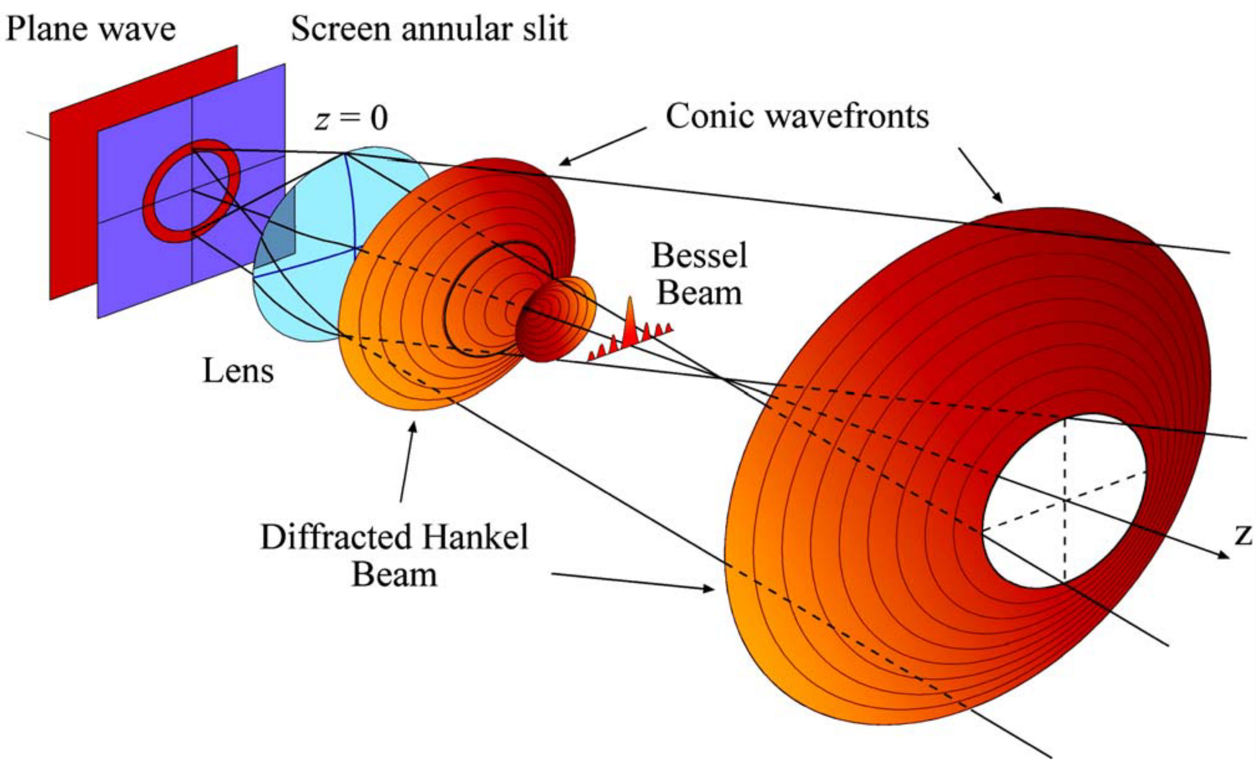



[1] S. Chávez-Cerda et al., "Nondiffracting Beams: travelling, standing, rotating and spiral waves", Opt. Commun **123**, 225 (1996).
[2] S. Chávez-Cerda, "A New Approach to Bessel Beams", J. Mod Opt. **46**, 923-930 (1999).
[3] J. C. Gutiérrez-Vega, "Formal analysis of the propagation of invariant optical fields with elliptical symmetry," Ph.D. Thesis (2001)

# *Mathieu beams as Mathieu-Hankel waves*

$$U_m^e = [Je_m(\xi;q) \pm iNe_m(\xi;q)]\; ce_m(\eta;q)\exp[i(k_z z - \omega t)]$$

$$U_m^o = \underbrace{[Jo_m(\xi;q) \pm iNo_m(\xi;q)]}_{MH_m^{(1),(2)}(\xi,q)} se_m(\eta;q)\exp[i(k_z z - \omega t)]$$

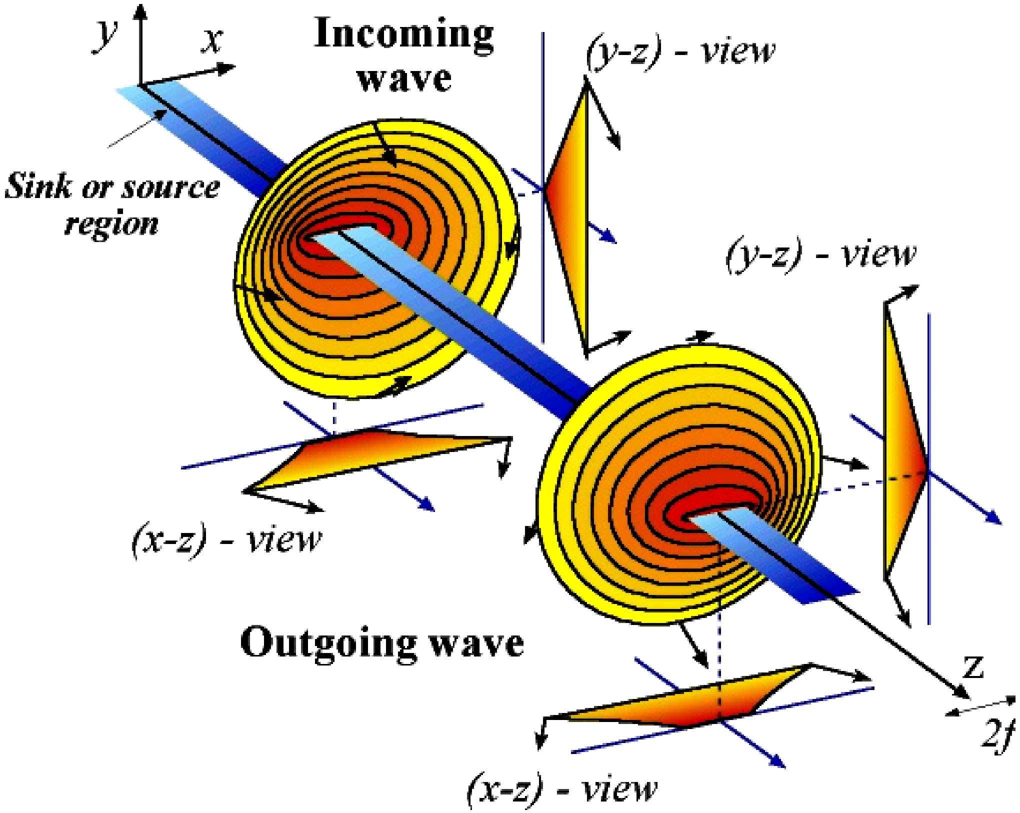


[1] J. C. Gutiérrez-Vega, "Formal analysis of the propagation of invariant optical fields with elliptical symmetry," Ph.D. Thesis (2001)

## *An application of Mathieu beams in optical manipulation*

**In the LAMP seminars**

**Observation of**
**Orbital Angular Momentum Transfer to Particles**
**Trapped in a Mathieu Beam**
**by Carlos López-Mariscal**

**Today at 14:30**

# Mathieu modes: Analogy with mechanics

1) Probability distributions in elliptic quantum billiards
2) Vibrating modes in elliptic membranes

$$
\begin{aligned}
{}_eU_m(\mathbf{r}) &= Je_m(\xi,q)\,ce_m(\eta,q), \quad m=\{0,1,2,3\ldots\},\\
{}_oU_m(\mathbf{r}) &= Jo_m(\xi,q)\,se_m(\eta,q), \quad m=\{1,2,3\ldots\}.
\end{aligned}
$$

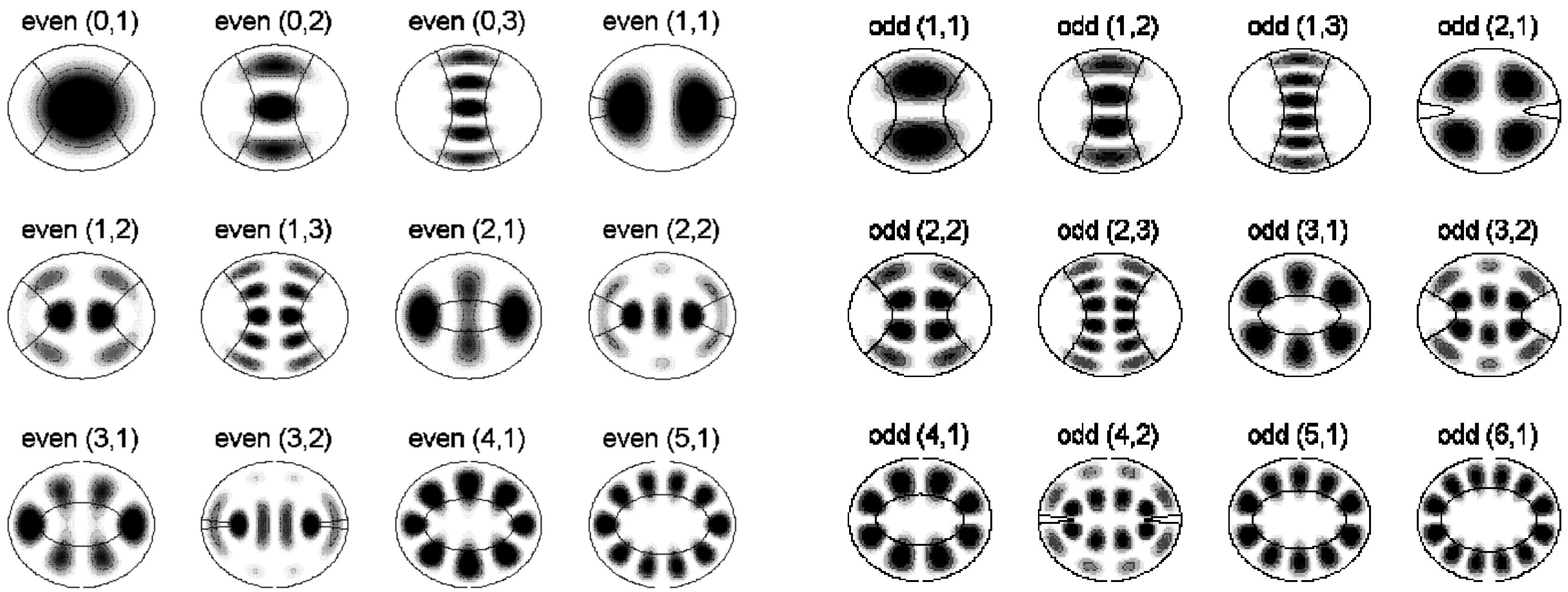


J. C. Gutiérrez-Vega, *et al.*, Am. J. Phys. 71 (3), 233-242, Mar. 2003
J. C. Gutiérrez-Vega, *et al.*, *Rev. Mex. Fis.*, **47** (5), 480-488, Oct. 2001

## *Summary of key points of the Mathieu beams*

1. MBs are characterized by an "ellipticity" parameter $q$ and the order $m$.
2. MBs are transition beams between BBs $(q = 0)$ and finite width cosine beams ($q$ tends to infinite).
3. The transverse intensity shape of MBs is composed by confocal ellipses.
4. MBs have a continuous gradient of phase around the interfocal line.
5. Contrary to HOBBs, the even and odd MBs are structurally different.
6. The angular spectrum is given directly by the Angular Mathieu functions.
7. The $m$ in-line vortices of a $m$-th order BB split into $m$ vortices of a $m$-th order MB along the interfocal line.
8. It is possible to construct rotating waves with elliptical trajectories.
9. Similar to BBs, MBs form a complete and orthogonal set of Invariant Optical Fields, such that any IOF can be reconstructed by linearly superposing MBs.

# Parabolic beams

# Parabolic beams: Parabolic coordinates

$$x = \frac{1}{2}\left(\eta^2 - \xi^2\right)$$
$$y = \xi\eta$$
$$z = z$$

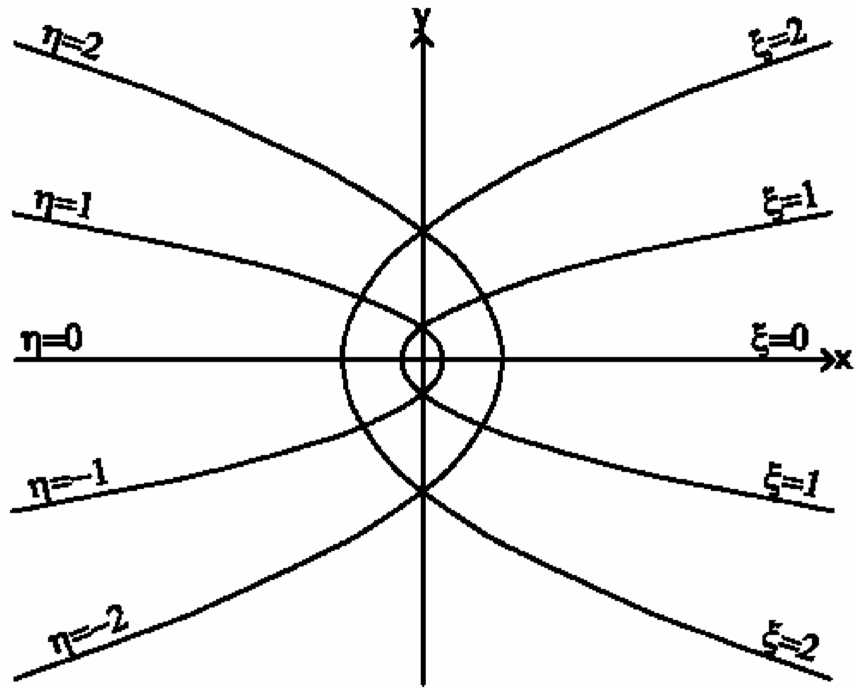


$$\eta^2 = \sqrt{x^2 + y^2} + x, \qquad \xi^2 = \sqrt{x^2 + y^2} - x,$$
$$\eta = \sqrt{2r}\cos(\frac{\theta}{2}), \qquad \xi = \sqrt{2r}\sin(\frac{\theta}{2}),$$

## Parabolic beams: Separation of the Helmholtz equation

Taking $U(\mathbf{r}) = R(\xi)\Theta(\eta)Z(z),$

Helmholtz equation in parabolic coordinates separates into

$$\begin{aligned} R''(\xi) + (k_t^2\xi^2 - 2k_t a)R(\xi) &= 0, \\ \Phi''(\eta) + (k_t^2\eta^2 + 2k_t a)\Phi(\eta) &= 0, \\ Z''(z) + k_z^2 Z(z) &= 0. \end{aligned}$$

$$2k_t a = sep.\ cons$$

$$k^2 = k_t^2 + k_z^2$$

By the simple change of variables $\xi\sqrt{2k_t} \to v,$

above equations become the canonical form of the Parabolic cylinder equation

$$P''(v) + \left(v^2/4 - a\right)P(v) = 0$$

PFs can be expressed in terms of a Taylor expansion about $v = 0$.

$$P(v,a) = \sum_{n=0}^{\infty} c_n \frac{v^n}{n!}, \quad where \quad c_{n+2} = ac_n - \frac{n(n-1)c_{n-2}}{4}$$

Miguel A. Bandres et al "Parabolic nondiffracting optical wavefields," Opt. Lett., **29**, 44 (2004)

# Parabolic cylinder functions

$$Even\ solution: Pe(v,a)$$

$$c_0 = 1, \quad c_1 = 0$$

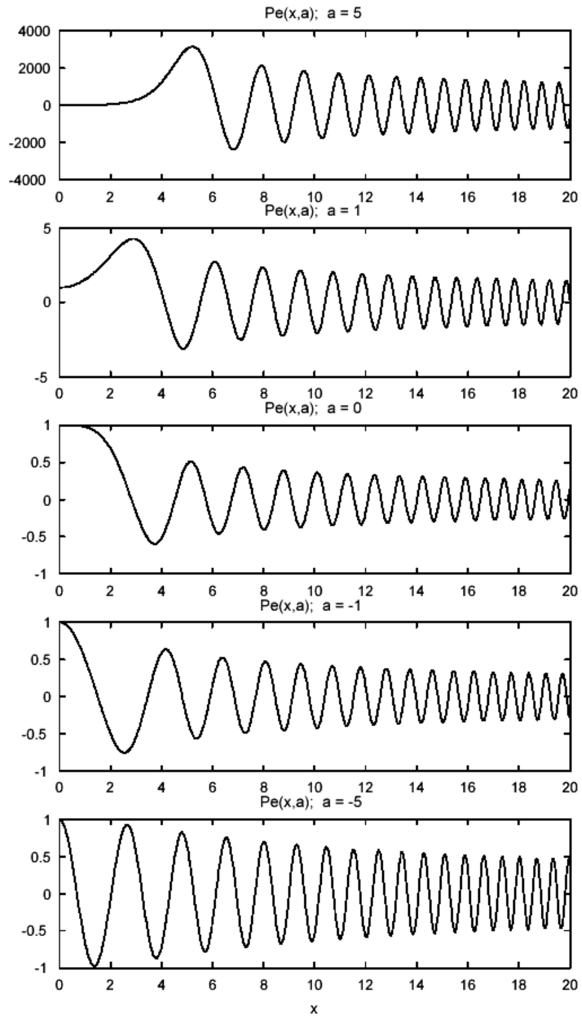


+

$a$

-

$$Odd\ solution: Po(v,a)$$

$$c_0 = 0, \quad c_1 = 1$$

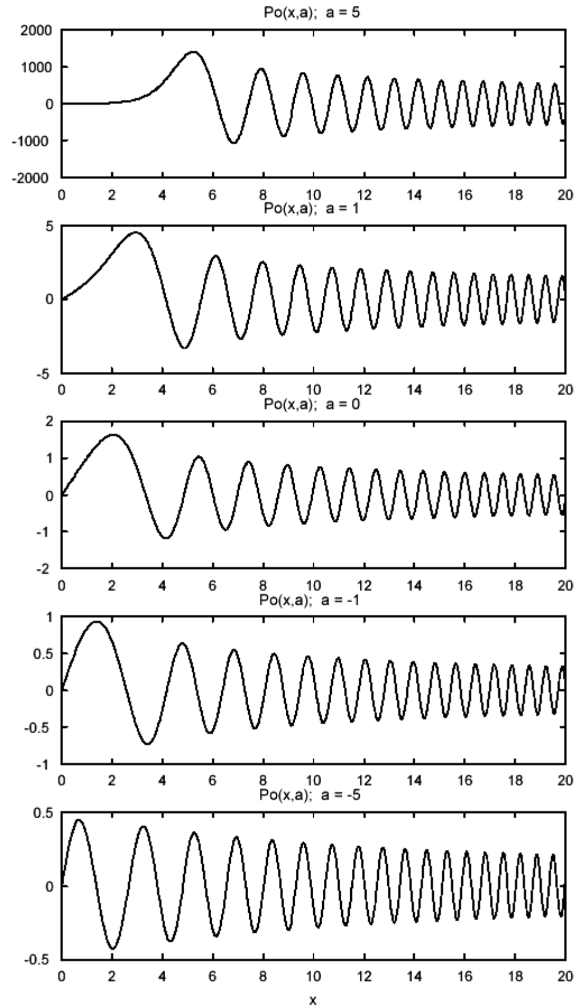

# Parabolic beams:  Angular spectrum

$$Ue(\xi,\eta,a) = C_a Pe(\xi,a) Pe(\eta,-a) \exp(ik_z z),$$
$$Uo(\xi,\eta,a) = C_a Po(\xi,a) Po(\eta,-a) \exp(ik_z z).$$

$$U(\mathbf{r}) = \exp(ik_z z) \int_0^{2\pi} A(\Phi) \exp[ik_t (x\cos\Phi + y\sin\Phi)] d\Phi,$$

$$Ae(\varphi,a) = \frac{1}{2\sqrt{\pi|\sin\varphi|}} \exp\left( ia\ln\left|\tan\frac{\varphi}{2}\right|\right),$$

$$Ao(\varphi,a) = \frac{1}{i}\begin{cases} -Ae, & \varphi\in(-\pi,0) \\ Ae, & \varphi\in(0,\pi) \end{cases}$$

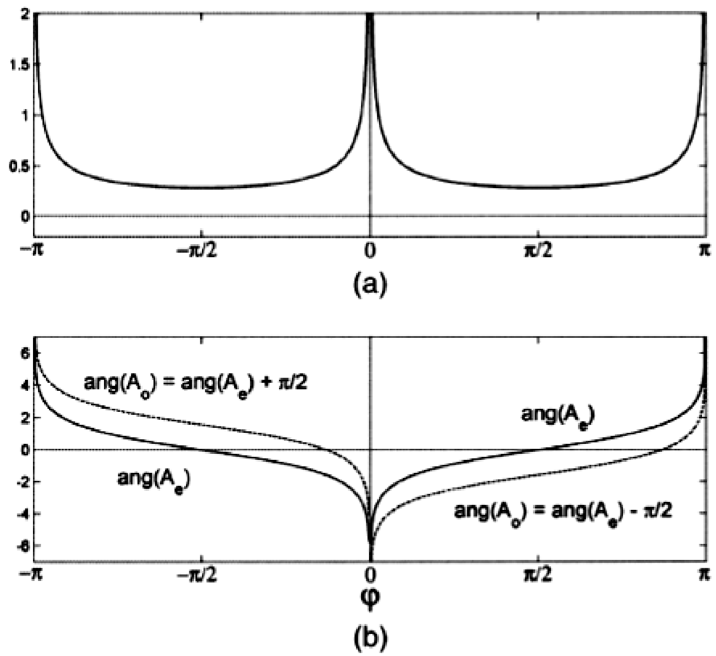


Miguel A. Bandres et al "Parabolic nondiffracting optical wavefields," Opt. Lett., **29**, 44 (2004)

# *Parabolic beams: Transverse intensity distributions*

$$Ue(\xi,\eta,a) = C_a Pe(\xi,a) Pe(\eta,-a) \exp(ik_z z),$$
$$Uo(\xi,\eta,a) = C_a Po(\xi,a) Po(\eta,-a) \exp(ik_z z).$$

**Theory:**

***a* = 0**

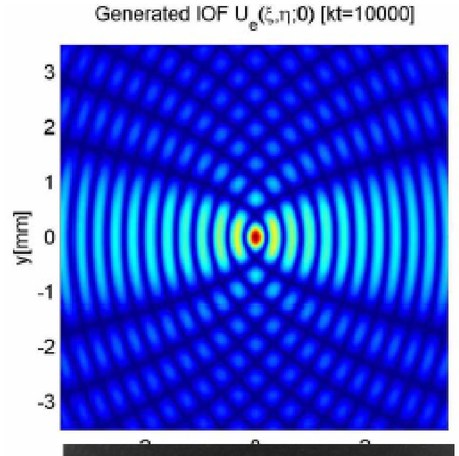


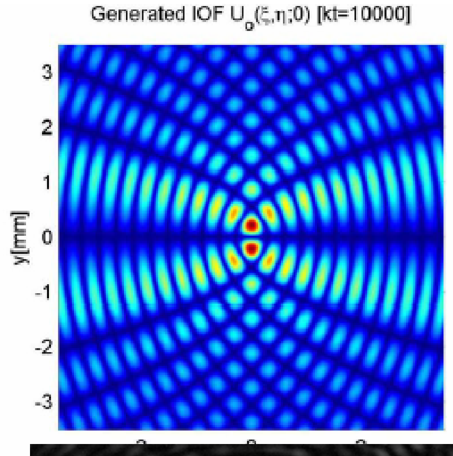


**Experimental observatiom using the Durnin's setup**

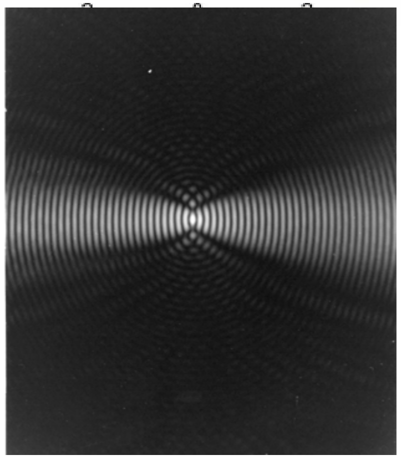

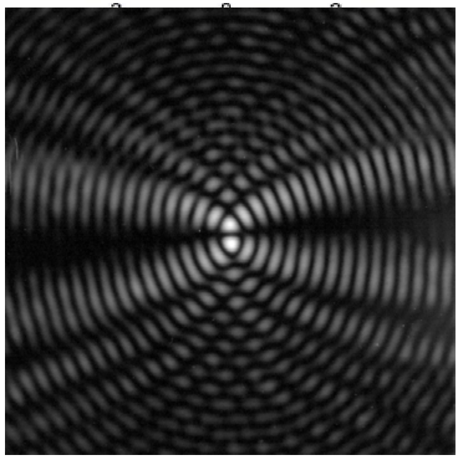

C. López-Mariscal, "Observation of Parabolic nondiffracting wave fields," Opt. Express, **13**, 2364 (2005)

# *Parabolic beams: Transverse intensity distributions*

$$Ue(\xi,\eta,a) = C_a Pe(\xi,a) Pe(\eta,-a) \exp(ik_z z),$$
$$Uo(\xi,\eta,a) = C_a Po(\xi,a) Po(\eta,-a) \exp(ik_z z).$$

*a = 1*

*a = -3*

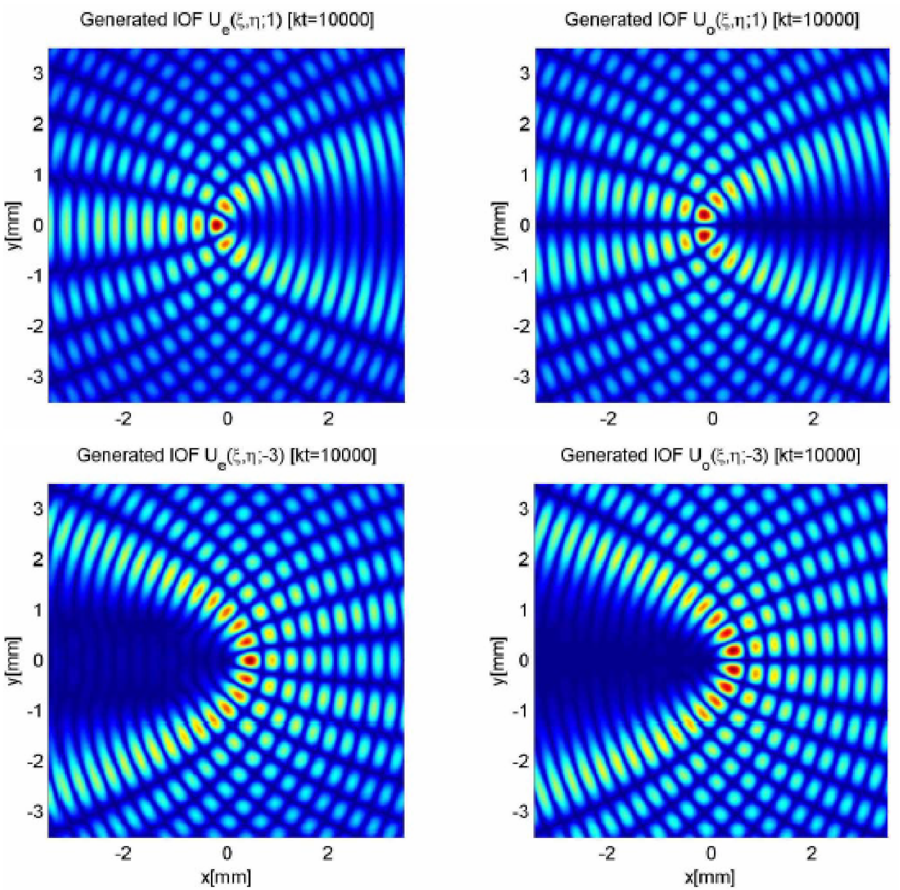


**Effect of changing *a*:**

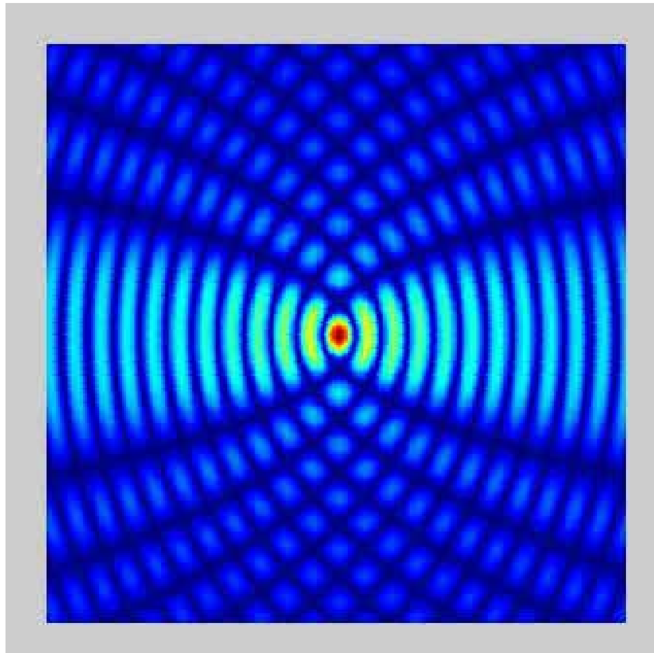

Parameter $a$ is a measure of the concavity of parabolae

## *Parabolic beams: Transverse intensity distributions*

$$Ue(\xi,\eta,a) = C_a Pe(\xi,a) Pe(\eta,-a) \exp(ik_z z),$$
$$Uo(\xi,\eta,a) = C_a Po(\xi,a) Po(\eta,-a) \exp(ik_z z).$$

- Even

*a = 4*

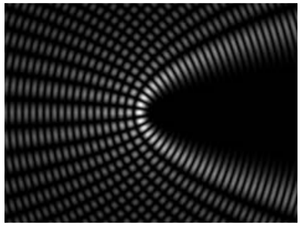

- Odd

*a = 4*

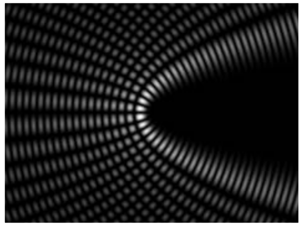

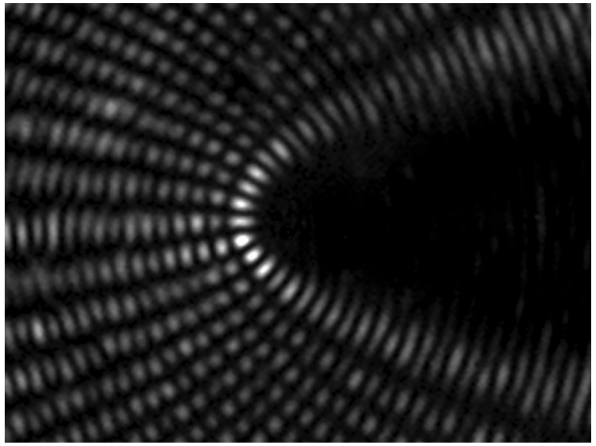

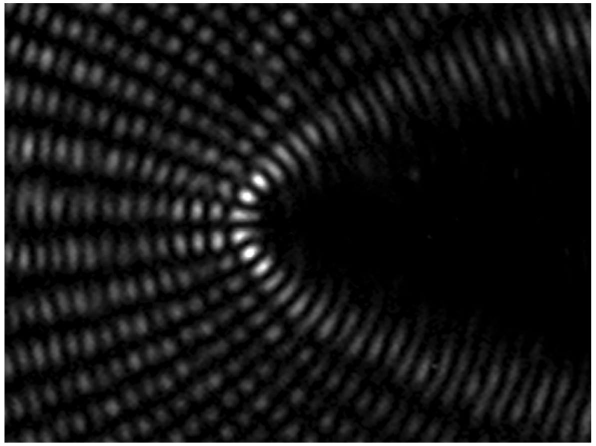

3 mm

C. López-Mariscal, "Observation of Parabolic nondiffracting wave fields," Opt. Express, **13**, 2364 (2005)

# *Parabolic beams: Travelling solutions*

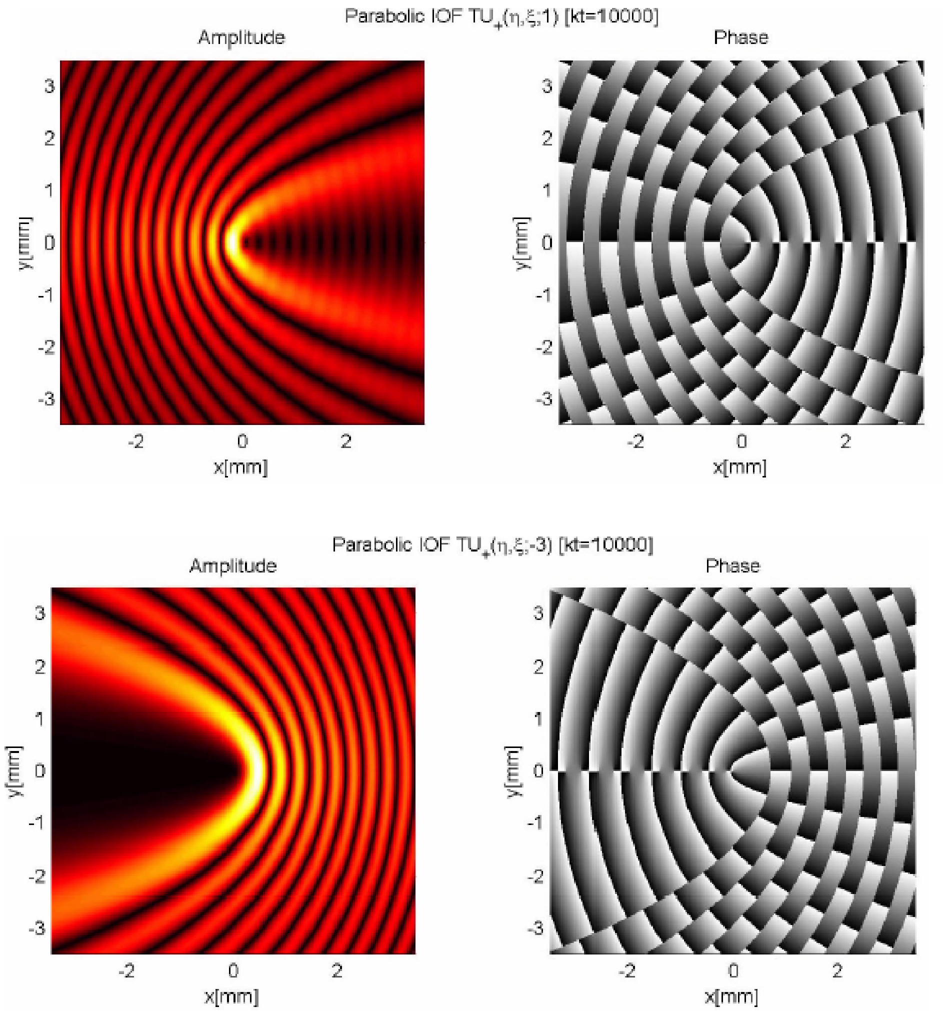


$$TU^{\pm}(\xi,\eta,a)=Ue\pm iUo$$

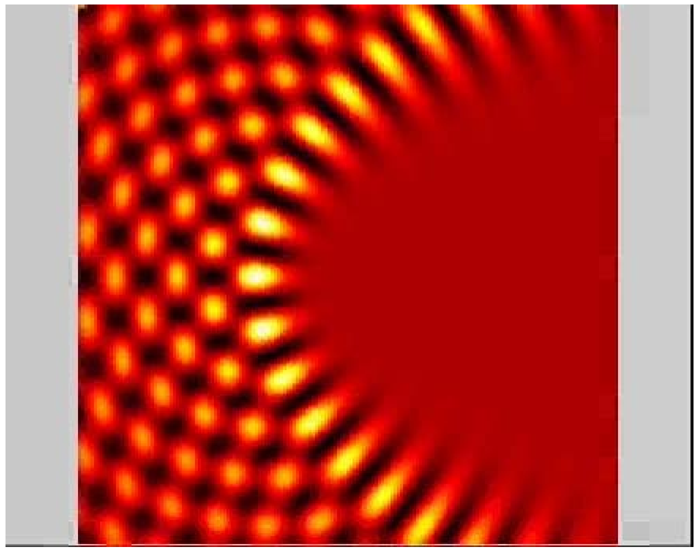

**Real part of TU**

# *Vortices along the positive (or negative) x-axis:*

Fork-like patterns resulting from the interferogram with a plane wave

$a = 1$

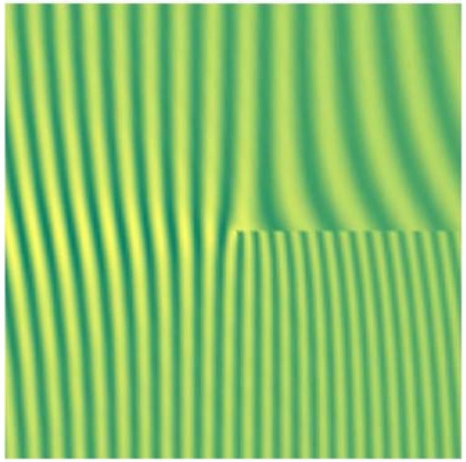

$a = 2$

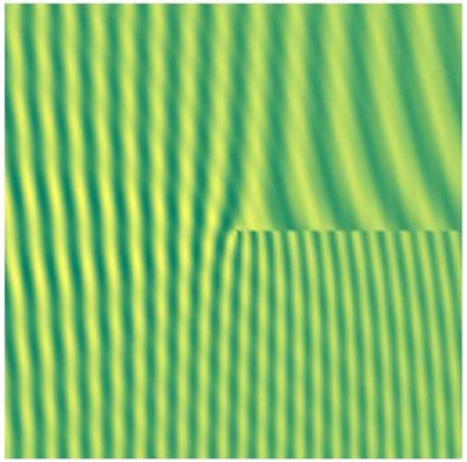

$a = 3$

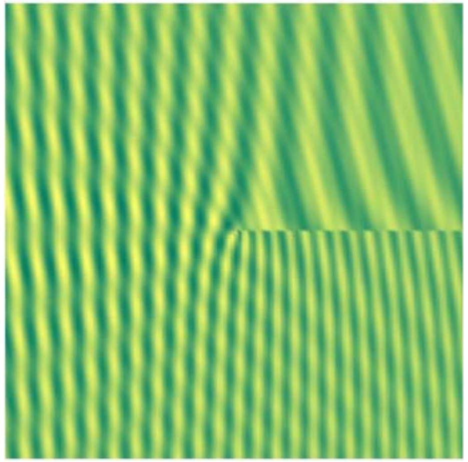

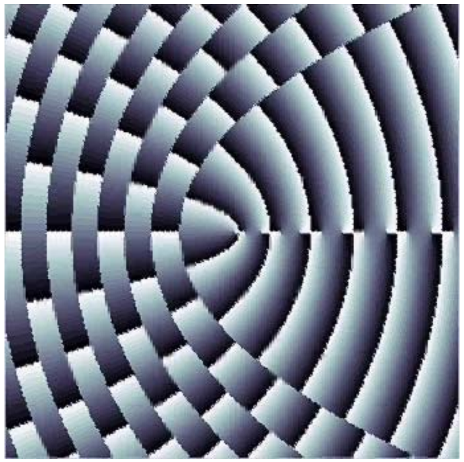

**Phase evolution under propagation of a traveling PB**

## *Experimental evidence: phase structure*

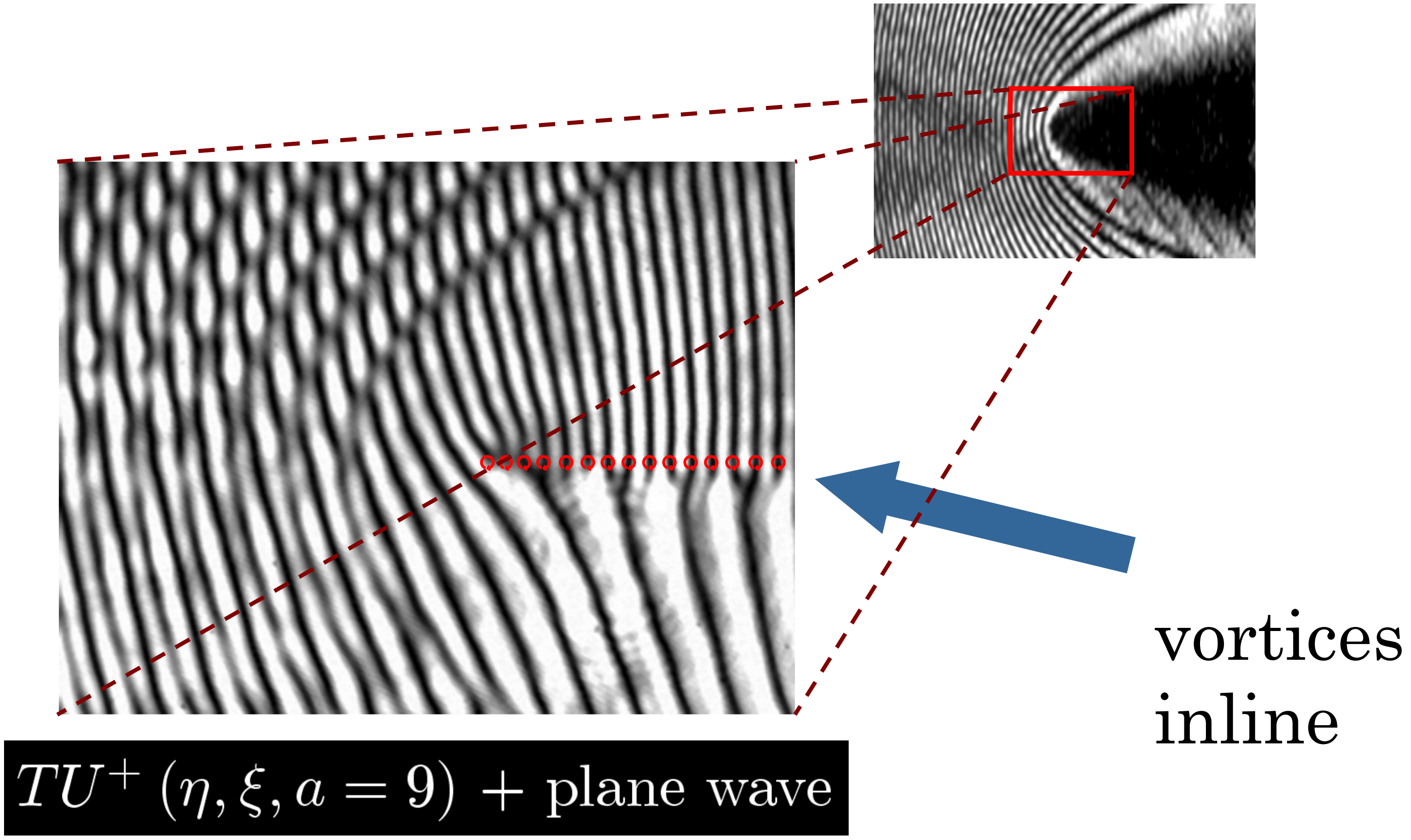


C. López-Mariscal, "Observation of Parabolic nondiffracting wave fields," Opt. Express, **13**, 2364 (2005)

# *Energy flux in apertured Parabolic beams*

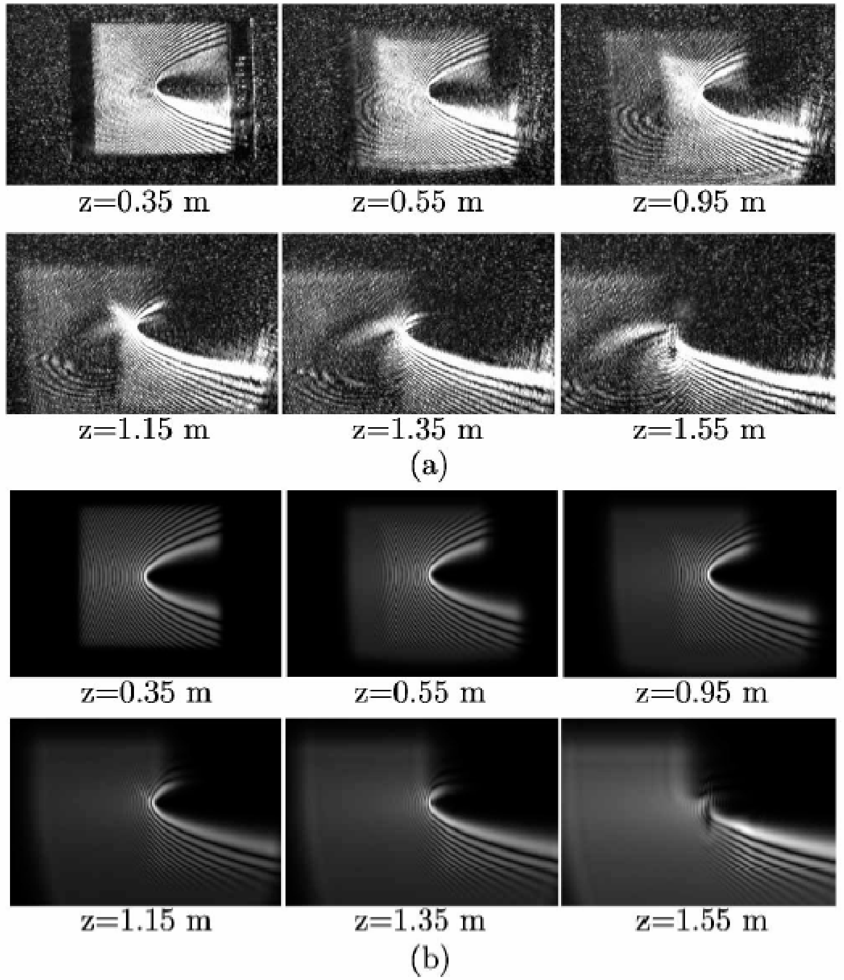


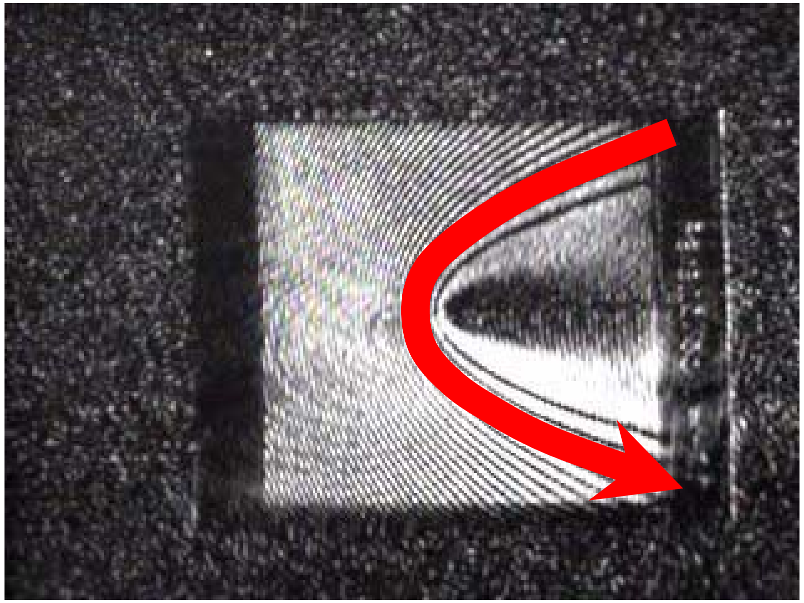

Fig. 3. a) Photographic sequence of the propagation of a bounded traveling PB $TU^{-}(\eta,\xi;a=4)$. (b) Computer simulated propagation.

C. López-Mariscal, "Observation of Parabolic nondiffracting wave fields," Opt. Express, **13**, 2364 (2005)

## *Summary of key points of the Parabolic beams*

1. PBs are characterized by a "parabolicity" parameter $a$.
2. PBs have a continuous order $a$.
3. The transverse intensity shape of PBs is composed by confocal parabolae.
4. PBs have a continuous gradient of phase around the positive (or negative) $x$-axis.
5. The angular spectrum is given directly by a general algebraic expresion.
6. PBs exhibit an infinite number of vortices along the positive (or negative) $x$-axis.
7. It is possible to construct travelling waves with parabolic trajectories.
8. Similar to BBs and MBs,  PBs form a complete and orthogonal set of Invariant Optical Fields, such that any IOF can be reconstructed by linearly superposing PBs.

# Papers related to Mathieu and Parabolic beams

[1] J. C. Gutiérrez-Vega, M.D.Iturbe-Castillo, and S.Chávez-Cerda, "Alternative formulation for invariant optical fields: Mathieu beams," Opt. Lett., 25 (20), 1493-1495, Oct. 15, 2000

[2] J. C. Gutiérrez-Vega, M. D. Iturbe-Castillo, E. Tepichin, and S. Chávez-Cerda, "New Member in the Family of Propagation Invariant Optical Fields: Mathieu beams," Opt. and Phot. News, 11 (12), 35-36, Dec. 2000

[3] J. C. Gutiérrez-Vega, M. D. Iturbe-Castillo, G. A. Ramírez, S. Chávez-Cerda, and G.H.C. New, "Experimental demonstration of optical Mathieu beams," Opt. Comm., 195 (1-4), 35-40, 1 Aug. 2001

[4] J. C. Gutiérrez-Vega, S. Chávez-Cerda y R. M. Rodríguez-Dagnino, "Probability distributions in classical and quantum elliptic billiards," Rev. Mex. Fis., 47 (5), 480-488, Oct. 2001

[5] S. Chávez-Cerda, J. C. Gutiérrez-Vega, and G.H.C. New, "Elliptic vortices of electromagnetic wavefields," Opt. Lett., 26 (22), 1803-1805, 15-Nov. 2001

[6] S. Chávez-Cerda, M.J. Padgett, I. Allison, G.H.C. New, J. C. Gutiérrez-Vega, A.T. O'Neil, and J. Courtial, "Holographic generation and orbital angular momentum of high-order momentum", J. Opt. B 4, S52–S57, Apr. 2002

[7] J. C. Gutiérrez-Vega, R. M. Rodríguez-Dagnino, M. A. Meneses-Nava, and S. Chávez-Cerda, "Mathieu functions, a visual approach," Am. J. Phys. 71 (3), 233-242, Mar. 2003

[8] Miguel A. Bandres, Julio C. Gutiérrez-Vega, and S. Chávez-Cerda, "Parabolic nondiffracting optical wavefields," Opt. Lett., 29 (1), 44-46, 01-Jan. 2004

[9] Carlos López-Mariscal, Miguel A. Bandrés, S. Chávez-Cerda, and Julio. C. Gutiérrez-Vega, "Observation of Parabolic nondiffracting wave fields," Opt. Express, 13 (7), 2364-2369, April 2005

# Scalar Helmholtz-Gauss beams

- Ideal nondiffracting beams have an infinite extent and energy (they are not square integrable), and thus they are not physically realizable.

- In view of this, some papers have been devoted to describing modified versions of Bessel beams, which carry finite energy and may be said to be nearly nondiffracting because they can propagate over a large range without significant divergence.

# Classical paper: Bessel-Gauss beams by Gori et al.

Volume 64, number 6 OPTICS COMMUNICATIONS 15 December 1987

## BESSEL–GAUSS BEAMS

F. GORI, G. GUATTARI
*Dipartimento di Fisica, Università di Roma "La Sapienza", P. le A. Moro, 2, 00185 Roma, Italy*

and

C. PADOVANI
*Dipartimento di Ingegneria Elettrica, Università di L'Aquila, Monteluco di Roio, L'Aquila, Italy*

Received 13 August 1987

A new type of solution of the paraxial wave equation is presented. It encompasses as limiting cases both the diffraction-free beam and the gaussian beam. The propagation features of this solution are discussed.

### 1. Introduction

Propagation of coherent or partially coherent light in the form of beams is of obvious importance from both the theoretical and the experimental point of view. Although light beams of one form or another are simple to produce in practice, the corresponding analytical description is not that easy. This occurs because the evaluation of the integrals involved in the propagation formulas seldom leads to closed expressions. As a celebrated example, we recall that the deceptively simplest way of shaping a light pencil, namely limiting a plane wave by a circular aperture, prompted the introduction of a new family of special functions, known as Lommel functions [1], for its paraxial analysis. Nevertheless, a number of types of light beams both useful and analytically simple are known today. They range from the ubiquitous gaussian beam of zero order [2,3], to more sophisticated forms of both coherent [2–7] and partially coherent [8–26] beams.

Recently, new types of coherent light beams, called diffraction-free beams, have been studied [27,28]. They have the peculiar property of conserving the same disturbance distribution (apart from a phase factor) across any plane orthogonal to the direction of propagation, say the $z$-axis. An intuitive understanding of these beams can be gained by thinking of them as a superposition of plane waves whose wave vectors lie on a cone around the $z$-axis. All these plane waves have the same component of the wave vector along the $z$-axis. Accordingly, they all suffer the same phase change for any given pathlength along the $z$-axis. The mutual phase relations among the various plane waves do not change on propagation, so that the overall interference pattern has one and the same shape at any plane $z$=constant. For the simplest beam of this type, which is circularly symmetric, the transverse disturbance distribution has the form of a Bessel function of the first kind and zero order, $J_0(\beta r)$, where $r$ denotes the distance from the $z$-axis and $\beta$ is the length of the component, orthogonal to the $z$-axis, of any wave vector belonging to one of the plane waves producing the beam. As well known, the maxima of the oscillating function $J_0(x)$ tend to decrease like $1/x^{1/2}$ when $x$ goes to infinity. Because of this slow decrease law, it is impossible to realize experimentally a beam giving everywhere a good approximation to the ideal model. Note also that the ideal beam should carry an infinite power because of the divergence of the norm of $J_0(\beta r)$. In a laboratory test [27], an experimental beam was realized whose disturbance in the plane $z=0$ was of the form $J_0(\beta r)$ within a circular aperture and vanished elsewhere. It





F. Gori, G. Guattari, and C. Padovani, "Bessel–Gauss beams," Opt. Commun. **64**, 491–495 (1987).

**Field at $z$ = 0**

$$V(r,0)=A\,J_0(\beta r)\exp[-(r/w_0)^2]$$

**Propagated field for $z$ >= 0**

$$\begin{aligned} V(r,z) &= (Aw_0/w(z)) \\ &\times \exp\{i[(k-\beta^2/2k)z-\Phi(z)]\} \\ &\times J_0[\beta r/(1+iz/L)]\exp\{[-1/w^2(z) \\ &+ik/2R(z)]\,(r^2+\beta^2z^2/k^2)\}\,, \end{aligned} \tag{2.7}$$

where the parameter $L$ is given by

$$L=kw_0^2/2\,, \tag{2.8}$$

and where the functions $w(z)$, $\Phi(z)$ and $R(z)$ are as follows

$$w(z)=w_0\,[1+(z/L)^2]^{1/2}\,, \tag{2.9}$$

$$\Phi(z)=\arctan(z/L)\,, \tag{2.10}$$

$$R(z)=z+L^2/z\,. \tag{2.11}$$

## Scalar Helmholtz-Gauss beams

We call Helmholtz-Gauss (HzG) beam a general solution to the paraxial wave equation.

$$\left(\frac{\partial^2}{\partial x^2}+\frac{\partial^2}{\partial y^2}+2ik\frac{\partial}{\partial z}\right)\Psi\left(\mathbf{r}\right)=0.$$

whose disturbance across the plane $z = 0$ is given by the product of a Gaussian factor and the transverse shape of an arbitrary nondiffracting beam

$$U_0\left(\mathbf{r}_t\right)=\exp\left(-\frac{r^2}{w_0^2}\right)W\left(\mathbf{r}_t;k_t\right),$$

$W(x,y;\, k_t)$ satisfies the two-dimensional Helmholtz equation

$$\left(\frac{\partial^2}{\partial x^2}+\frac{\partial^2}{\partial y^2}+k_t^2\right)W\left(\mathbf{r}_t;k_t\right)=0,$$

and can be expanded in terms of plane waves (angular spectrum)

$$W\left(\mathbf{r}_t;k_t\right)=\int_{-\pi}^{\pi}A(\varphi)\exp\left[ik_t(x\cos\varphi+y\sin\varphi)\right]\,\mathrm{d}\varphi,$$

## Analitical expression of Helmholtz-Gauss beams

The analytical expression of the HzG waves is given by the product of three factors:

- a complex amplitude dependent on *z* only
- a Gaussian beam and
- a complex scaled version of the transverse profile of the nondiffracting beam.

$$\underbrace{U(\mathbf{r})}_{\text{HzG beam}} = \overbrace{\exp\left(-i\frac{k_t^2}{2k}\frac{z}{\mu}\right)}^{\text{z-dependent function}} \underbrace{\mathrm{GB}(\mathbf{r})}_{\text{Gaussian envelope}} \underbrace{W}_{\text{Nondiffracting function}}\left(\frac{x}{\underbrace{\mu}_{\text{Scaling complex factor}}}, \frac{y}{\mu}; k_t\right)$$

where $\mathrm{GB}(\mathbf{r}) = \dfrac{\exp(ikz)}{\mu}\exp\left(-\dfrac{r^2}{\mu w_0^2}\right).$

$$\mu = \mu(z) = 1 + iz/z_R, \quad z_R = kw_0^2/2.$$

Julio C. Gutiérrez-Vega and Miguel A. Bandres, "Helmholtz-Gauss beams," JOSA A, **22**, 289 (2005)

# *Angular spectrum of Helmholtz-Gauss beams*

Two-dimensional Fourier transform

$$\mathfrak{U}(u,v;z) = \frac{1}{2\pi} \iint U(x,y,z) \exp\left(-ixu - iyv\right) \mathrm{d}x\mathrm{d}y,$$

Angular spectrum of the HzG waves

$$\mathfrak{U}(u,v;z) = D(z) \exp\left(-\frac{w_0^2 \mu}{4} \rho^2\right) W_{\mathrm{t}}\left(\frac{w_0^2}{2i} u, \frac{w_0^2}{2i} v; k_t\right).$$

where $\rho = (u^2 + v^2)^{1/2}$, $D(z) = \frac{w_0^2}{2} \exp\left(-\frac{1}{4} k_t^2 w_0^2\right) \exp(ikz).$

Exact NDBs
Ideal plane waves

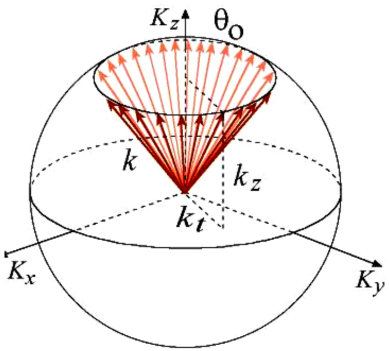


HzG beams
Tilted plane-wave-Gaussian beam

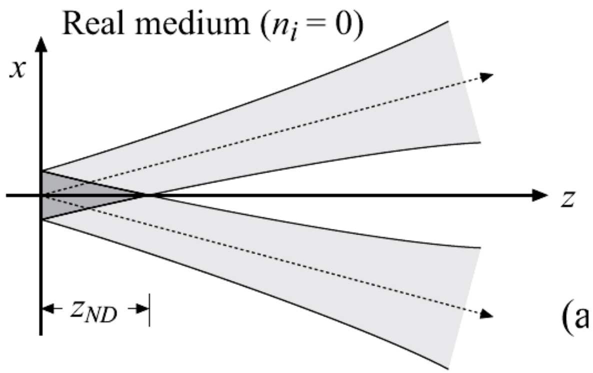

# Cosine-Gauss beams

$$W\left(\mathbf{r}_t; k_t\right) = \cos\left(k_t y\right)$$

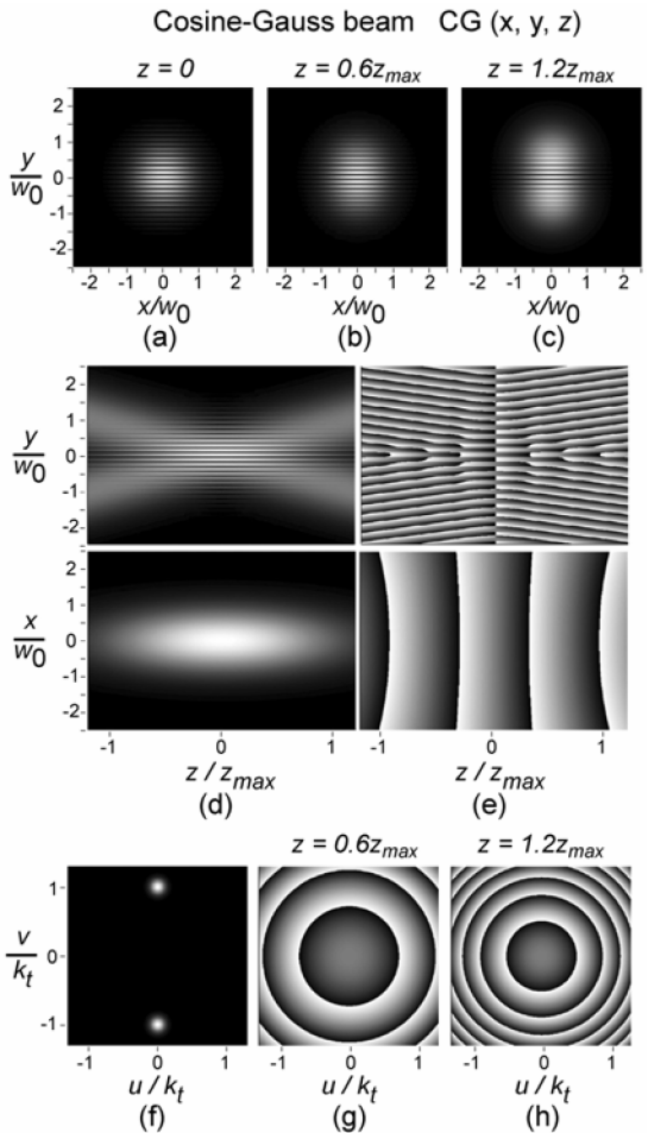


Field

$$\mathrm{CG}\left(\mathbf{r}\right) = \exp\left(-i\frac{k_t^2}{2k}\frac{z}{\mu}\right)\ \mathrm{GB}\left(\mathbf{r}\right)\ \ \cos\left(\frac{k_t y}{\mu}\right)$$

Spectrum

$$\mathfrak{CG}(u, v; z) = D(z)\exp\left(-\frac{\mu w_0^2}{4}\rho^2\right)\cosh\left[2\gamma^2(v/k_t)\right]$$

Fig. 2. (a)-(c) Transverse amplitude distribution of a Cosine–Gauss beam at different $z$ planes. (d)-(e) Propagation of the amplitude and phase profiles along the planes $(y, z)$ and $(x, z)$. (f)-(h) Amplitude and phase distribution of the angular spectrum at different $z$ planes. f2NDG.eps.

# *Bessel-Gauss beams*

$$\mathrm{BG}_m(\mathbf{r}) = \exp\left(-i\frac{k_t^2}{2k}\frac{z}{\mu}\right)\ \mathrm{GB}(\mathbf{r})\ J_m\left(\frac{k_t r}{\mu}\right)\exp(im\phi).$$

$$\mathfrak{BG}_m(u,v;z) = (-i)^m D(z)\exp\left(-\frac{\mu w_0^2}{4}\rho^2\right)\ I_m\left(2\gamma^2\rho/k_t\right)\exp\left(im\phi\right).$$

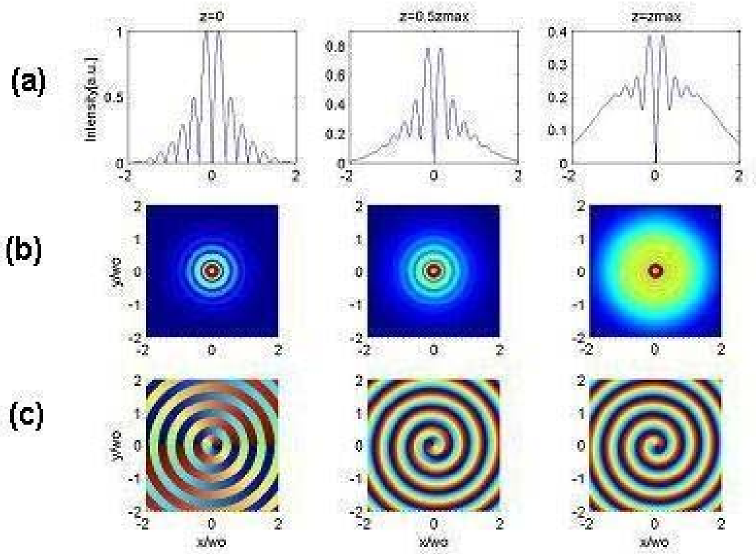


Propagation of a Bessel-Gauss beam of order 1.
(a) Intensity profile at y=0 and at z=0, 0.5zmax and zmax.
(b) Transverse profile at z=0, 0.5zmax and zmax.
(c) Phase profile at the plane (x,y)

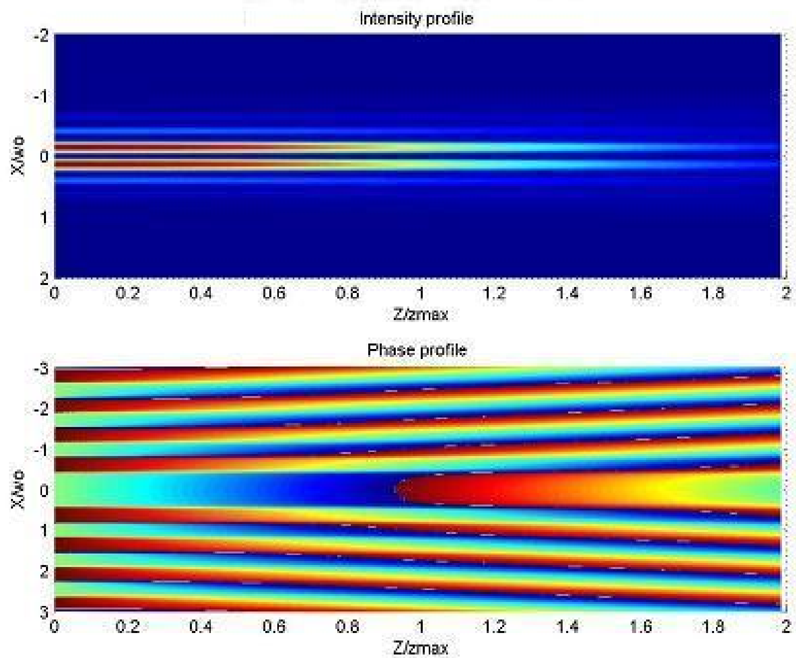


Propagation of the amplitude and phase profiles along the (x,z) plane in the range [0,2Zmax].

# Mathieu-Gauss beams

$$W^e(\mathbf{r}_t;k_t) = \mathrm{Je}_m(\xi,q)\ \mathrm{ce}_m(\eta,q)$$

$$W^o(\mathbf{r}_t;k_t) = \mathrm{Jo}_m(\xi,q)\ \mathrm{se}_m(\eta,q)$$

## Field

$$\mathrm{MG}^e_m(\mathbf{r}) = \exp\left(-i\frac{k_t^2}{2k}\frac{z}{\mu}\right)\ \mathrm{GB}(\mathbf{r})\ \mathrm{Je}_m(\overline{\xi},q)\,\mathrm{ce}_m(\overline{\eta},q)$$

$$x = f_0(1+iz/z_R)\cosh\overline{\xi}\cos\overline{\eta}$$

$$y = f_0(1+iz/z_R)\sinh\overline{\xi}\sin\overline{\eta},$$

## Spectrum

$$\mathfrak{MG}^e_m(u,v;z) = D(z)\exp\left(-\frac{\mu w_0^2}{4}\rho^2\right)\mathrm{Je}_m\left(\widehat{\xi},q\right)\ \mathrm{ce}_m(\widehat{\eta},q)$$

$$u = \frac{2i}{w_0^2}f_0\cosh\widehat{\xi}\cos\widehat{\eta},$$

$$v = \frac{2i}{w_0^2}f_0\sinh\widehat{\xi}\sin\widehat{\eta}.$$

Complex elliptic variables (ξ,η) !!

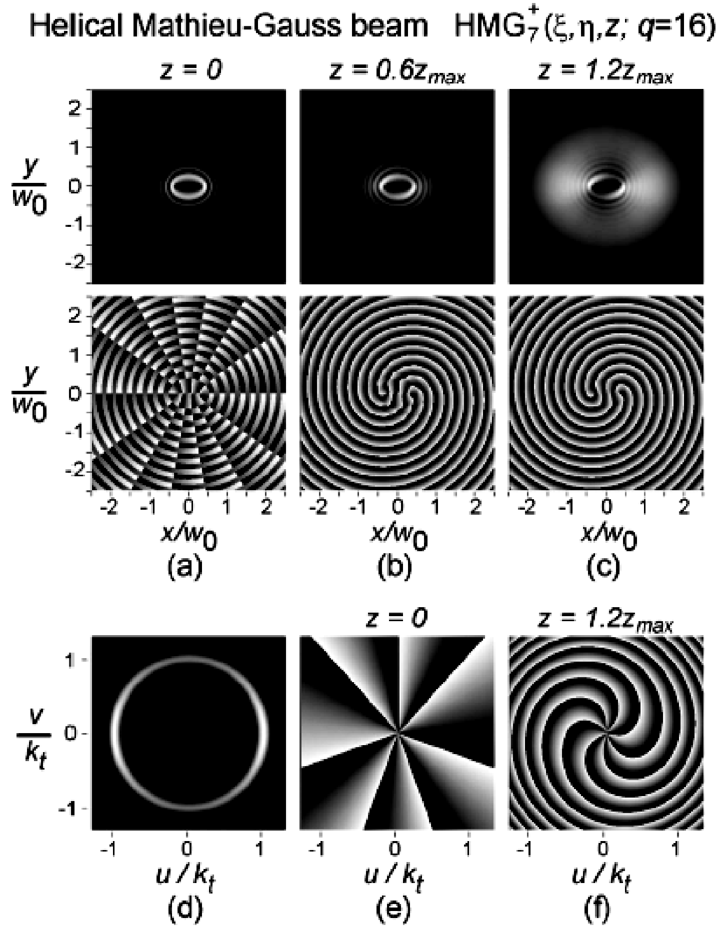


Fig. 5. (a)–(c) Transverse amplitude and phase distributions of a seventh-order HMG beam at different $z$ planes, (d)–(f) amplitude and phase distributions of the angular spectrum as a function of the normalized coordinates $(u/k_t, v/k_t)$.

## *Helical Mathieu-Gauss beams: experiment*

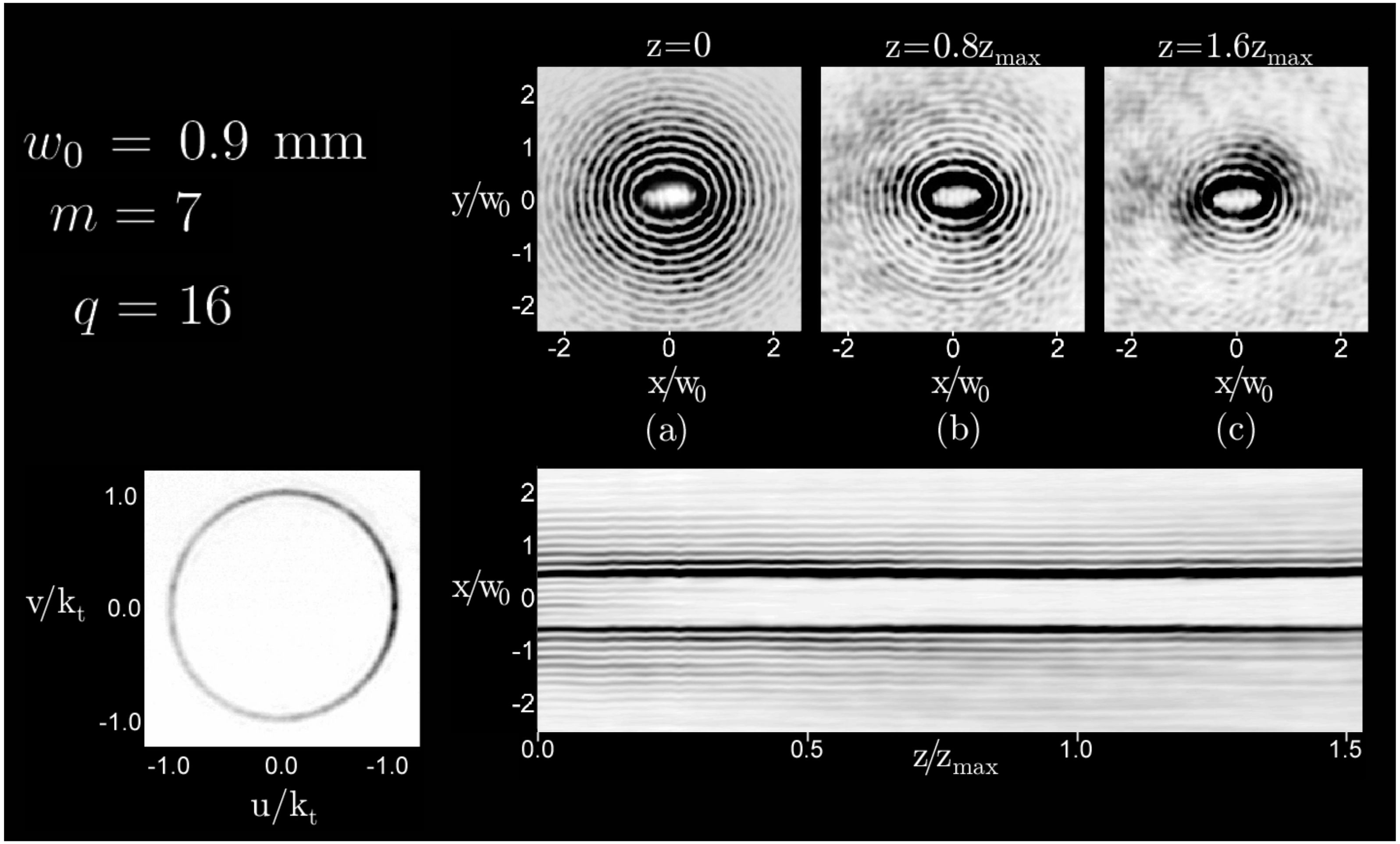


Carlos López-Mariscal et al, "Observation of the experimental propagation properties of Helmholtz-Gauss beams," To be published in Opt. Eng. 2006

# *Parabolic-Gauss beams*

$$W^e(\xi,\eta;k_t) = \frac{|\Gamma_1|^2}{\pi\sqrt{2}} \mathrm{P}_e\left(\sqrt{2k_t}\xi;a\right) \mathrm{P}_e\left(\sqrt{2k_t}\eta;-a\right)$$

$$W^o(\xi,\eta;k_t) = \frac{|\Gamma_1|^2}{\pi\sqrt{2}} \mathrm{P}_e\left(\sqrt{2k_t}\xi;a\right) \mathrm{P}_e\left(\sqrt{2k_t}\eta;-a\right)$$

## Field

$$\mathrm{PG}^e(\mathbf{r};a) = \exp\left(-i\frac{k_t^2}{2k}\frac{z}{\mu}\right)\ \mathrm{GB}(\mathbf{r})\ \frac{|\Gamma_1|^2}{\pi\sqrt{2}}$$
$$\mathrm{P}_e\left(\sqrt{2k_t/\mu}\xi;a\right) \mathrm{P}_e\left(\sqrt{2k_t/\mu}\eta;-a\right)$$

## Spectrum

$$\mathfrak{PG}^e(u,v;z) = D(z)\exp\left(-\frac{\mu w_0^2}{4}\rho^2\right)\frac{|\Gamma_1|^2}{\pi\sqrt{2}}$$
$$\mathrm{P}_e\left(\sqrt{-ik_t w_0^2}\tilde{\xi};a\right) \mathrm{P}_e\left(\sqrt{-ik_t w_0^2}\tilde{\eta};-a\right)$$

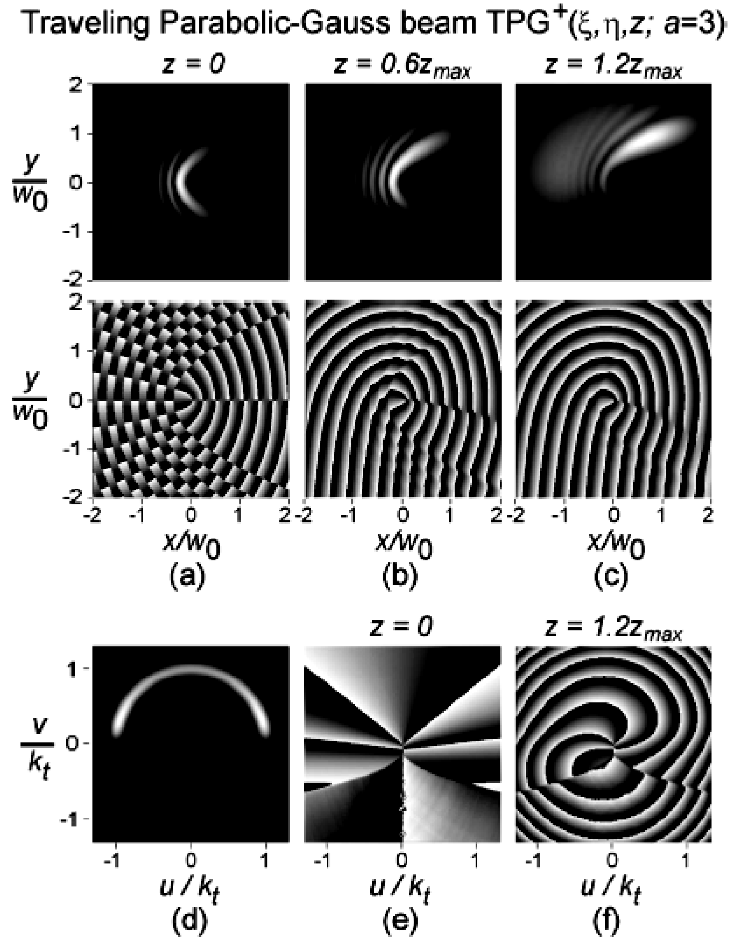


Fig. 7. (a)–(c) Transverse amplitude and phase distributions of a TPG beam with $a = 3$ at different $z$ planes, (d)–(f) amplitude and phase distributions of the angular spectrum.

# *Helical Parabolic-Gauss beams: experiment*

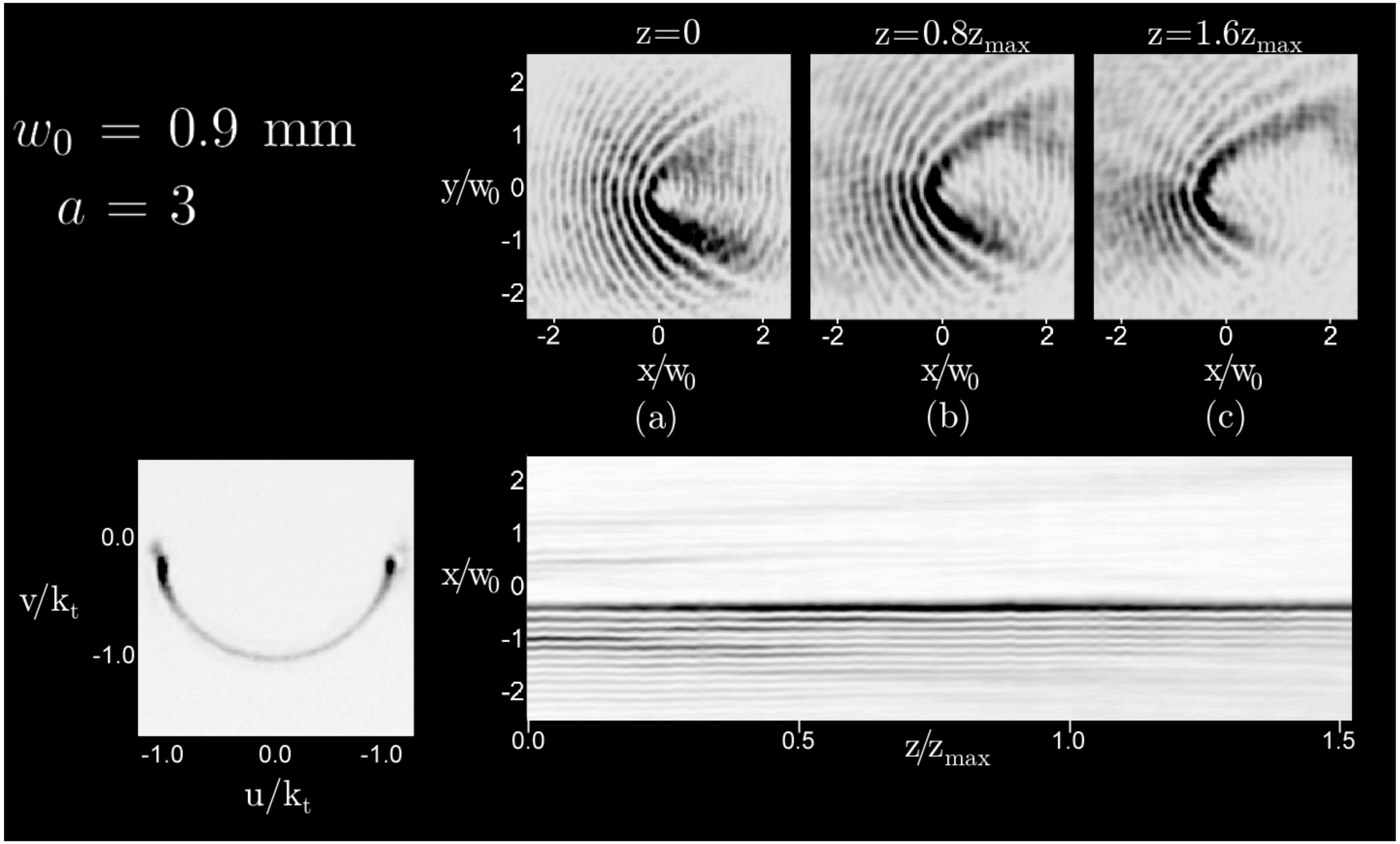


Carlos López-Mariscal et al, "Observation of the experimental propagation properties of Helmholtz-Gauss beams,"
To be published in Opt. Eng. 2006

# Vector HzG beams

We introduce a general family of localized vector beam solutions of the Maxwell equations in the paraxial regime.

The family of solutions is constructed starting from the scalar solutions of the 2D Helmholtz equation, thus we refer to them as vector Helmholtz-Gauss (vHzG) beams.

The transverse fields appear naturally as solutions of the vector paraxial wave equation (vPWE) by applying the separation of variables method.

Under the appropriate limits, the vHzG beams reduce to the special cases of

- Scalar Helmholtz-Gauss beams [1,2,3]
- TE and TM Gaussian vector beams [4,5]
- Nondiffracting vector Bessel beams [6]
- Vector Bessel-Gauss beams [7]
- Propagating modes supported by waveguides and cavities with constant cross-section [8].

# Vector Paraxial wave equation

Consider the free space propagation of a monochromatic electromagnetic beam along the positive $z$ axis of a coordinate system $\mathbf{r} = (\mathbf{r}_t, z)$ where $\mathbf{r}_t = (\widehat{\mathbf{x}}x + \widehat{\mathbf{y}}y)$ is the transverse radius vector. The electric and magnetic fields are written as

$$\mathbf{E} = (\mathbf{E}_t + \widehat{\mathbf{z}}E_z)\exp(ikz) \text{ and } \mathbf{H} = (\mathbf{H}_t + \widehat{\mathbf{z}}H_z)\exp(ikz),$$

From the perturbative series expansion of Maxwell equations provided by Lax *et al.*, [PRA **11**, 1365 (1975)] it is known that zeroth-order fields are purely transverse and satisfy the vector paraxial wave equation

$$\left[\nabla_t^2 + 2ik\frac{\partial}{\partial z}\right]\begin{Bmatrix}\mathbf{E}_t\\ \mathbf{H}_t\end{Bmatrix} = 0,$$

where $\nabla_t = \widehat{\mathbf{x}}\partial/\partial x + \widehat{\mathbf{y}}\partial/\partial y$ is the transverse nabla operator. Lax expansion also showed that in next-order correction a small longitudinal field component must be present and its value is obtained from the transverse components through

$$\begin{Bmatrix}E_z\\ H_z\end{Bmatrix} = \frac{i}{k}\nabla_t \cdot \begin{Bmatrix}\mathbf{E}_t\\ \mathbf{H}_t\end{Bmatrix}.$$

Additionally, to be consistent with Maxwell equations, the transverse fields and the unit vector $\widehat{\mathbf{z}}$ are mutually perpendicular and satisfy

$$\mathbf{H}_t = (\epsilon_0/\mu_0)^{1/2}\widehat{\mathbf{z}} \times \mathbf{E}_t.$$

## *Extracting the Gaussian envelope of the PWE*

**vPWE**

$$\left[\nabla_t^2 + 2ik\frac{\partial}{\partial z}\right]\begin{Bmatrix}\mathbf{E}_t \\ \mathbf{H}_t\end{Bmatrix} = 0,$$

A rigorous analytical solution to the vPWE is obtained by writing

$$\mathbf{E}_t(\mathbf{r}) = \mathbf{U}\left(X, Y, \zeta\right)\mathrm{G}(\mathbf{r}), \tag{5}$$

where $(X, Y) = (x/\zeta, y/\zeta)$ are scaled Cartesian coordinates,

$\zeta(z) = 1 + iz/z_R$, and

$$\mathrm{G}(\mathbf{r}) = \frac{1}{\zeta}\exp\left(-\frac{r^2}{\zeta w_0^2}\right) \tag{6}$$

is the familiar Gaussian beam with waist size $w_0$, and Rayleigh range $z_R = kw_0^2/2$. Inserting Eq. (5) into (2) produces the equation for $\mathbf{U}$:

**Reduced vPWE**

$$\nabla_T^2\mathbf{U} - \frac{4\zeta^2}{w_0^2}\frac{\partial \mathbf{U}}{\partial \zeta} = 0, \tag{7}$$

where $\nabla_T = \widehat{\mathbf{x}}\partial/\partial X + \widehat{\mathbf{y}}\partial/\partial Y$ is the transverse nabla in the scaled coordinates

# Applying the separation of variables method

Equation (7) admits the separation of variables $\mathbf{U} = \mathbf{\Psi}\left(X, Y\right) Z\left(\zeta\right)$

upon which we find that

$$Z\left(\zeta\right) = \exp\left(-i\frac{k_t^2 z}{2k\zeta}\right), \tag{8}$$

where $k_t^2$ is the separation constant and $\mathbf{\Psi}\left(X, Y\right)$ satisfies the 2D vector Helmholtz equation

$$\nabla_T^2 \mathbf{\Psi} + k_t^2 \mathbf{\Psi} = 0. \tag{9}$$

Now Eq. (9) admits the two independent vector solutions of the form [J. A. Stratton, Electromagnetic theory (McGraw-Hill, New York, 1941)]

$$\mathbf{\Psi}^{(1)} = \nabla_T W(X, Y), \tag{10a}$$

$$\mathbf{\Psi}^{(2)} = -\widehat{\mathbf{z}} \times \mathbf{\Psi}^{(1)}, \tag{10b}$$

where $W(X, Y)$ is a solution of the 2D scalar Helmholtz equation

$$\nabla_T^2 W + k_t^2 W = 0. \tag{11}$$

## Collecting the partial results

### First class vector beam solution

$$\mathbf{E}_t^{(1)} = Z(\zeta)\,\mathrm{G}(\mathbf{r})\nabla_T W,$$

$$E_z^{(1)} = -\frac{iZ(\zeta)\,\mathrm{G}(\mathbf{r})}{\zeta}\left(\frac{k_t^2}{k}W + \frac{2}{kw_0}\nabla_T W \cdot \frac{\mathbf{r}_t}{w_0}\right),$$

$$\mathbf{H}_t^{(1)} = \sqrt{\frac{\epsilon_0}{\mu_0}}Z(\zeta)\,\mathrm{G}(\mathbf{r})\left(\widehat{\mathbf{z}} \times \nabla_T W\right),$$

$$H_z^{(1)} = -\sqrt{\frac{\epsilon_0}{\mu_0}}\frac{2i}{kw_0}\frac{Z(\zeta)\,\mathrm{G}(\mathbf{r})}{\zeta}\left(\widehat{\mathbf{z}} \times \nabla_T W\right) \cdot \frac{\mathbf{r}_t}{w_0},$$

where $W(X,Y)$ is a solution of the 2D scalar Helmholtz equation

$$\nabla_T^2 W + k_t^2 W = 0.$$

M. A. Bandres and J. C. Gutiérrez-Vega, "Vector Helmholtz-Gauss and vector Laplace-Gauss beams," Opt. Lett., **30**, 2155 (2005)

## Collecting the partial results

### *Second class vector beam solution*

$$\mathbf{E}_t^{(2)} = -Z(\zeta)\,\mathrm{G}(\mathbf{r})(\widehat{\mathbf{z}} \times \nabla_T W),$$

$$E_z^{(2)} = \frac{2i}{kw_0}\frac{Z(\zeta)\,\mathrm{G}(\mathbf{r})}{\zeta}(\widehat{\mathbf{z}} \times \nabla_T W) \cdot \frac{\mathbf{r}_t}{w_0},$$

$$\mathbf{H}_t^{(2)} = \sqrt{\frac{\epsilon_0}{\mu_0}} Z(\zeta)\,\mathrm{G}(\mathbf{r}) \nabla_T W,$$

$$H_z^{(2)} = -\sqrt{\frac{\epsilon_0}{\mu_0}} \frac{iZ(\zeta)\,\mathrm{G}(\mathbf{r})}{\zeta}\left(\frac{k_t^2}{k}W + \frac{2}{kw_0}\nabla_T W \cdot \frac{\mathbf{r}_t}{w_0}\right)$$

where $W(X, Y)$ is a solution of the 2D scalar Helmholtz equation

$$\nabla_T^2 W + k_t^2 W = 0.$$

# *Vector distributions for some families*

The fundamental and orthogonal families of eigenfunctions of the 2D Helmholtz equation

Circular coordinates: .
Vector Bessel-Gauss beams

$$W = J_m(k_t r)\exp(\pm im\phi)$$

Elliptic coordinates [9]: .

Vector Mathieu-Gauss beams

$$W = \mathrm{Je}_m(\xi, q)\mathrm{ce}_m(\eta, q)$$

Parabolic coordinates [10]:
Vector Parabolic-Gauss beams

$$W = \mathrm{Pe}\left(u\sqrt{2k_t}; a\right)\mathrm{Pe}\left(v\sqrt{2k_t}; -a\right)$$

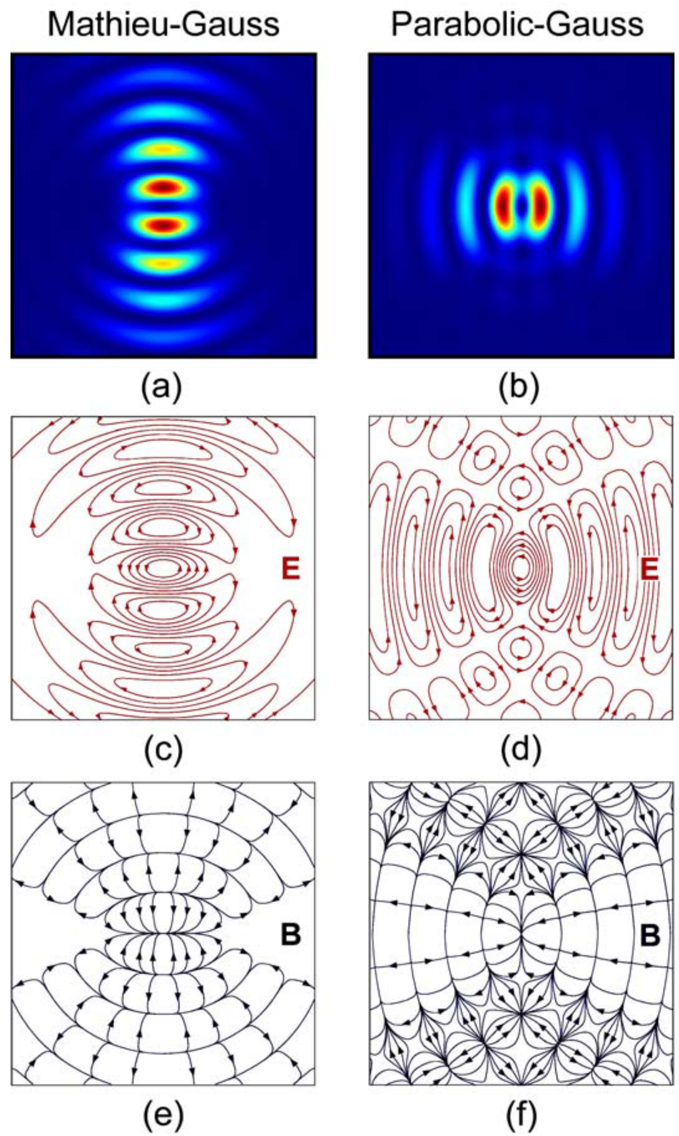

## Special case: vector Bessel-Gauss beams

The first class vector beam solution

$$\boxed{\begin{aligned}
\mathbf{E}_t^{(2)} &= -Z\,(\zeta)\,\mathrm{G}(\mathbf{r})(\widehat{\mathbf{z}} \times \nabla_T W),\\
E_z^{(2)} &= \frac{2i}{kw_0}\,\frac{Z\,(\zeta)\,\mathrm{G}(\mathbf{r})}{\zeta}(\widehat{\mathbf{z}} \times \nabla_T W)\cdot\frac{\mathbf{r}_t}{w_0},\\
\mathbf{H}_t^{(2)} &= \sqrt{\frac{\epsilon_0}{\mu_0}}Z\,(\zeta)\,\mathrm{G}(\mathbf{r})\nabla_T W,\\
H_z^{(2)} &= -\sqrt{\frac{\epsilon_0}{\mu_0}}\frac{iZ\,(\zeta)\,\mathrm{G}(\mathbf{r})}{\zeta}\left(\frac{k_t^2}{k}W + \frac{2}{kw_0}\nabla_T W\cdot\frac{\mathbf{r}_t}{w_0}\right)
\end{aligned}}$$

reduces to the Vector-beam solutions of Maxwell's wave equation found by:

D. G. Hall, "Vector-beam solutions of Maxwell's wave equation", Opt. Lett. **21**, 9 (1996).

S. R. Seshadri, "Electromagnetic Gaussian beam", JOSA A, **15,** 2712 (1998)

when circular cylindrical coordinates are used and $W = J_m(k_t r)\exp(\pm im\phi)$

## Special case: Vector TM and TE nondiffracting beams

When the Gaussian beam size becomes very large ( $w_0 \to \infty$ ) we have

$$\boxed{\begin{aligned}
\mathbf{E}^{\mathrm{TM}} &= \exp(ik_z z)\left(\nabla_t W - \hat{\mathbf{z}}\frac{ik_t^2}{k}W\right), \\
\mathbf{H}^{\mathrm{TM}} &= \sqrt{\frac{\epsilon_0}{\mu_0}}\exp(ik_z z)(\hat{\mathbf{z}} \times \nabla_t W), \\
\mathbf{E}^{\mathrm{TE}} &= -\exp(ik_z z)(\hat{\mathbf{z}} \times \nabla_t W), \\
\mathbf{H}^{\mathrm{TE}} &= \sqrt{\frac{\epsilon_0}{\mu_0}}\exp(ik_z z)\left(\nabla_t W - \hat{\mathbf{z}}\frac{ik_t^2}{k}W\right)
\end{aligned}}$$

These expressions reduce to the vector Bessel beams discussed by
Z. Bouchal and M. Olivík, "Nondiffractive Bessel beams," J. Mod. Opt. **42**, 1555 (1995)
when circular cylindrical coordinates are used:

$$W = J_m(k_t r)\exp(\pm im\phi)$$

# Laplace-Gauss beams

The case when $k_t = 0$ is important. From Eq. (7) we have $Z = 1$, thus the function $\mathbf{U} = \mathbf{\Psi}(X, Y)$ depends only on the transverse coordinates $(X, Y)$. From Eq. (8) it is evident that $\mathbf{\Psi}$ satisfies now the 2D vector Laplace equation $\nabla_T^2 \mathbf{\Psi} = 0$, whose solutions are also given by Eqs. (9) where $W \to \overline{W}(X, Y)$ is now a solution of the scalar Laplace equation $\nabla_T^2 \overline{W} = 0$. Setting $k_t = 0$ in Eqs. (11), the first-class vHzG beams reduce to

$$\boxed{\begin{aligned}
\mathbf{E}_t^{(1)} &= \mathrm{G}(\mathbf{r}) \nabla_T \overline{W}, \\
E_z^{(1)} &= -\frac{2i}{kw_0} \frac{\mathrm{G}(\mathbf{r})}{\zeta} \left( \nabla_T \overline{W} \cdot \frac{\mathbf{r}_t}{w_0} \right), \\
\mathbf{H}_t^{(1)} &= \sqrt{\frac{\epsilon_0}{\mu_0}} \mathrm{G}(\mathbf{r}) \left( \widehat{\mathbf{z}} \times \nabla_T \overline{W} \right), \\
H_z^{(1)} &= -\sqrt{\frac{\epsilon_0}{\mu_0}} \frac{2i}{kw_0} \frac{\mathrm{G}(\mathbf{r})}{\zeta} \left( \widehat{\mathbf{z}} \times \nabla_T \overline{W} \right) \cdot \frac{\mathbf{r}_t}{w_0}.
\end{aligned}}$$

where $\bar{W}(X,Y)$ is a solution of the 2D scalar Laplace equation

M. A. Bandres and J. C. Gutiérrez-Vega, "Vector Helmholtz-Gauss and vector Laplace-Gauss beams," Opt. Lett., **30**, 2155 (2005)

# Thanks to my Nondiffracting collegues

Carlos López-Mariscal
Tecnológico de Monterrey, México

Miguel A. Bandres
Tecnológico de Monterrey, México

Prof. Sabino Chávez-Cerda
INAOE, México